BERICHTE
aus dem Fachbereich Geowissenschaften
der Universität Bremen

No. 123

V. Spiess, C. Hübscher, M. Breitzke, W. Böke, A. Krell, T. v. Larcher,
T. Matschkowski, T. Schwenk, A. Wessels, L. Zühlsdorff, S. Zühlsdorff

REPORT AND PRELIMINARY RESULTS OF R/V SONNE CRUISE 125 COCHIN - CHITTAGONG, 17.10. - 17.11.97

FAHRTBERICHT UND ERSTE ERGEBNISSE DER FS SONNE FAHRT 125 COCHIN - CHITTAGONG, 17.10. - 17.11.97

Berichte, Fachbereich Geowissenschaften, Universität Bremen, No. 123,
128 pages, Bremen 1998

ISSN 0931-0800

The "Berichte aus dem Fachbereich Geowissenschaften" are produced at irregular intervals by the Department of Geosciences, Bremen University.

They serve for the publication of experimental works, Ph.D.-theses and scientific contributions made by members of the department.

Reports can be ordered from:

Gisela Boelen

Sonderforschungsbereich 261

Universität Bremen

Postfach 330 440

D 28334 BREMEN

Phone: (49) 421 218-4124

Fax: (49) 421 218-3116

Citation:

V. Spiess, C. Hübscher, M. Breitzke, W. Böke, A. Krell, T. v. Larcher, T. Matschkowski, T. Schwenk, A. Wessels, L. Zühlsdorff, S. Zühlsdorff

REPORT AND PRELIMINARY RESULTS OF R/V SONNE CRUISE 125, COCHIN - CHITTAGONG, 17.10. - 17.11.97

FAHRTBERICHT UND ERSTE ERGEBNISSE DER FS SONNE FAHRT 125, COCHIN - CHITTAGONG, 17.10. - 17.11.97

Berichte, Fachbereich Geowissenschaften, Universität Bremen, No. 123, 128 pages, Bremen, 1998.

ISSN 0931-0800

Contents

1. Participants and Crew List

1.1 SO125 - List of Scientific Crew

Name	Function	Reserach Field	Institution
Prof. Volkhard Spieß	Ch/Scientist	Geophysics	GeoB
Dipl.-Ing. Wolfgang Böke	Engineer	Geophysics	GeoB
Dr. Monika Breitzke	Scientist	Geophysics	GeoB
Dr. Christian Hübscher	Scientist	Geophysics	GeoB
Andreas Krell	Student	Geophysics	GeoB
Thorsten Matschkowski	Technician	Geophysics	GeoB
Tilmann Schwenk	Student	Geophysics	GeoB
Thomas von Larcher	Student	Geophysics	GeoB
Arne Wessel	Student	Geophysics	GeoB
Lars Zühlsdorff	Scientist	Geophysics	GeoB
Sven Zühlsdorff	Student	Geophysics	GeoB

GeoB: Fachbereich Geowissenschaften
Universität Bremen
Postfach 330 440
28334 Bremen

1.2 SO125 - Crew List

Name	Rank
Dirk Kalthoff	Master
Roland Priebe	Ch/Mate
Detlef Corte	1st Mate
Wolfgang Sturm	Radio Officer
Stephan Baade	Doctor
Volker Hartig	Ch. Eng.
Peter Uwe Schade	2nd Eng.
Dieter Geithner	2nd Eng.
Steffen Beekan	Electrician
Hilmar Hoffmann	El./Eng.
Rainer Duthel	El./Eng.
Jens Griegel	Sys. Manager
Andreas Klein	Sys. Manager
Rudolf Tscharntke	Fitter
Gerhard Paul	Motorman
Hans G. Bethge gen. Becher	Motorman
Helmut Meyer	Motorman
Johannes Georg Arronet	Motorman
Wolfgang Evers	Ch/Cook
Adolf Cwienk	2nd Cook
Johann Bronn	Ch/Steward
Jan Hoppe	2nd Steward
Werner Scheller	2nd Steward
Heiko Baron	Bosun
Günther Ventz	A.B.
Werner Hoedl	A.B.

Günter Stängl	A.B.
Ralf Etzdorf	A.B.
Ingo Witkowski	A.B.
Volkmar Neitsch	A.B.

2. *Research Program*

The scientific program of R/V SONNE Cruise SO125 was assigned to collect sediment echosounder, swath sounder and multichannel reflection seismic profiles to study the

- general depositional processes on the Bengal Fan,
- down-fan development of the recent channel-levee system,
- sedimentation history at DSDP Leg 22, Site 218 in the lower fan,
- relationship of meander geometry and depositional terraces within the channels,
- channel shifting and channel jumping in the middle Bengal Fan,
- channel termination and attached channel mouth lobes.

Working areas are located in the international waters of the Gulf of Bengal between 8°N and 17°N (Fig. 1). Drill site 218 of DSDP Leg 22 was crossed on the southern most seismic line to constrain seismostratigraphic interpretation.

Acoustic and seismic systems in 4 different frequency domains were used to optimize resolution in different levels of sub-bottom depths (Fig. 2). The Hydrosweep swath sounder and the Parasound sediment echosounder are permanently installed on R/V SONNE. The Hydrosweep system provides topographic information of a width of twice the water depth. The Parasound sediment echosounder uses frequencies around 4 kHz, which allow signal penetration between 10 and 100 m depending on sediment composition and grain size. Digital echosounder data were routinely collected with the help of all scientists onboard by participating in the 24-hour watch keeping duties.

Multichannel seismic measurements were carried out with a new instrumentation of the Department of Earth Sciences, Bremen University, utilizing two seismic sources of different volume in an alternating mode. A water gun with a frequency range from 200 to 2000 Hz provides information of the upper 100 to 300 m of the sediment column, whereas a GI-Gun™ with signal

energy up to 500 Hz allows seismic imaging of sedimentary layers down to 1000-2000 m below see floor. A total of 4000 km of multi-channel data were collected along 50 seismic lines (see chapter 6).

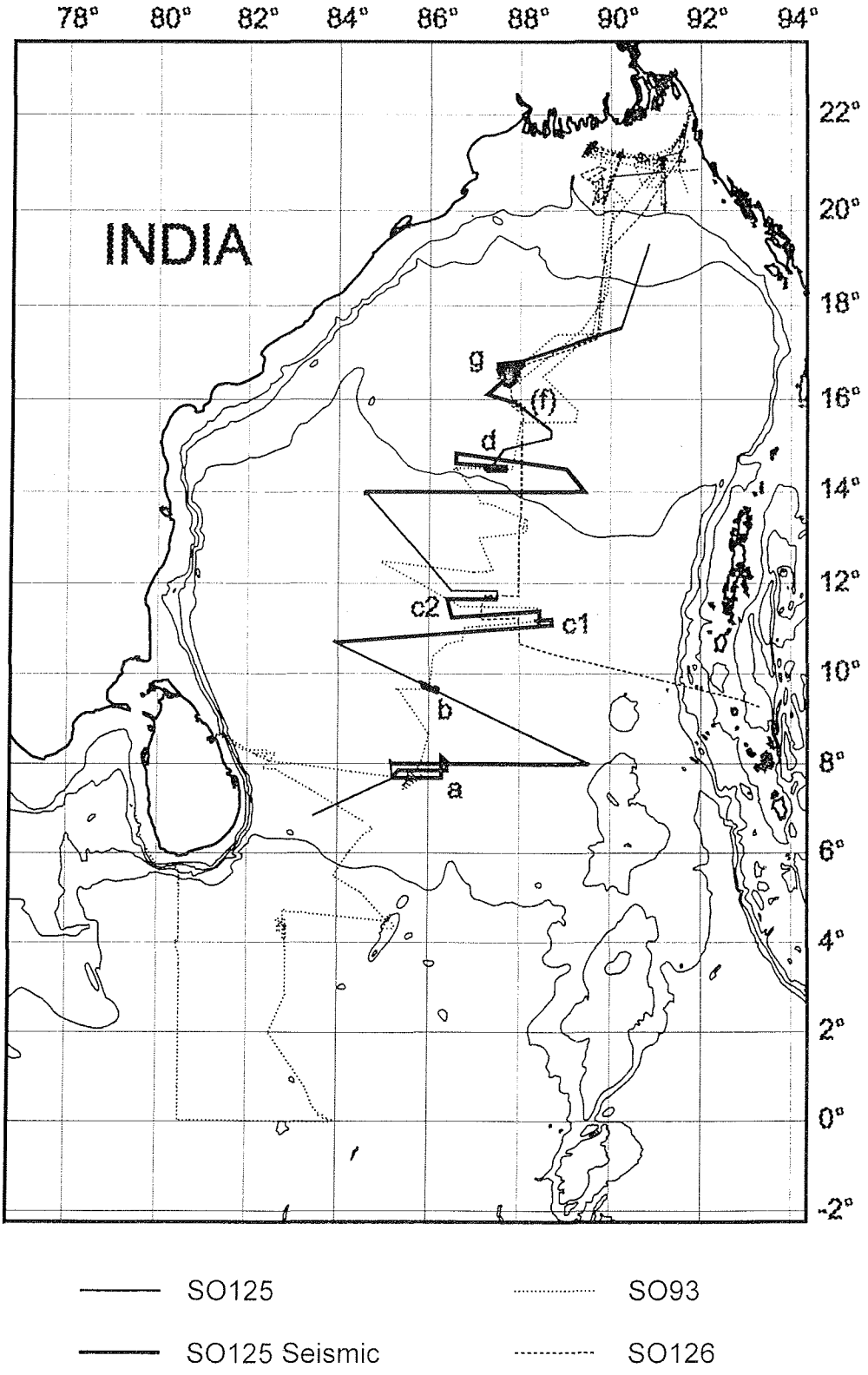

Fig. 1. Map of the Gulf of Bengal with tracks from RV Sonne cruises SO93, SO125, SO126.

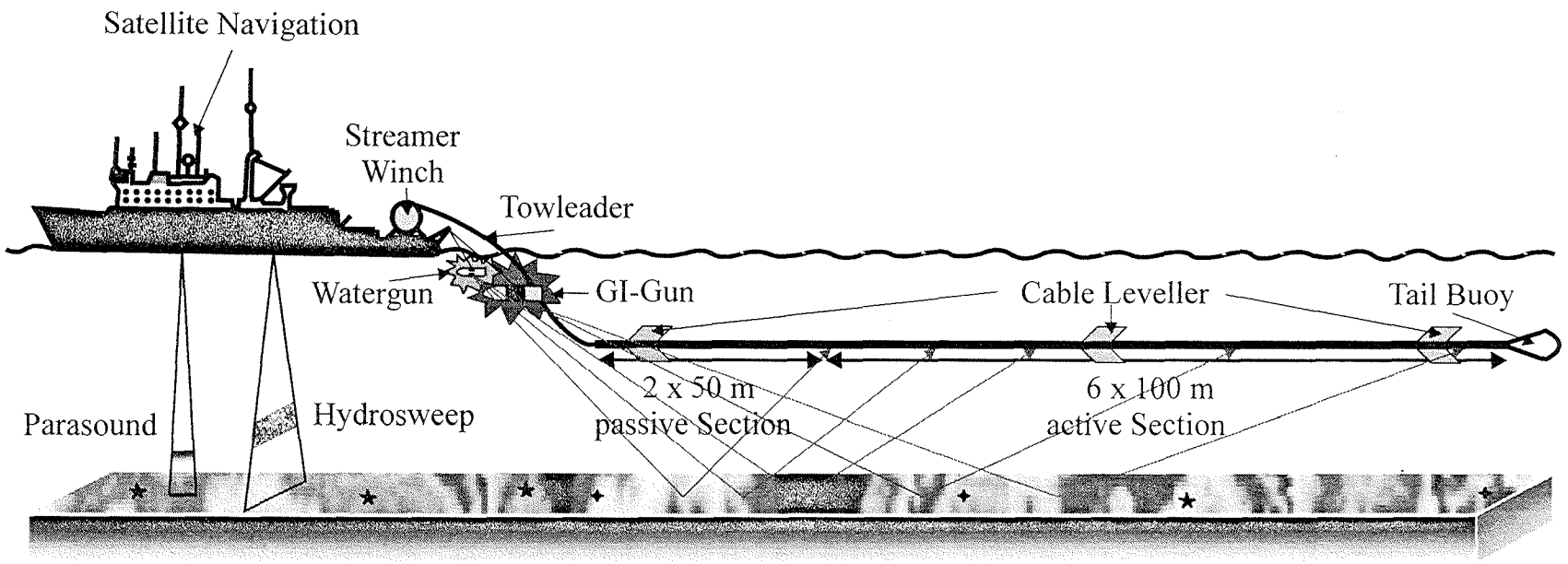

Fig. 2. Hydroacoustic and seismic systems on board of RV Sonne.

3. *Narrative of the Cruise*

The charter period of R/V SONNE started in Cochin on October, 17th, just when Queen Elizabeth visited Southern India and Cochin. This caused some confusion and delay, which, however, did not affect the logistics. All participants as well as all pieces of air and sea freight arrived before departure, partially due to the intensive support by the local agency. The cruise started in time on October, 18th, at 3 pm.

The transit to the working area passed the island of Sri Lanka, heading to position 7°40'N/85°12'E outside of the 200 nm zone of Sri Lanka. Underway the equipment was set up and streamer, guns and instruments were tested just before arrival. After the successful test a first detailed multichannel seismic and echosounder survey of 4 days was started around 8° northern latitude. A long E-W transect to study the overall structural and seismic characteristics was combined with a net of seismic lines in the vicinity of DSDP Site 218 and the nearby active channel. The penetration of the seismic energy was with 1500 m for the GI Gun sufficiently high to look far back in geologic time and to cover the length of the drill hole. The data quality was extremely high due to optimum weather conditions.

At the end of the transect (8°N/89°30E) profiling was continued with the Parasound and Hydrosweep systems to (10°42N/83°55E), which revealed interesting data about the evolution of terraces within broad channels.

The second week started with another long seismic line across the Bengal Fan from 10°42N/83°55E to 11°06N/88°40E. It was evident that the number of older, filled channels had increased towards the North. Based on the echosounder data several channels could be identified and correlated which had been observed during R/V SONNE Cruise SO 93. Some of the channels seem to run parallel to the slope indicating an extreme meandering in combination with large lateral offsets, which makes the correlation of channels downslope more difficult than expected.

At the end of the line, on which seismic data were recorded continuously for 2.5 days, a detailled survey focussed on the evolution of terraces which were observed within a broad valley during the SO 93 cruise. The objective was to understand the builtup sequence in time of these terraces in relation to sea level changes, the meandering process and the associated remobilisation of sediment and the climatically-driven variation of sediment input. A preliminary evaluation indicated that channel jumping as part of the meandering process is responsible for the observed relicts of internal levees and channel fills. Acoustically transparent zones were investigated with different source frequencies, which revealed their likely nature as interference patterns of highly laminated turbiditic sequences.

From previous work it was known that the life time of channel levee systems in the Bengal Fan seemed to be limited to some thousand years only. During the subsequent survey in the second half of the second week under again optimum weather conditions we identified a depositional lobe with numerous small channels which most likely evolved downslope during most recent depositional events, possibly inhibiting transport of sediment into the distal fan.

In the third week another 3-day transect across the fan was measured at 14° northern latitude, which revealed the increasing complexity compared to the survey areas further south and which served as a reference line to image the stacking pattern of channel levee systems through time. Detailled seismic surveys were planned during the third and fourth week to understand the responsible processes. A large scale survey at 14°40'N was conducted during the rest of the third week to study the downslope variability of the active channel within channels, levees, internal terraces and meander geometry. Fast destruction and fill of underlying channels was observed.

Although a strong taifun wind system was approaching the Bay of Bengal, the work was not considerably affected and data quality could be maintained at a high level.

The northernmost working area at 16°30'N / 87°30'E was one of the most interesting and at the same time most complex parts of the Bengal Fan to be

investigated during the cruise. Several days of seismic and echosounder surveying were dedicated to collect data around the active channel. A 10 km wide channel seemed to be filled successively by internal levees and terraces. The new data should serve to reconstruct phases of sedimentation, channel jumping, narrowing and meandering. The complex nature required a narrow distance of profiles down to 1 km in conjunction with a three times higher shot rates over an area of 40 km x 50 km.

The data revealed a dynamic environment undergoing significant changes also in the Holocene. Further processing of the different data sets and their integration will be required to understand the spatial and temporal evolution in the area.

A final seismic line was recorded on departure of the last detailed survey area. The data recording was stopped on November, 14th at 11 pm, when we approached the 200 nm zone of Bangladesh. Chittagong was reached on November, 16th, at 8 am.

4. *Methods and Instruments*

4.1 PARASOUND

The PARASOUND system works both as a low-frequency sediment echosounder and as high-frequency narrow beam sounder to determine the water depth. It makes use of the parametric effect, which produces additional frequencies through nonlinear acoustic interaction of finite amplitude waves. If two sound waves of similar frequencies (here 18 kHz and e.g. 22 kHz) are emitted simultaneously, a signal of the difference frequency (e.g. 4 kHz) is generated for sufficiently high primary amplitudes. The new component is traveling within the emission cone of the original high frequency waves, which are limited to an angle of only 4° for the equipment used. Therefore, the footprint size of 7% of the water depth is much smaller than for conventional systems and both vertical and lateral resolution are significantly improved.

The PARASOUND system is permanently installed on the ship. The hull-mounted transducer array has 128 elements on an area of ~1 m^2. It requires up to 70 kW of electric power due to the low degree of efficiency of the parametric effect. In 2 electronic cabinets, beam forming, signal generation and the separation of primary (18, 22 kHz) and secondary frequencies (4 kHz) is carried out. With the third electronic cabinet in the echosounder control room the system is operated on a 24 hour watch schedule.

Since the two-way travel time in the deep sea is long compared to the length of the reception window of up to 266 ms, the PARASOUND System sends out a burst of pulses at 400 ms intervals, until the first echo returns. The coverage of this discontinuous mode depends on the water depth and produces non-equidistant shot distances between bursts. On average, one seismogram is recorded about every second providing a spatial resolution on the order of a few meters on seismic profiles at 4.9 knots.

The main tasks of the operators are system and quality control and the adjustment of the start of the reception window. Because of the limited

penetration of the echosounder signal into the sediment, only a short window close to the sea floor is recorded.

Beyond the analog recording features with the b/w DESO 25 device, the PARASOUND System was equipped with the digital data acquisition system PARADIGMA, which was developed at the University of Bremen (Spieß, 1993). The data were stored directly on 6250 bpi, 1/2" magnetic tapes using the standard, industry-compatible SEGY-format. The 486-processor based PC allows the buffering, transfer and storage of the digital seismograms at very high repetition rates. From the emitted series of pulses usually every second pulse could be digitized and stored, resulting in recording intervals of 800 ms within a pulse sequence. The seismograms were sampled at a frequency of 40 kHz, with a typical registration length of 266 ms for a depth window of ~200 m. The source signal was a band limited, 2-6 kHz sinusoidal wavelet of 4 kHz dominant frequency with a duration of 1 periods (~250 μs total length).

Already during the acquisition of the data an online processing was carried out. For all profiles Parasound sections were plotted with a vertical scale of several hundred meters. Most of the changes in window depth could thereby be eliminated. From these plots a first impression of variations in sea floor morphology, sediment coverage and sedimentation patterns along the ships track could be gained. To improve the signal-to-noise ratio, the echogram sections were filtered with a wide band pass filter. In addition the data were normalized to a constant value much smaller than the average maximum amplitude, to amplify in particular deeper and weaker reflections.

To study the influence of frequency and length of the source signal on the reflection pattern, these parameters were systematically varied at sites, where gravity or piston cores were recovered ('source signal test'). The frequency of the source signal was changed in 0.5 kHz steps over the available frequency range from 2.5 to 5.5 kHz, while the pulse length was set to 1, 2, and 4 sinus periods. The setting was kept for a time span of 2 minutes to enable later signal stacking and an evaluation of the variability of seismograms from the same location. In order to quantify interference phenomena, seismograms recorded

with different frequencies will be studied in more detailed, shore based analyses in comparison with physical property logs from the cores.

During the entire cruise the combined PARASOUND/PARADIGMA worked without significant problems. From time to time the tape drives had to be cleaned. Owing to some problems with the ship's own data distribution network no navigation data are written in the header of the PARASOUND data during some time intervals.

4.2 HYDROSWEEP

The multibeam echosounder HYDROSWEEP on R/V SONNE was routinely used during the cruise and serviced by the system operator and the electronics engineers. During a 24 hour watch the scientific crew operated continuously both the HYDROSWEEP and the PARASOUND echosounder systems in parallel. The HYDROSWEEP System worked without major technical problems. The multi-beam sounder provided a complete coverage of the sea floor topography with a swath width of twice the water depth. The data quality was generally good with data losses at higher speeds and due to high sea states.

4.3 Very High-Resolution Multichannel Reflection Seismics

The particular components and their interdependencies of the used entire very high-resolution multichannel reflection seismic equipment are presented in Figure 3 and are described below.

Trigger Unit

The custom trigger unit controls seismic sources, seismograph, MultiTrak Controller, online-plotter and digital scope (near-field hydrophones). The primary building blocks are an IBM compatible PC, an amplifier unit and a gun amplifier unit. The PC runs a custom software, which controls a real-time controller interface card (SORCUS) with 16 I/O channels, synchronized by an

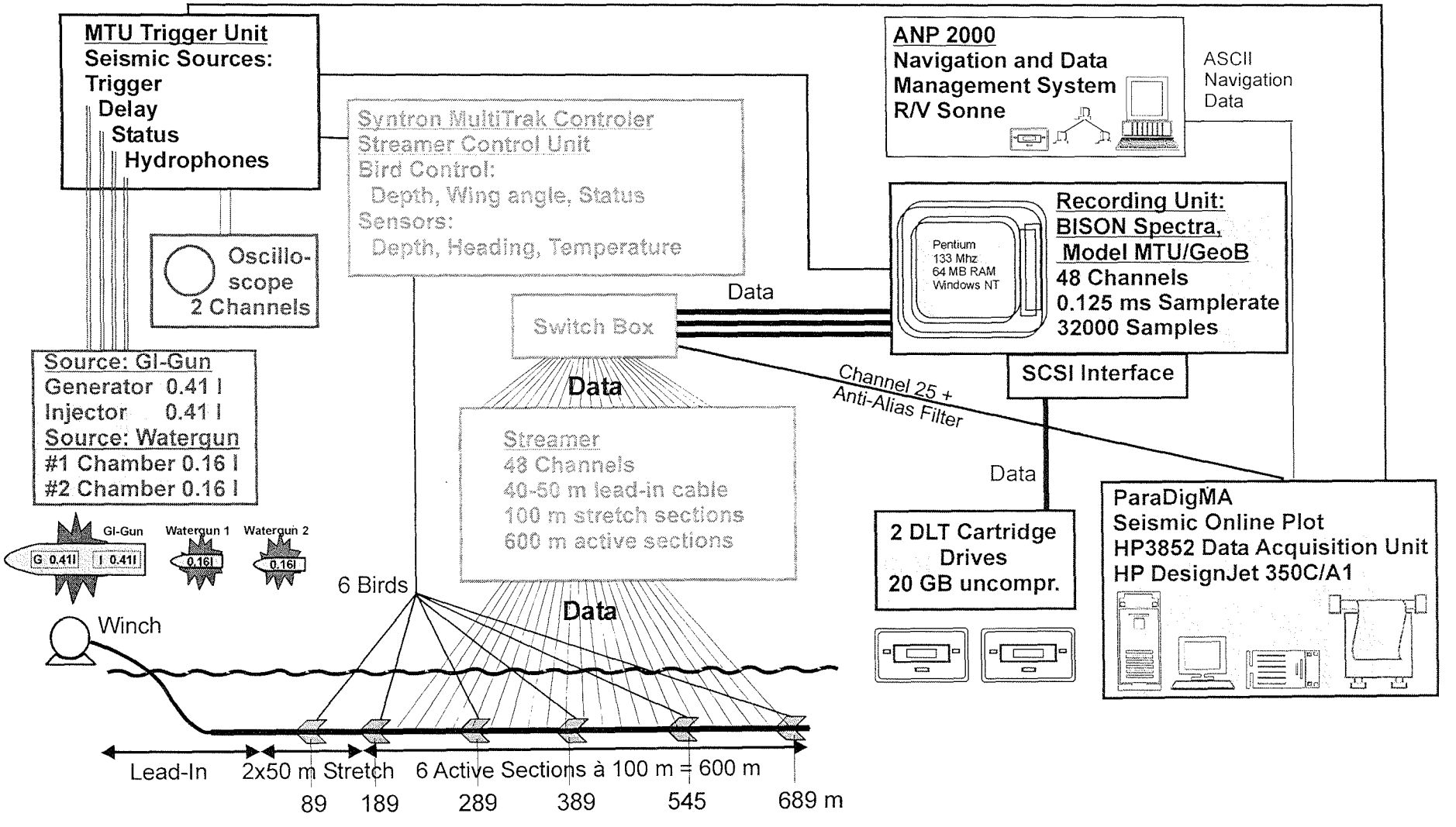

Fig. 3. Multichannel seismic instrumentation used during R/V Sonne Cruise SO 125.

internal clock. The program user interface enables the operator to change trigger times of each device online. The amplifier unit converts the controller output to TTL levels, which have to be negative for most of the devices. The gun amplifier unit was placed in the pulser station to avoid electronic noise in the seismic lab. It generates the required 60V/8 Amp. trigger level for the magnetic valves of the individual seismic sources.

Seismic sources and compressor

During seismic surveying two different seismic sources, a GI-Gun and two waterguns, were triggered in an alternating mode at a time interval of 13 s between the sources. On line GeoB 97-020 to GeoB 97-027 two waterguns were simultaneously triggered, a single watergun was shot on the subsequent lines. Owing to an average ship speed of 4.9 kn a shot distance of appx. 33 m between different sources and appx. 66 m between the same source were obtained. Both sources were operated with an air pressure of 145 bar. Each source type was shot more than 67000 times without failure, broken welds at the air exhausting pipes of the waterguns had no impact on the source signature. The handling of both sources during the measurements is shown in Fig. 4. Ship velocity during deployment and retrieval was 3 kn and 2 kn, respectively. A self constructed gun amplifier unit, located in the pulser station to avoid electronic noise in the seismic lab, generated the required 60V/8 Amp. trigger level for the magnetic valves of the individual seismic sources.

High-pressure air for gun operation was provided by a Junkers compressor that is installed on board R/V SONNE and maintained by the ship's crew. The compressors were operated according to the requirements of the chosen gun volumes.

The volume of the GI-Gun (Generator-Injector gun; Sodera) was reduced to 2x 0.41 l. It was towed starboard by a wire from the side crane 26 m behind the ship stern with a lateral offset of 6.3 m on the left hand side of the streamer. The towing wire was connected to a bow with the GI-Gun hanging on two

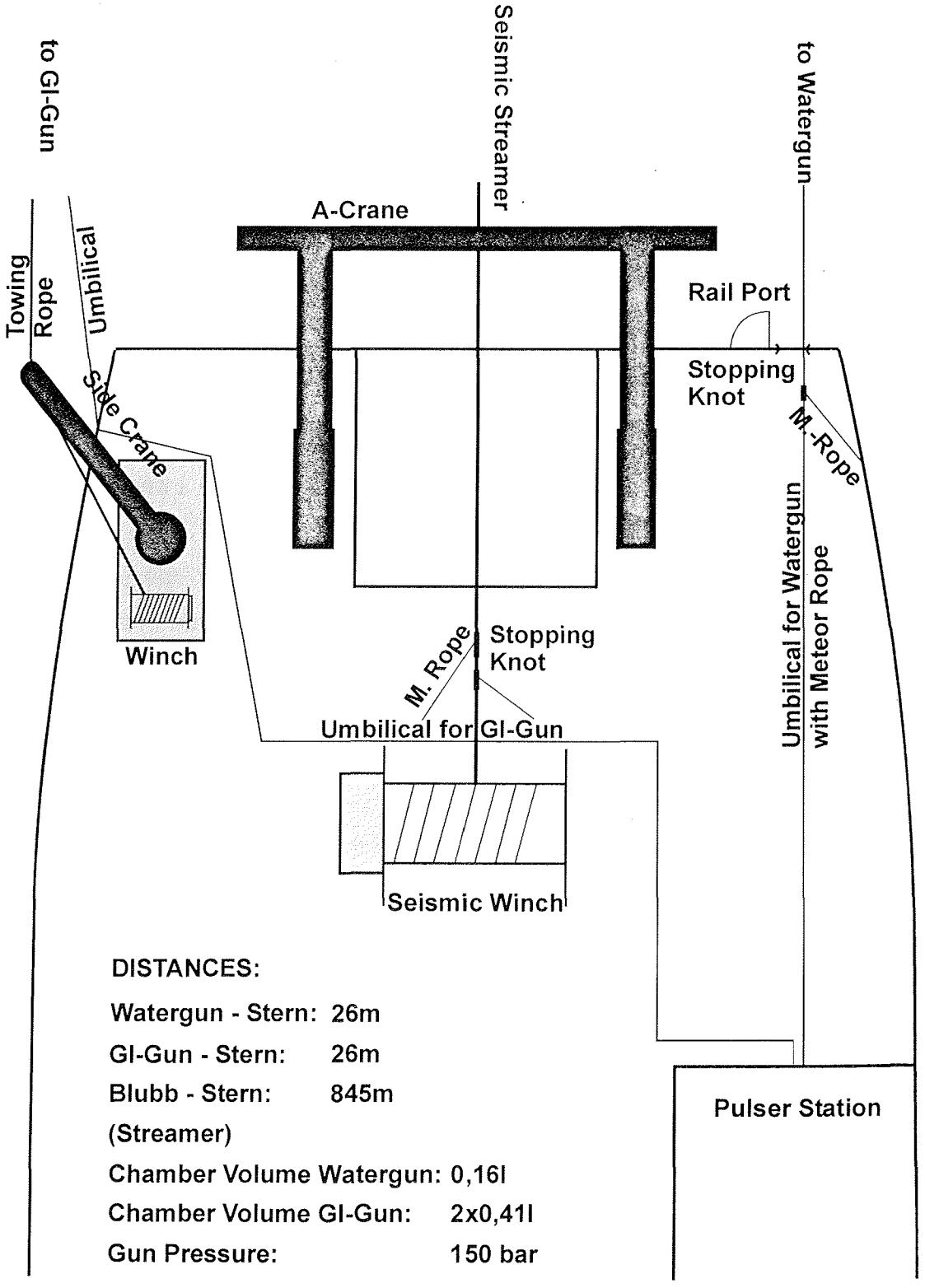

Fig. 4. Working deck during SO125.

chains 56 cm beneath (Fig. 5). An elongated buoy , which stabilized the gun in a horizontal position at a water depth of ~1.4 m, was connected to the bow by two rope loops. The Injector was triggered with a delay of 31 ms with respect to the Generator signal, which basically eliminated the bubble signal.

The second source type was a S15 watergun (Sodera) with a volume of 0.16 l. Two waterguns, connected with a Meteor rope in a distance of 1 m, were also towed by a Meteor rope, that was fixed to the umbilicals of the waterguns, 26 m behind the ship's stern 4.4 m port side of the streamer. A steel frame held the watergun in a tight position parallel to the elongated buoy in a depth of approximately 0.5 m (Fig. 5).

Frequency characteristics of both sources, measured under optimum conditions, are shown in Figures 6 and 7. During operations the seismic watch keeper in the seismic lab checked the near field source signature of both guns with a digital scope.

Streamer

The multichannel seismic streamer (SYNTRON) consisted of a tow-lead, two stretch sections of 50 m and six active sections of 100 m length each. A 100 m long Meteor rope with a buoy at the end was connected to the tail swivel. A 30 m long deck cable connected the streamer to the recording system. The winch location on the working deck is shown in Fig. 4. During operations the streamer (tow lead) was fixed with two Meteor ropes. The tow lead was paid out ~55 m, the distance from ship to stretch section was 45 m.

Active sections are subdivided in 16 hydrophone groups (Fig. 8). Each of the 6.25m long hydrophone groups is again subdivided into 5 subgroups of different length. One of the subgroups is a high-resolution hydrophone with pre-amplifier. A programming module distributes the subgroups of 4 hydrophone groups, i.e. a total of 20 groups, to 5 channels. As illustrated in Figure 8, every second 6.25 m hydrophone subgroup was used.

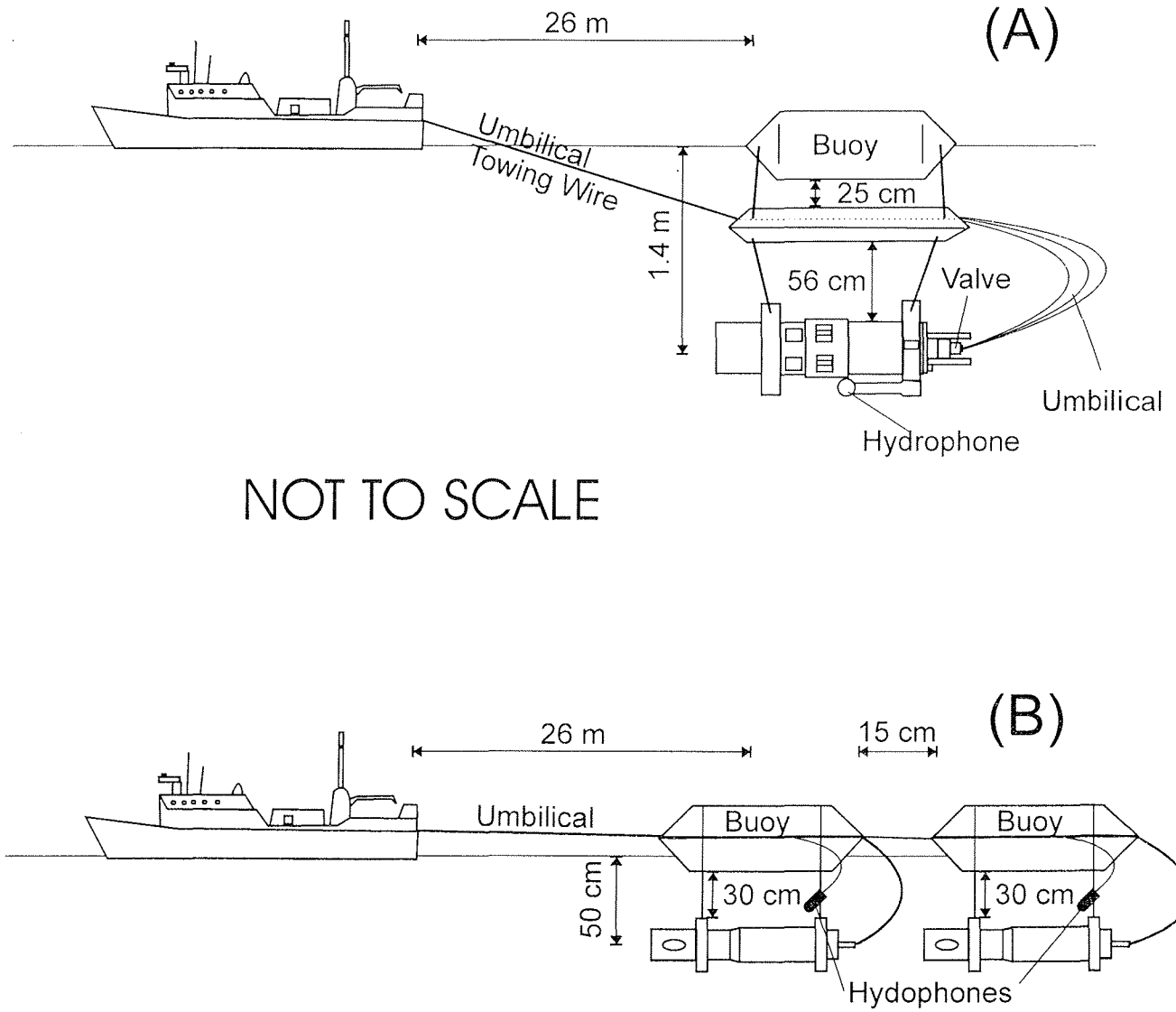

Fig. 5. Towing gear and arrangement for GI-Gun (A) and watergun (B).

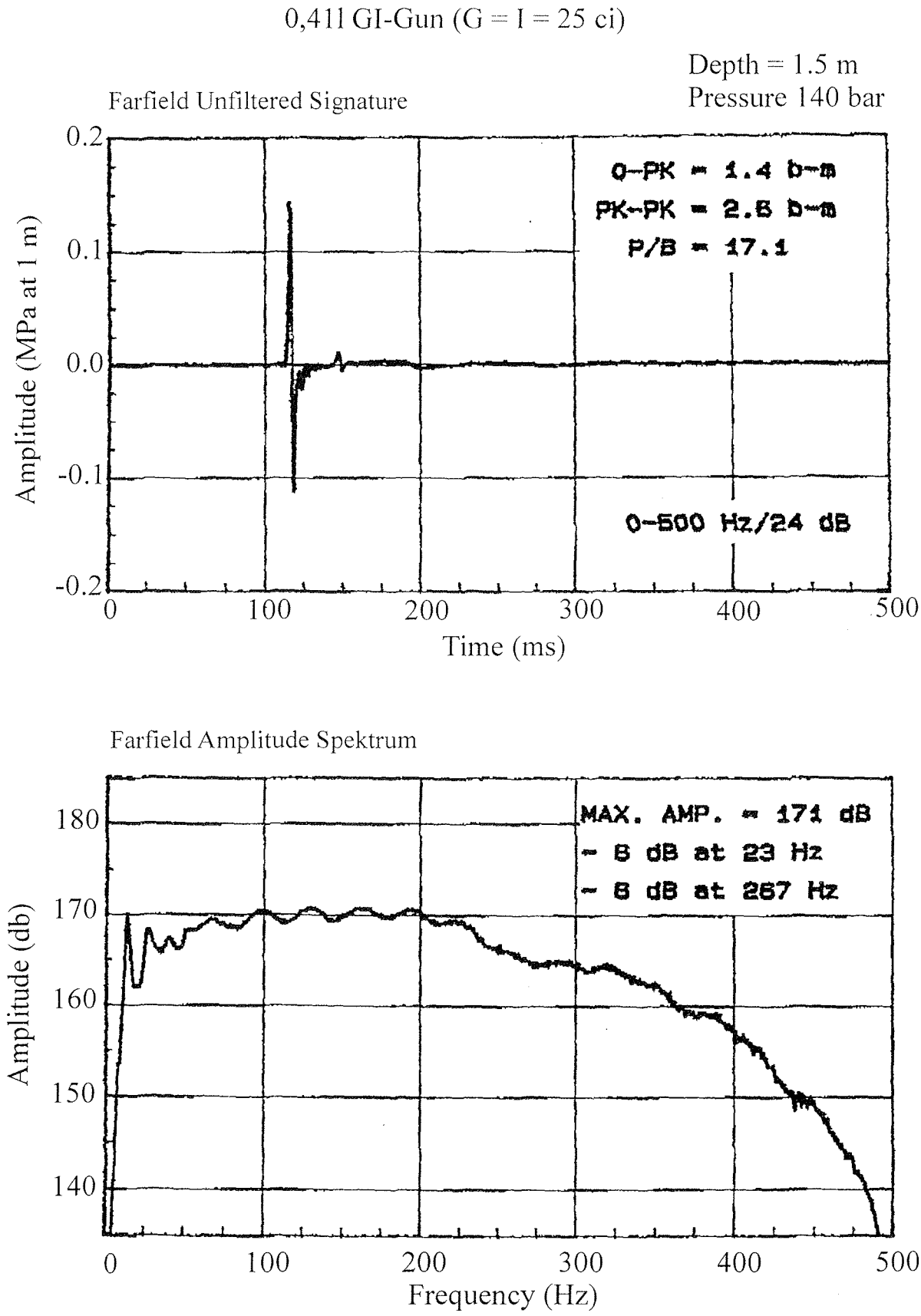

Fig. 6. Signal and spectrum of GI-Gun und optimum conditions.

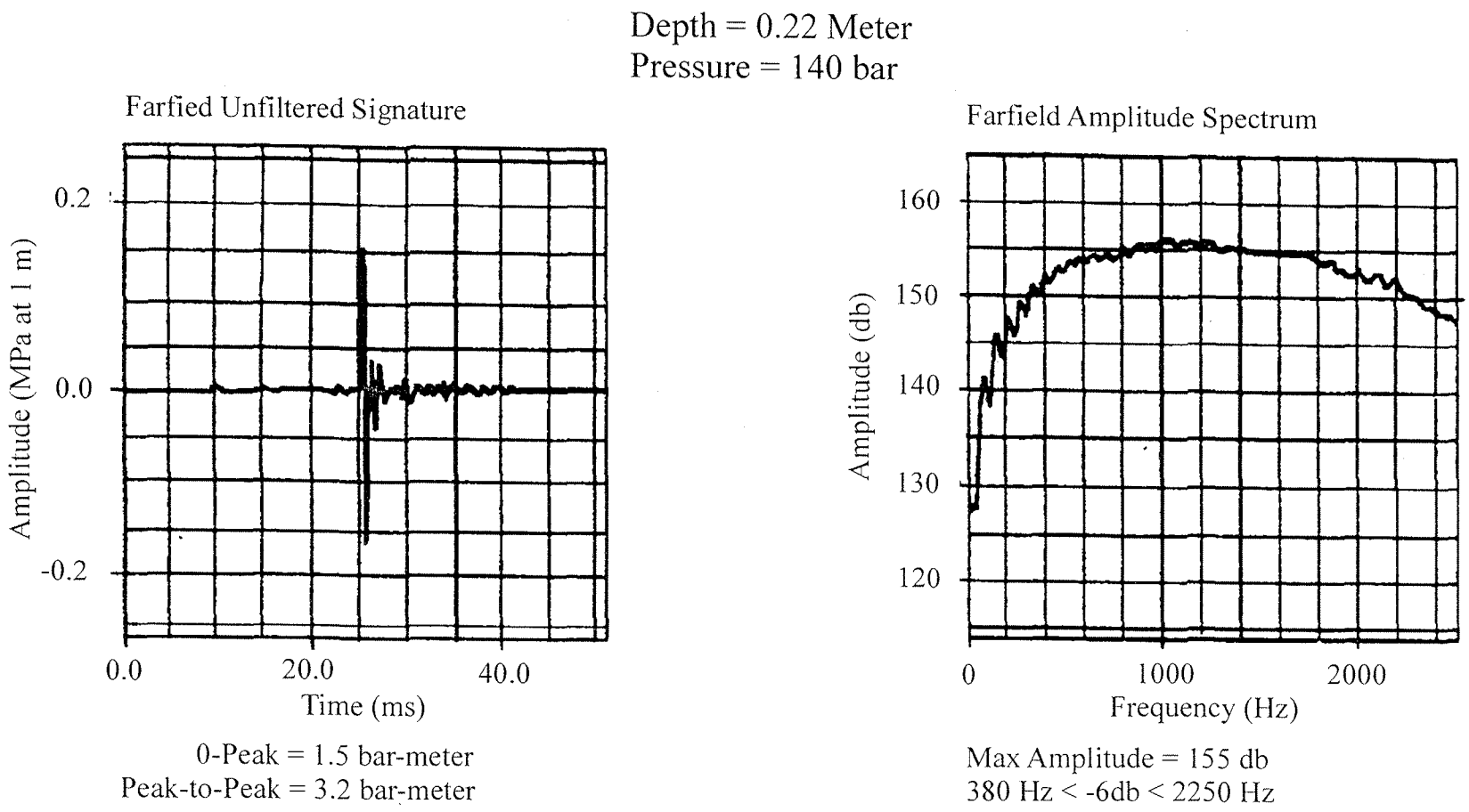

Fig. 7. Signal and spectrum of watergun under optimum conditions.

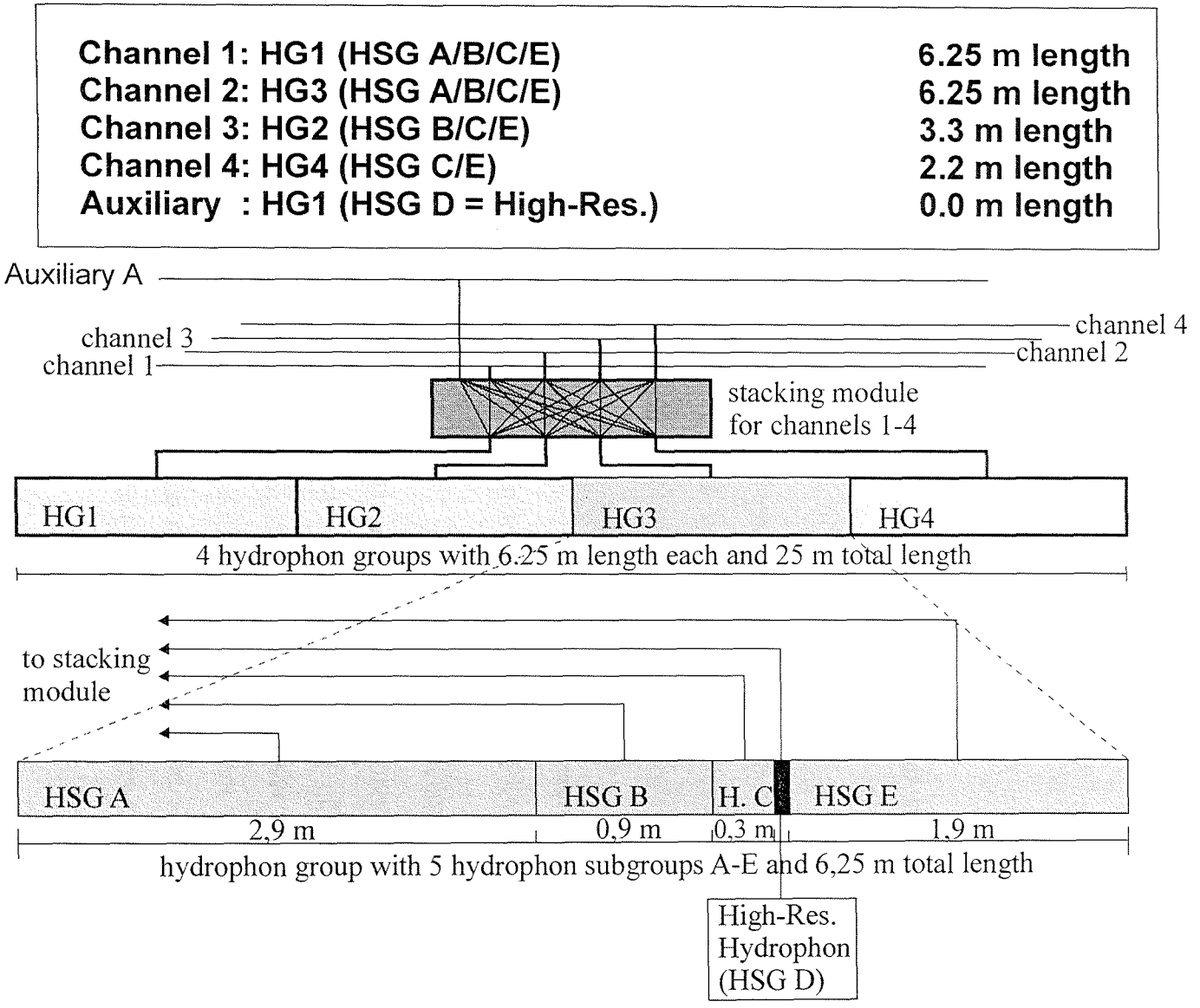

Fig. 8. Multichannel streamer design used during SO125 cruise. The hydrophone group combination repeats after every 5 channels..

Hydrophone Group No.	Midpoint Distance
1	9.3 m
2	21.8 m
3	33.3 m
4	43.8 m
5	59.3 m
6	71.8 m
7	83.3 m
8	96.8 m

Tab. 1: Midpoint distance between hydrophone groups and start of each active section.

These cover even channel numbers from 2 to 96 on the streamer cable and were connected to Bison channels 1 to 48. Single hydrophones (streamer channels 97 to 108) were not recorded due to the poor signal/noise ratio.

Ship's speed during deployment and retrieval was 3 kn and 2 kn, respectively. Deployment and retrieval lasted around 45 minutes including installation of the six Remote Bird Units (RUs; see below).

Multitrak Bird Controller

In operation 6 MultiTrak Remote Units (RU) were attached to the streamer. The position of RUs is listed in Tab. 2. Each RU includes a depth and a heading sensor as well as adjustable wings. The RUs are controlled by the MultiTrak controller in the seismic lab. Controller and RUs communicate via communication coils nested within the streamer. A twisted pair wire within the deck cable connects controller and coils. One wire had to be grounded to avoid communication errors.

RU (No.)	Position	Distance to Tow-Lead
1	End of Stretch Section No. 2	89 m
2	End of Active Section No. 1	189 m
3	End of Active Section No. 2	289 m
4	End of Active Section No. 3	389 m
5	Middle of Active Section No. 5	545 m
6	End of Active Section No. 6	689 m

Tab. 2: RU positions along seismic streamer.

Each shot trigger started the scan of water depth and heading (delay 0.5 s, duration 0.2 s). The current location of the streamer as depth or heading profile can be displayed on a monitor. All parameters are digitally stored on the controller PC, together with shot number, date and time.

There are two ways of controlling the streamer depth. The most common way is to send an operating depth range to the RUs, which was in most cases 2 - 3 m. The RUs try to force the streamer to the chosen depth by adjusting the wing angles accordingly. Another option is to set a constant wing angle, which was sometimes advisable for the distal RUs. Depth and wing angle statistics help to set appropriate parameters.

Data acquisition system

The recording unit includes a switch box, a seismograph and a single channel recording unit for online plotting. The switch box connects the streamer via deck cable with the seismograph and allows the assignment and optional stacking of streamer hydrophone subgroups to individual recording channels. The configuration during the cruise remained unchanged and sorts the streamer channels such, that hydrophone groups of the same length are available as a continuous series of channels (Figure 5).

The 48 channel seismograph (BISON) was specially designed for the University of Bremen, which allows a continuous operation mode for very high resolution seismic data. The seismograph allows online data display, online demultiplexing and storing in SEG-Y format. Analog filters were set to 8 Hz (low-cut) and 4000 Hz (high-cut). The sample rate was 0.125 ms for a recording length of 4000 ms. All channels were pre-amplified by a factor of 1000 (60 dB) to keep the incoming signal within the optimum digitizing voltage. The data were stored on 2 DLT4000 cartridge tapes with 20 GByte uncompressed capacity. The recording delay had to be adjusted according to the current water depth.

For immediate quality control and identification of sediment structures, a graphic output of the acquired GI-Gun data was generated with another recording system based on the ParaDigMA system design with a Hewlett Packard HP 3852 Data Acquisition Unit (DAU), a PC and a DesignJet 350 A1 roll paper plotter was used as an online plotting system. Also navigation data were stored using the second channel to the ship's GPS system.

5. *Preliminary Results*

5.1 Sedimentation history at DSDP Leg 22, Site 218, detail study area 'a' (8°N)

The southernmost survey of this cruise was carried out at 8° N (lines GeoB 97-020 - GeoB 97-027). The entire East-West transect crosses DSDP Site 218 (Leg 22), and a detail study was carried out in the vicinity (Fig. 9). Lithology and stratigraphic information from the DSDP cores will be later used to develop a seismostratigraphic framework.

Line GeoB 97-020 is the northernmost line in detail study area 'a' (Fig. 9), which crosses DSDP Site 218. The GI-Gun™ data (Fig. 10) reveal a channel-levee system in the center of the profile, DSDP site 218 is located at the eastern end. The approximate penetration depth of the core (773 m) is indicated using velocity estimates. The thick bars represent approximated depth ranges of four 'sandy pulses', that have been determined from grain size analysis (Shipboard Scientific Party, 1974). These sandy pulse were examined to interpret them in terms of channel shifting or variations of the sediment support due to climatic changes.

An important objective of this cruise was the investigation of meander geometry and internal structures of the internal sedimentary deposits, e.g., to compare to river processes. The reflection pattern of the terrace at the concave part of the meander loop is presented in Figure 11. The reflection pattern like the divergent (Div) reflections from the interior of the terrace allows a deeper insight into the growth patterns of those terraces. We expect a significant increase in lateral resolution after further processing of the raw data.

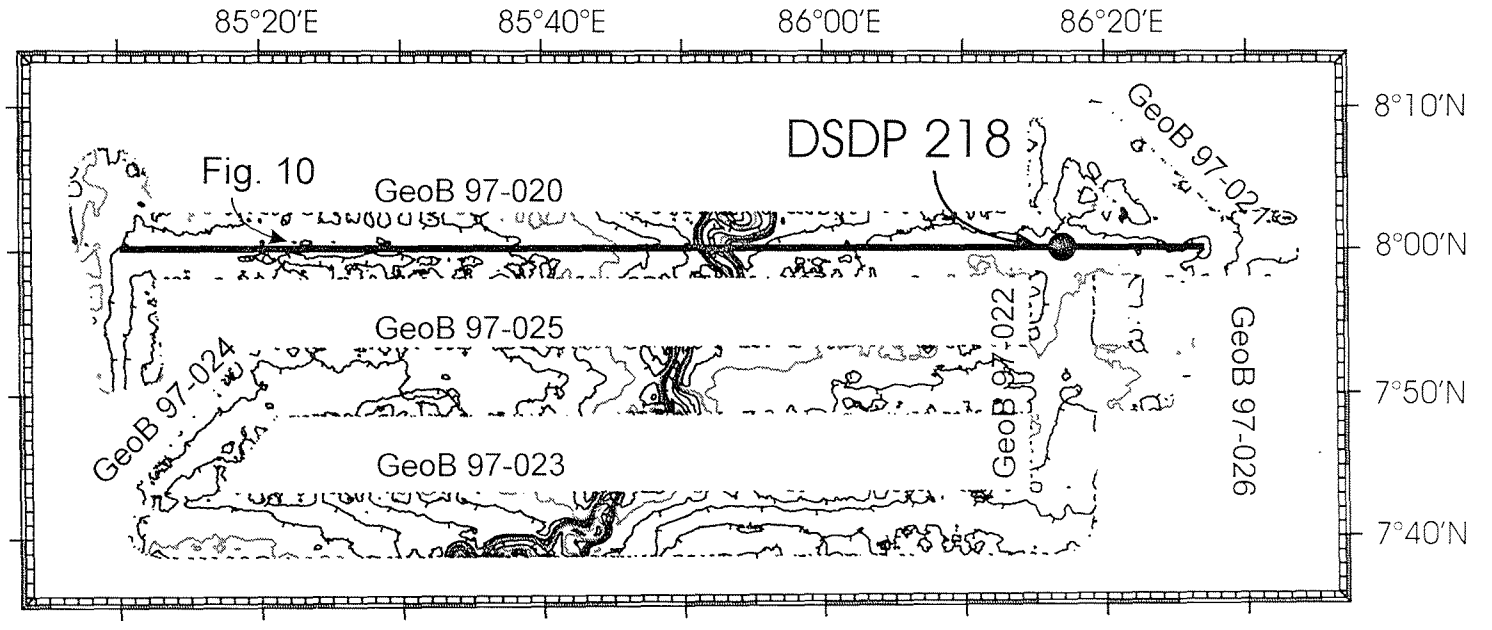

Fig. 9. Detail study 'a' at DSDP Site 22.

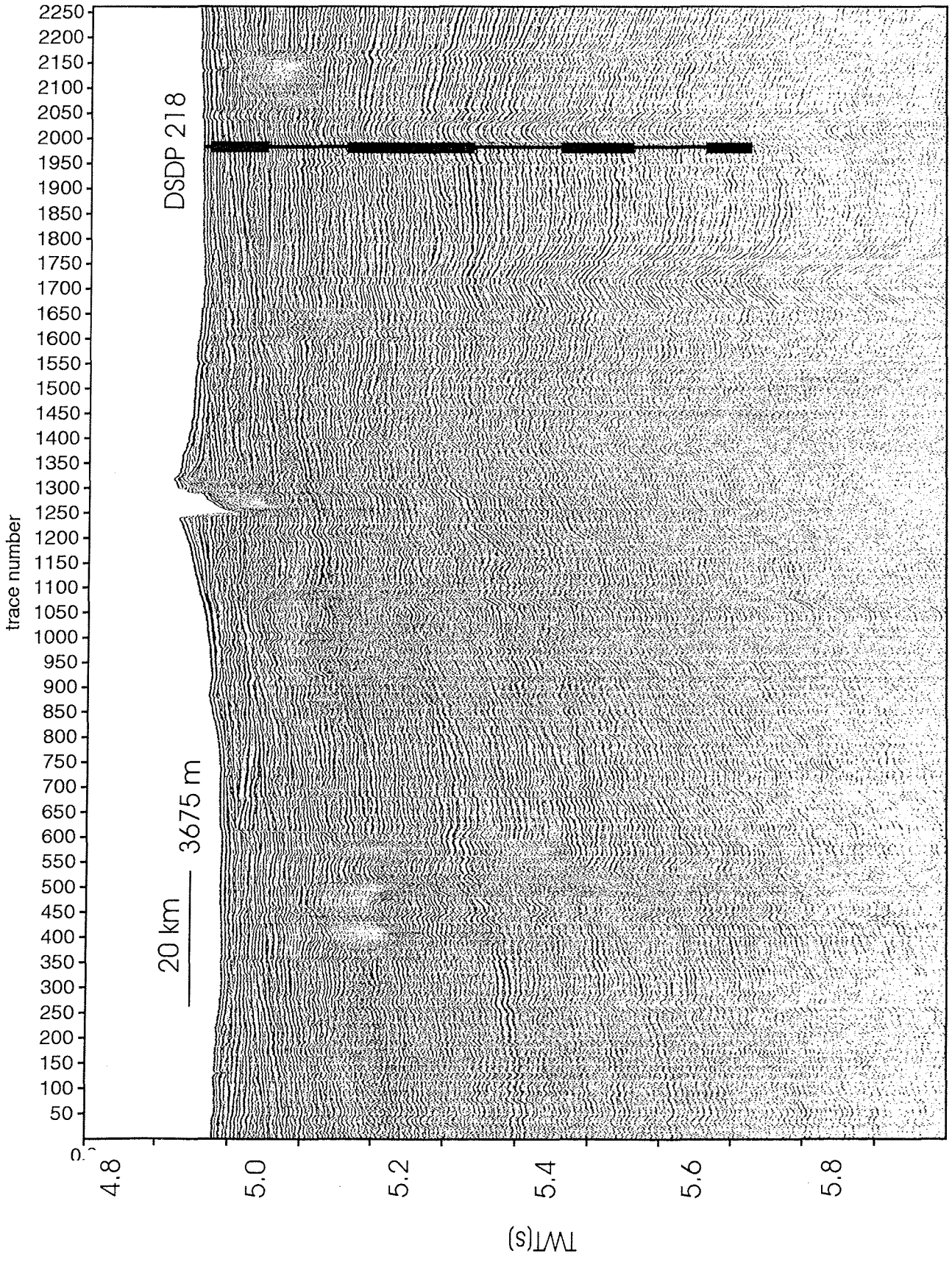

Fig. 10. Line GeoB 97-020 (GI-Gun data) crossing DSDP Site 22 (black bar). The thick segments mark four sandy pulses.

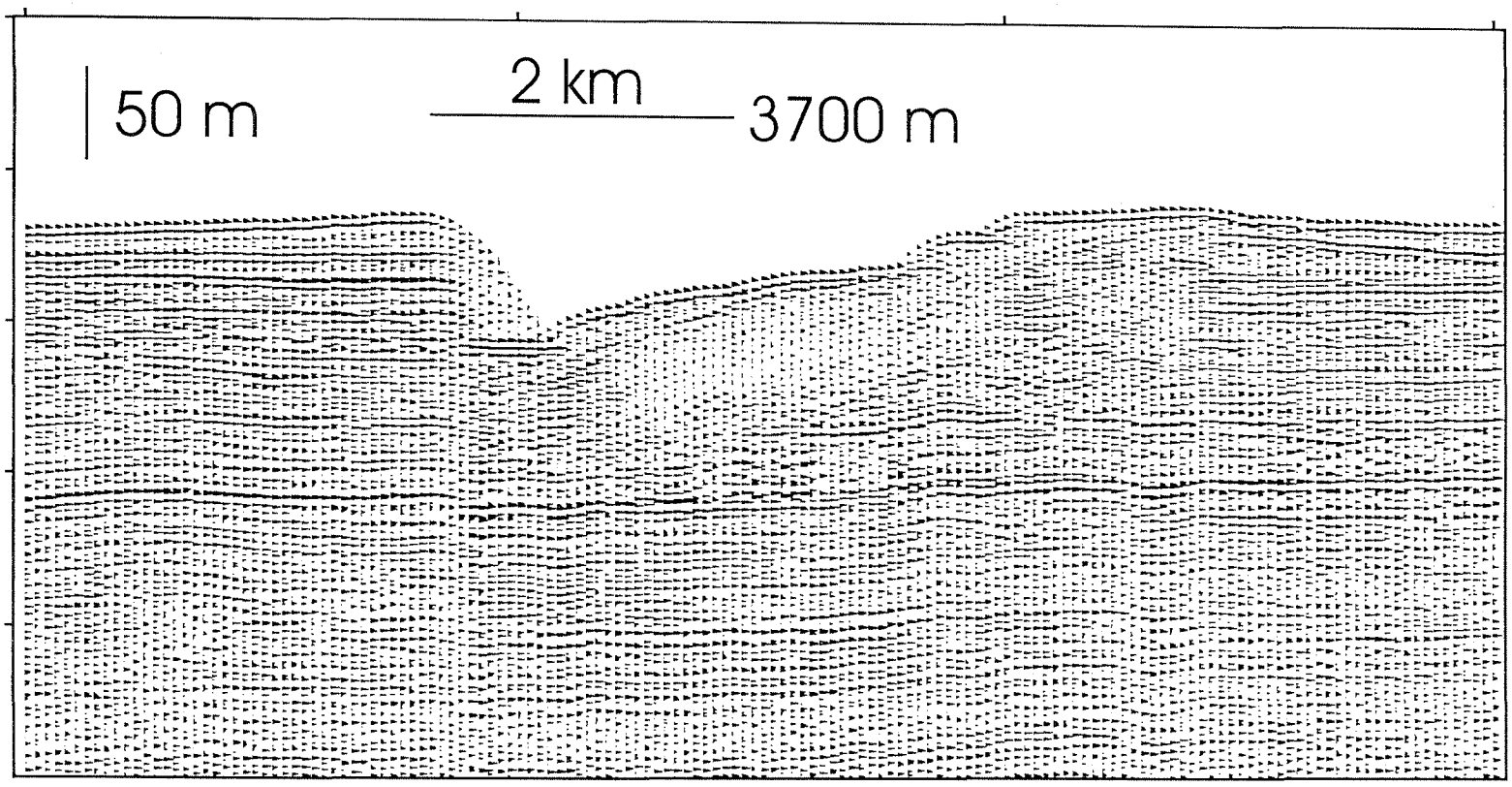

Fig. 11. Part of Figure 10. The data show a typical example for a cross-section of a meandering channel-leve system in the lower fan.

5.2 Detail study area 'c1' (11°10'N)

During R/V SONNE Cruise SO93 a terrace within an abandoned channel levee system, a so called point bar, was studied at 88°25'E, 11°10'N with the hydroacoustic systems (Fig. 12). The same area was revisited during SO125 cruise, this time multi-channel seismic data were also collected. The objective was to investigate the spatial extension and expression of the buried features. Another target was the base of this particular channel-levee system. The Hydrosweep and Parasound data reveal a 9 km wide and 90 m deep, highly meandering channel (Fig. 13). The rounded western edge of the point bar indicates channel jumping from the western to the east. The top of buried features, presumably older levee fragments, break through the top of the point bar. The seismic data (line GeoB 97-030) exhibit high-amplitude / discontinuous reflections at the base of the point bar (Fig. 14). Continuous reflections in-between are not related to the point bar, they support the interpretation of channel jumping.

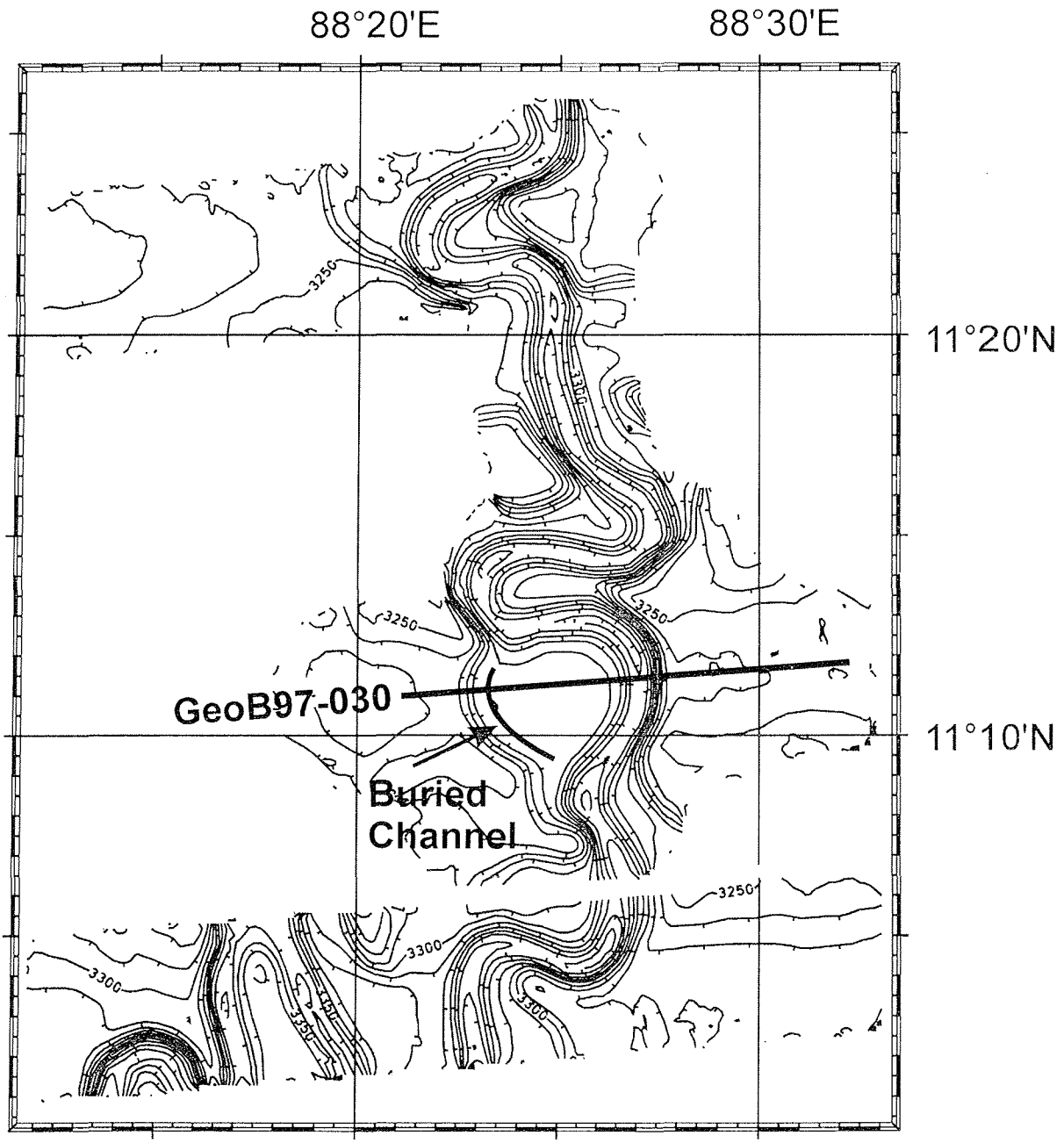

Fig. 12. Preliminary bathymetric map of detail study area 'c1'.

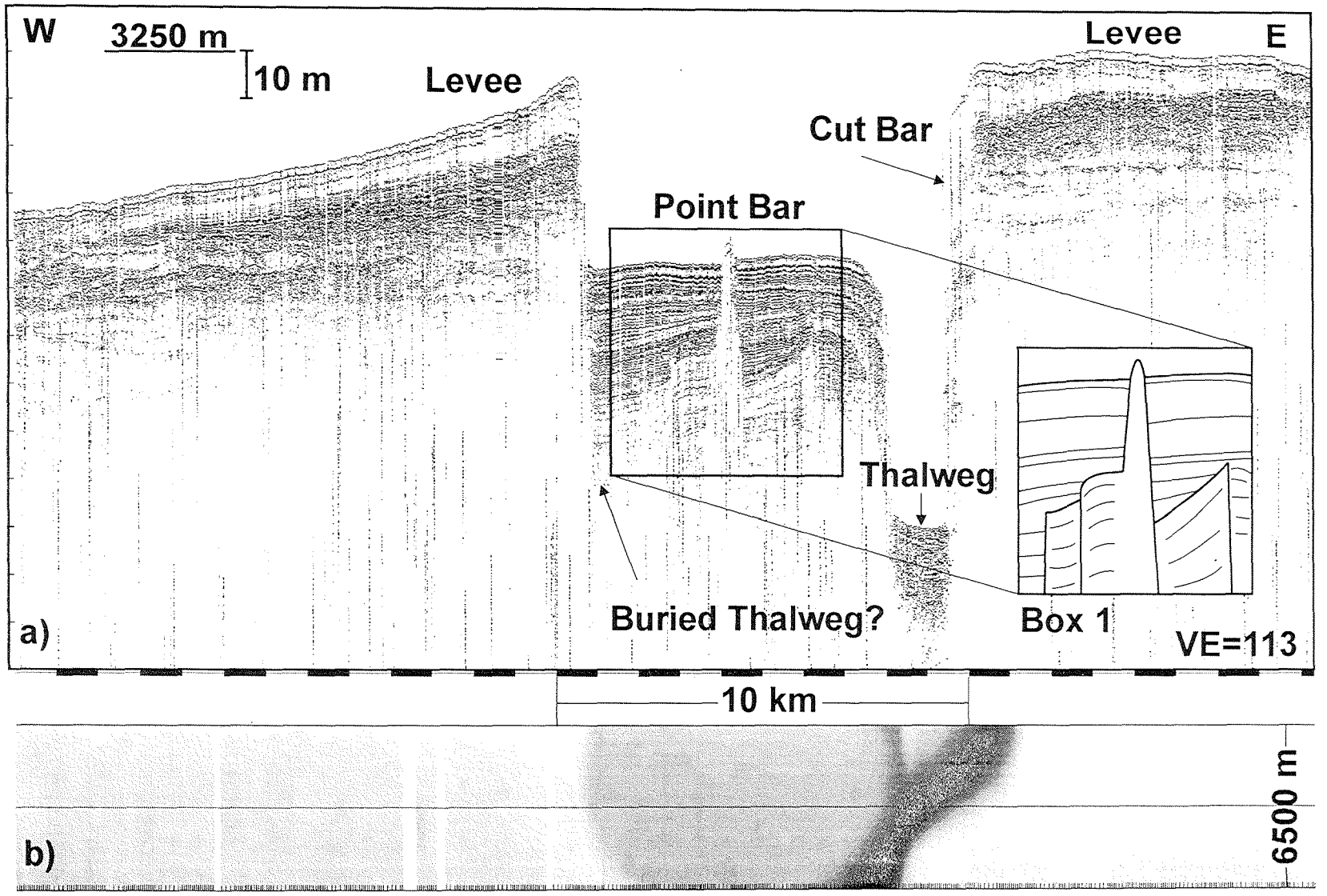

Fig. 13. Parasound and Hydrosweep data from Line GeoB 97-030 at detail study area 'c1'.

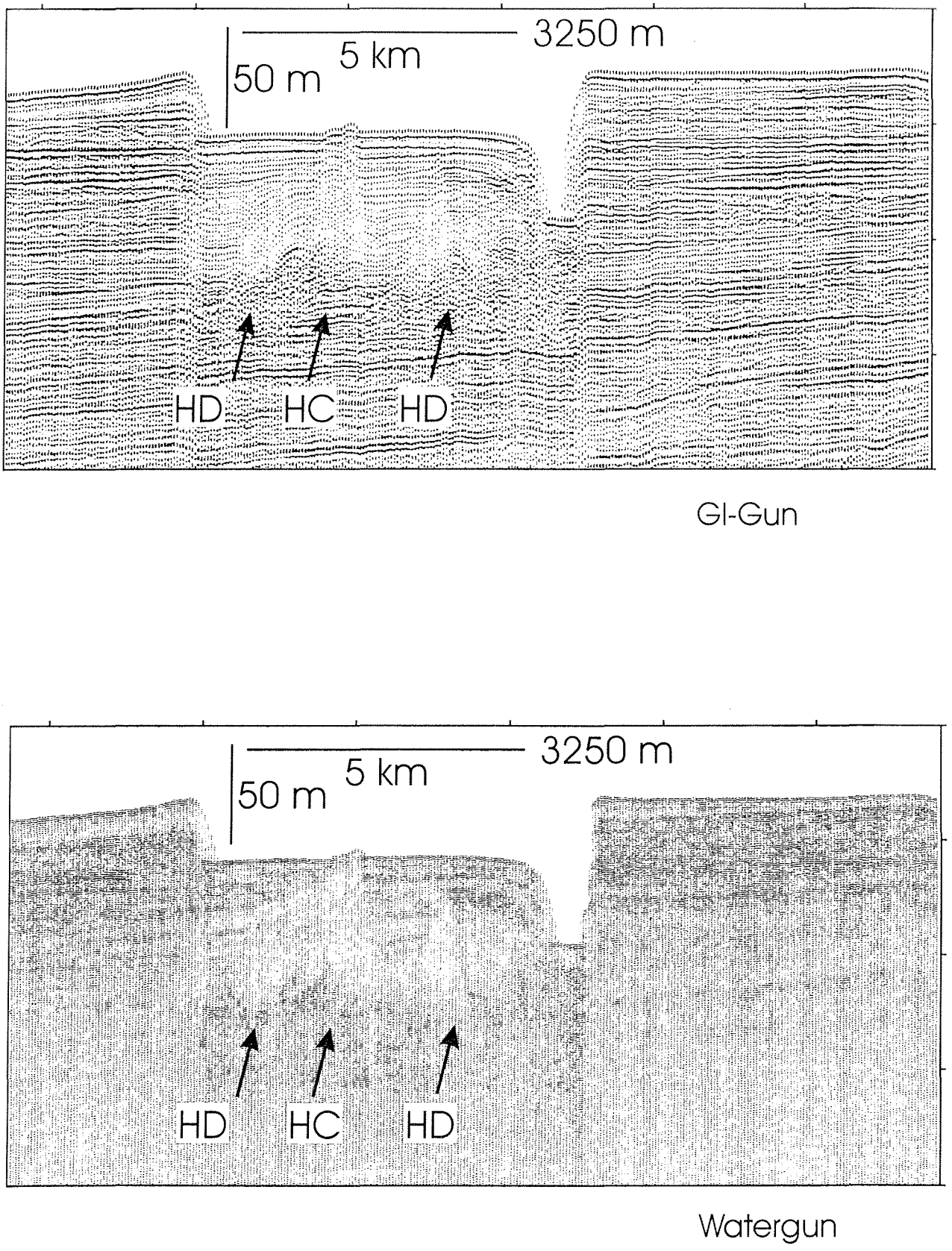

Fig. 14. GI-Gun and watergun data from Line GeoB 97-030, detail study area 'c1'.

5.3 Detail study area 'c2' (11°N-12°N)

The downstream termination of a near surface channel levee system was the main scientific objective for a combined hydroacoustic and seismic detail survey between 11°N and 12°N. The map (Fig. 15) shows the location of two channels, which are confirmed by Hydrosweep data and labeled with 'A' and 'B'. Line GeoB 97-040 (Fig. 16) shows the two channel levee systems at 11°20'N. The stacking pattern clearly proofs that system 'B' is the younger than system 'A'. A point bar at the inner side of a meander loop has developed within channel 'A'. The channel of system 'B' is more than 50 m deep, the width of the entire system is more than 50 km. Approximately 150 km further South at Line GeoB 97-028 the depth of channel 'B' has been reduced to only 10 m, at a width of less than 20 km (Fig. 17). The line crosses system 'A' exactly at the knee of a meander loop in the very West, which causes an apparent channel width of 5 km. This system was crossed a second time 15 km further to the east.

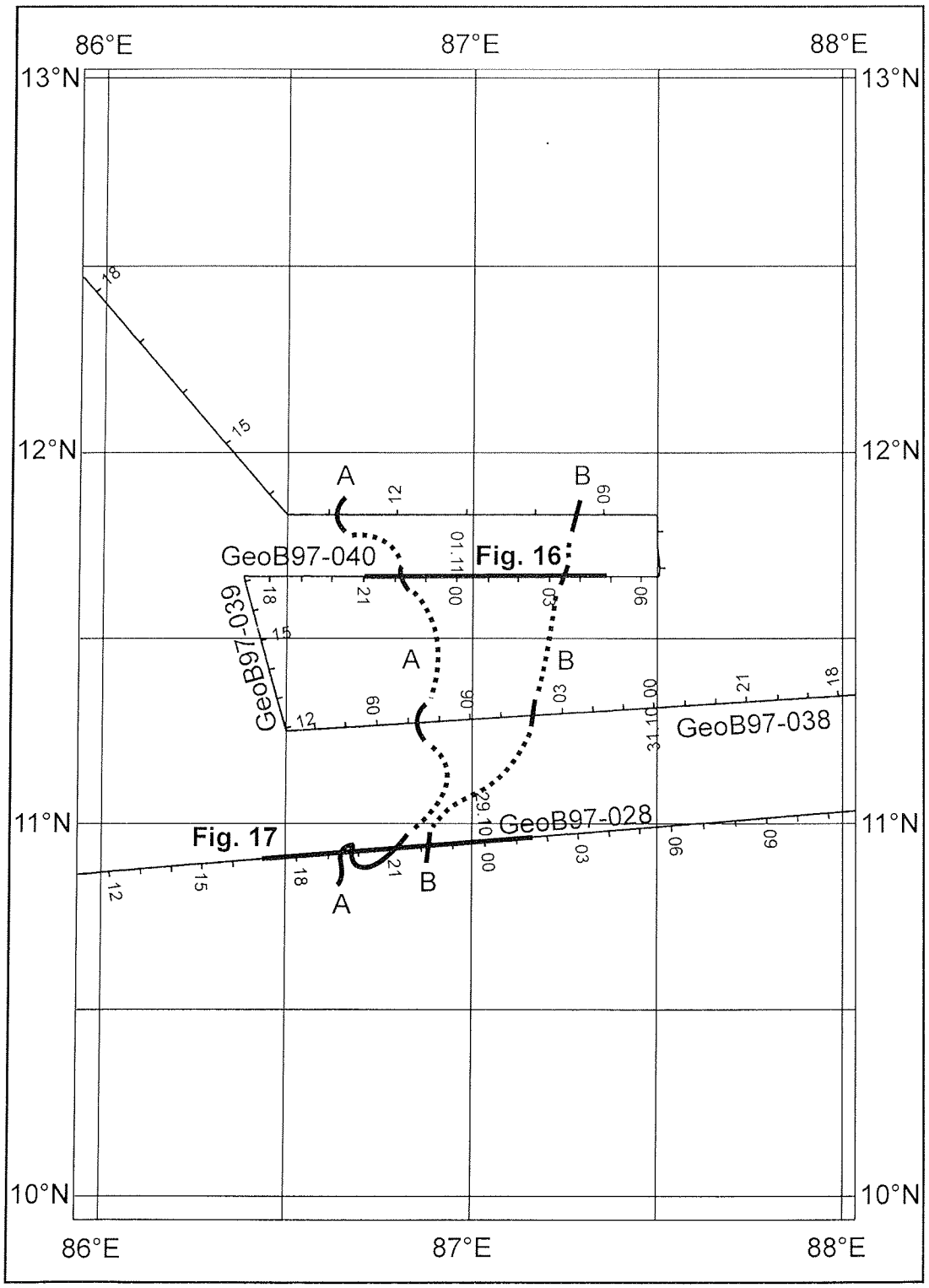

Fig. 15. Map of detail study area 'c2' with interpolated channels (dotted lines).

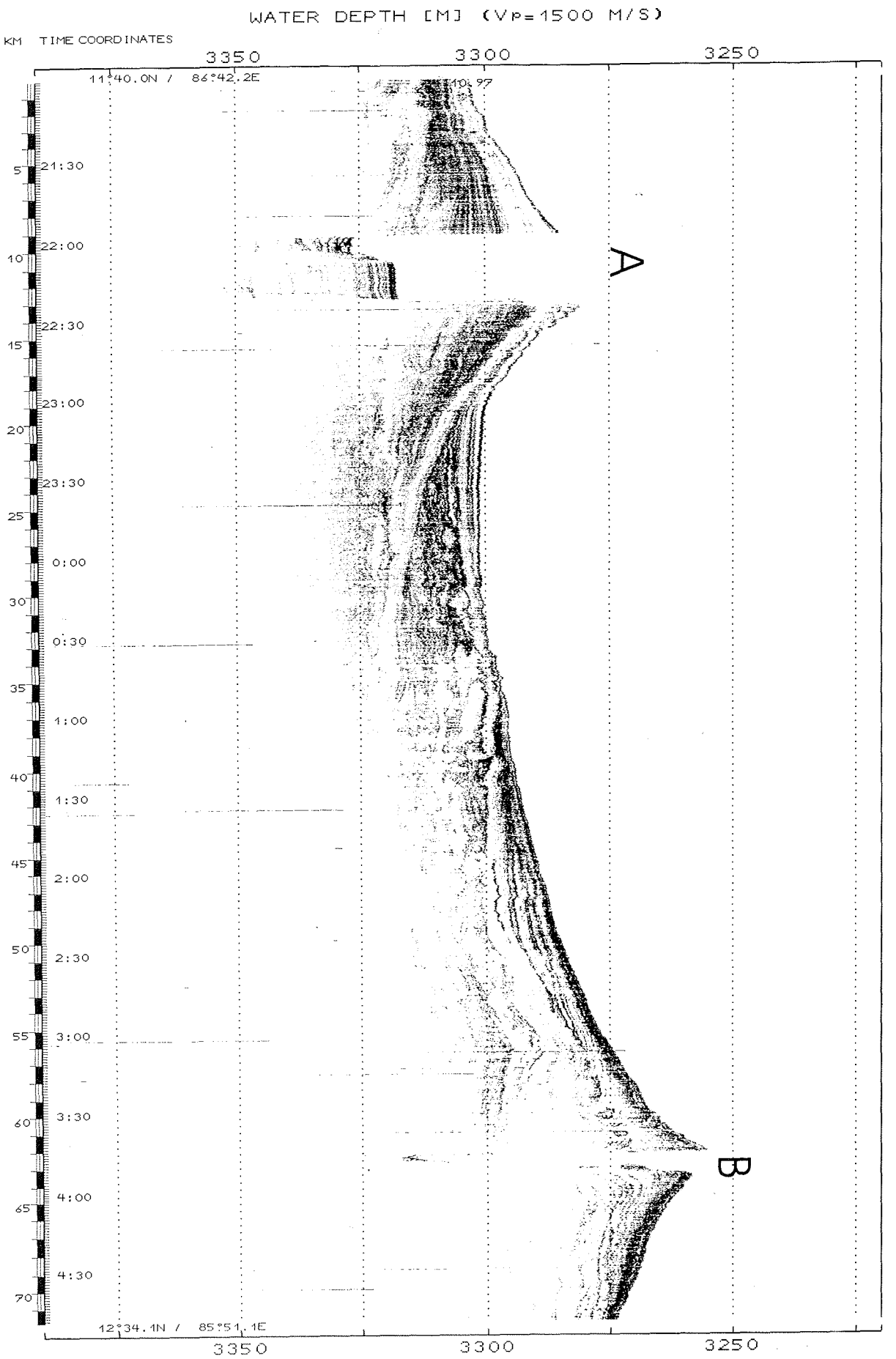

Fig. 16. Parasound section from detail study area 'c2', Line GeoB 97-040.

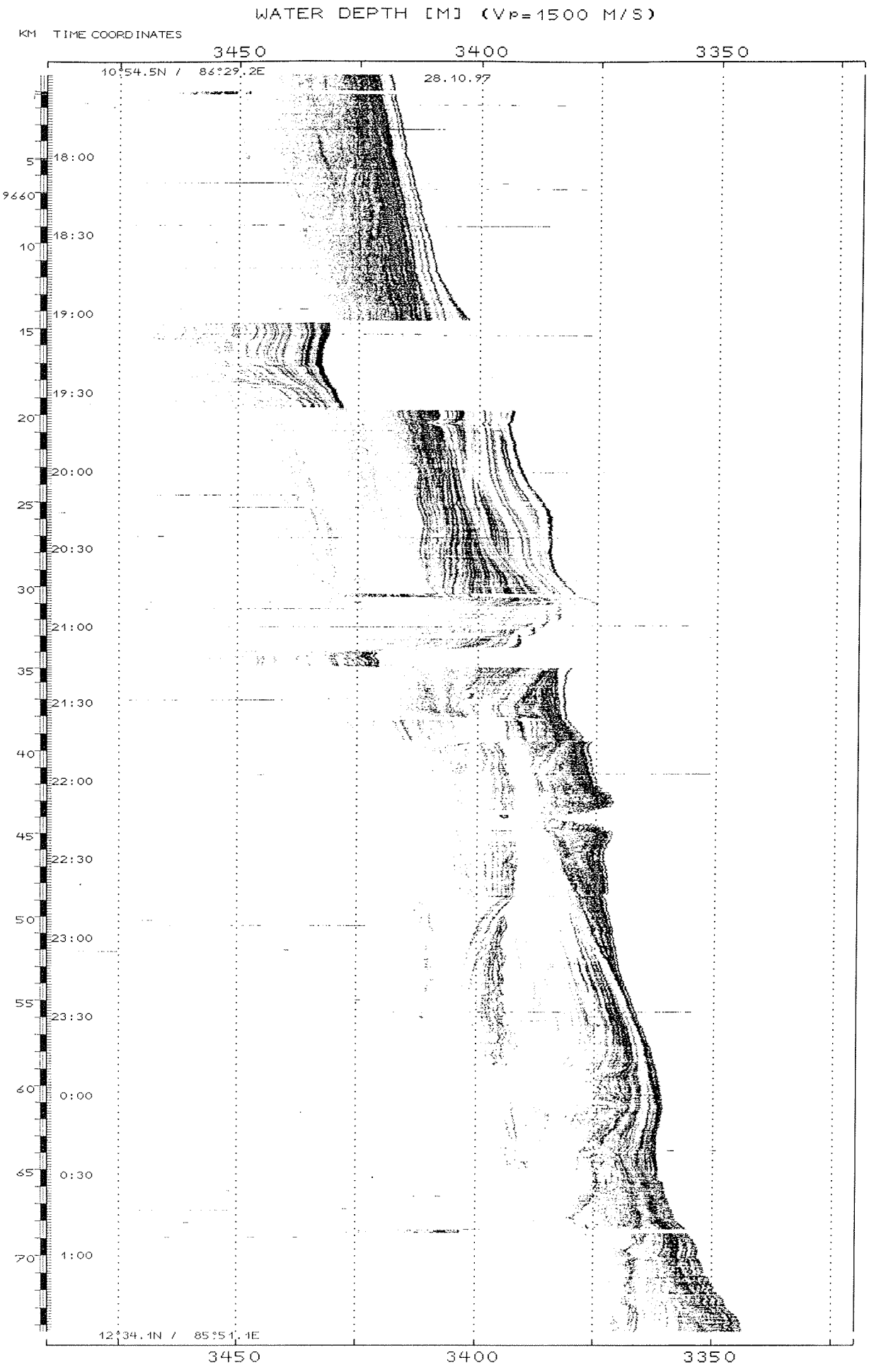

Fig. 17. Parasound section from detail study area 'c2', Line GeoB 97-028.

5.4 Middle Fan, detail study area 'g' (16°N-17°30'N)

Between 16°N and 17°30'N a cross-section through the middle fan area was obtained by two SW-NE trending seismic Lines (GeoB 97-059/069). The GI-Gun™ data from Line GeoB 97-059 reveal sequences with weak reflections and sequences with hummocky and discontinuous reflections (Fig. 18) by turns.

The evolution of the modern channel-levee system in the middle fan area was the scientific objective of a detail study in area 'g'. Starting with a Parasound survey which covered the working area, we obtained an overview about the channel geometry from Hydrosweep measurements (Fig. 19). A preliminary bathymetric map shows the main channel with varying meander-loop diameters. The PARASOUND data of the north-eastern part of Line GeoB 97-059 (Fig. 20) reveal several segments with the inner levees, which have been previously discussed by Hübscher et al. (1997). In order to understand the three-dimensional growth pattern of the observed sedimentary units we shot 35 Parasound and Hydrosweep profiles as well as 10 seismic lines (GeoB 97059 to -068; Fig. 21). The GI-Gun™ and watergun data show high-amplitude and discontinuous reflections beneath the inner levee segments which were not resolved in Parasound data. The levees exhibit low amplitude reflections except the levee segments directly on each side of the channel. The data of the other seismic lines showed striking variations in the growth patterns from line to line, therefore we narrowed the line spacing in the southern study area to 300 m.

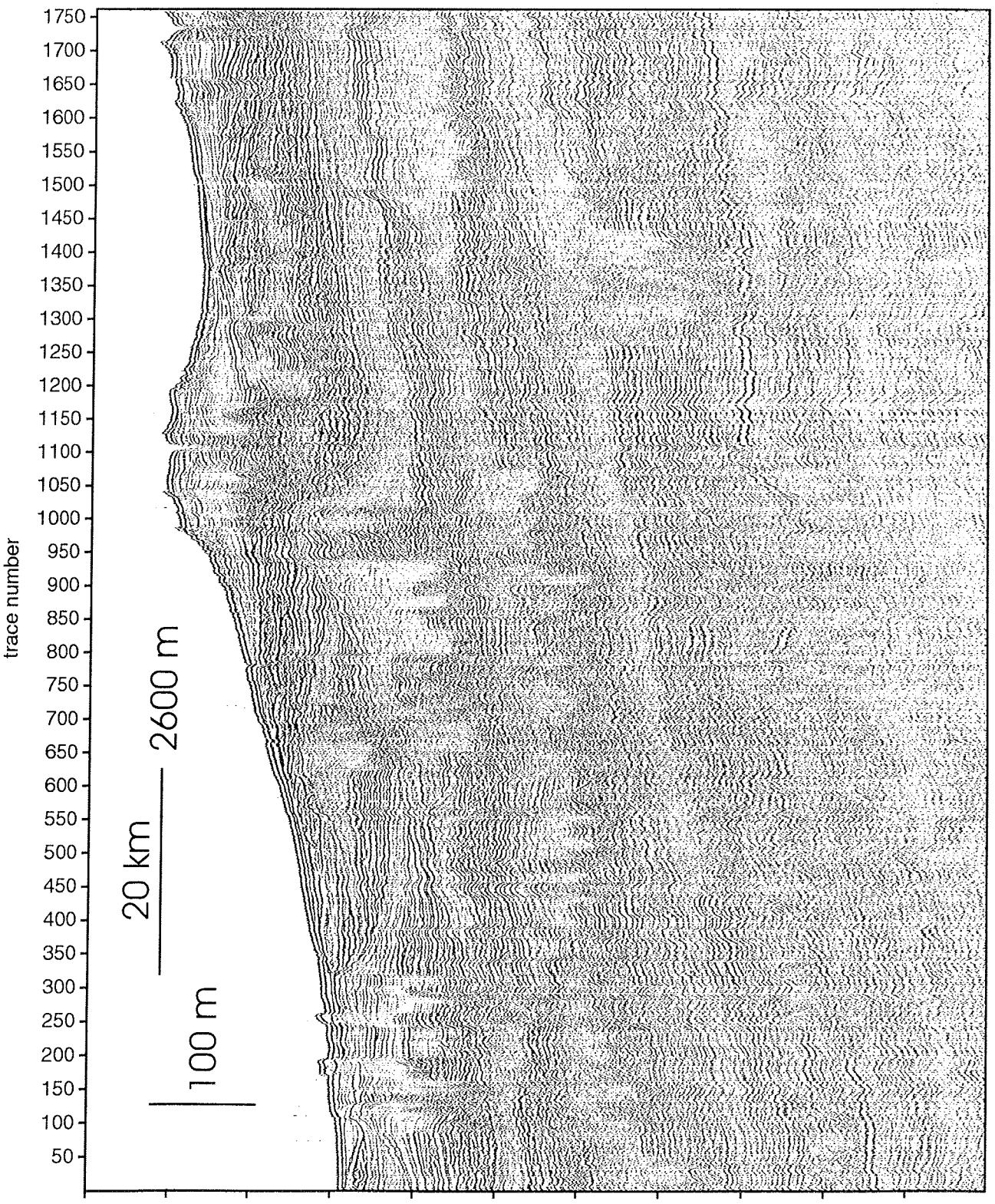

Fig. 18. Seismic data (GI-Gun) from Line GeoB 97-059

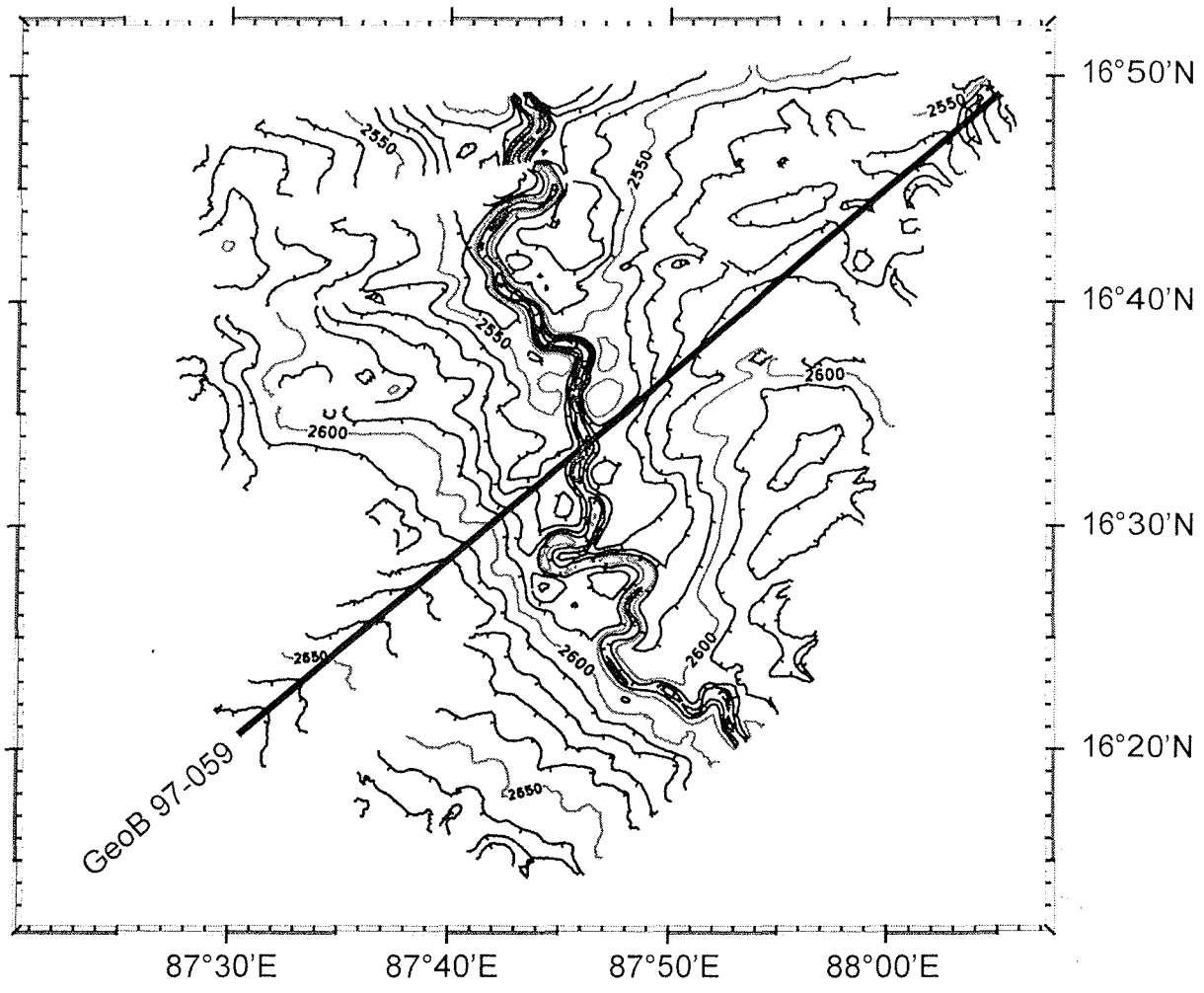

Fig. 19. Bathymetric map of detail study area 'g'.

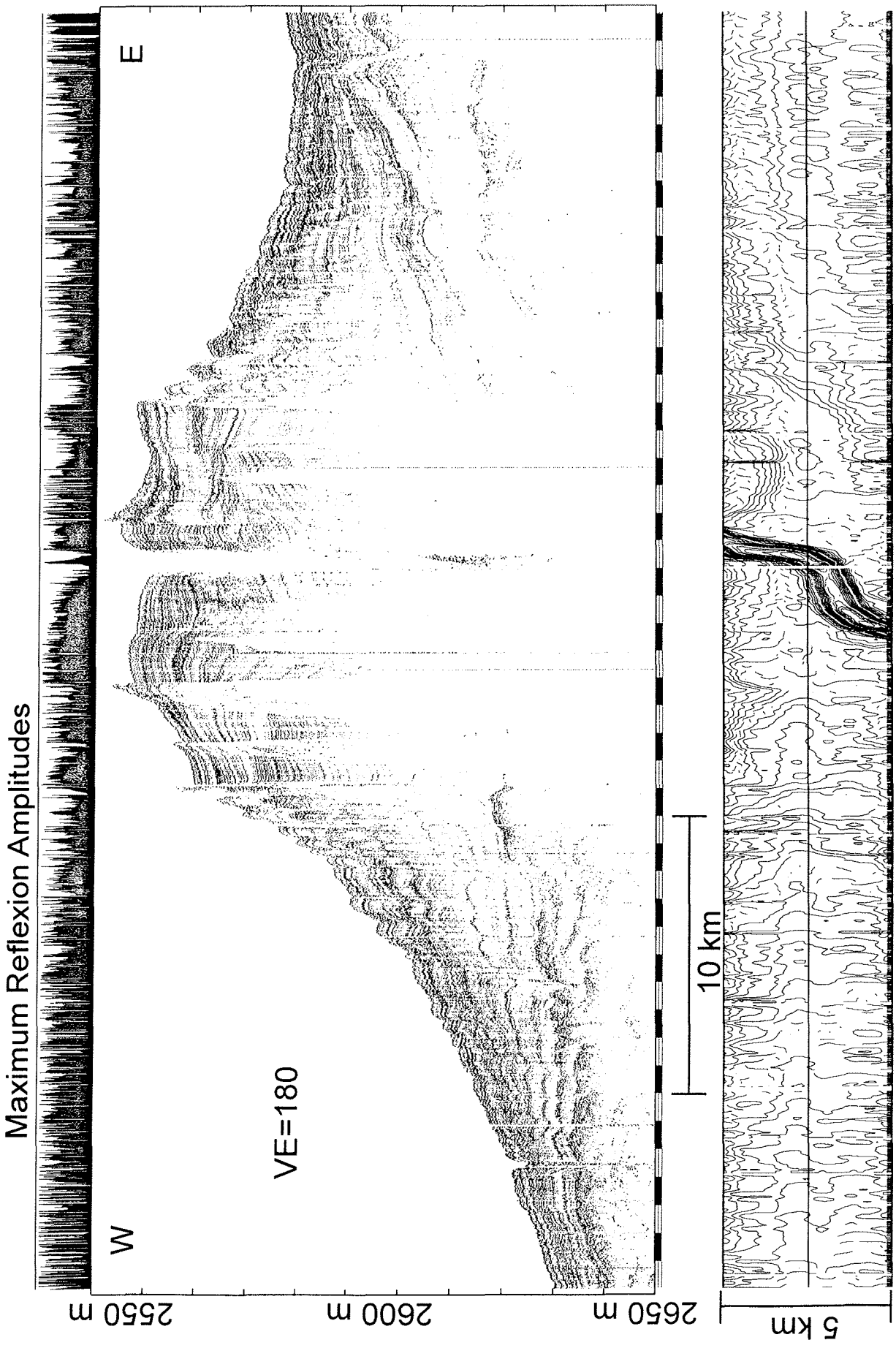

Fig. 20. Parasound section from Line GeoB 97-059, detail study area 'g'.

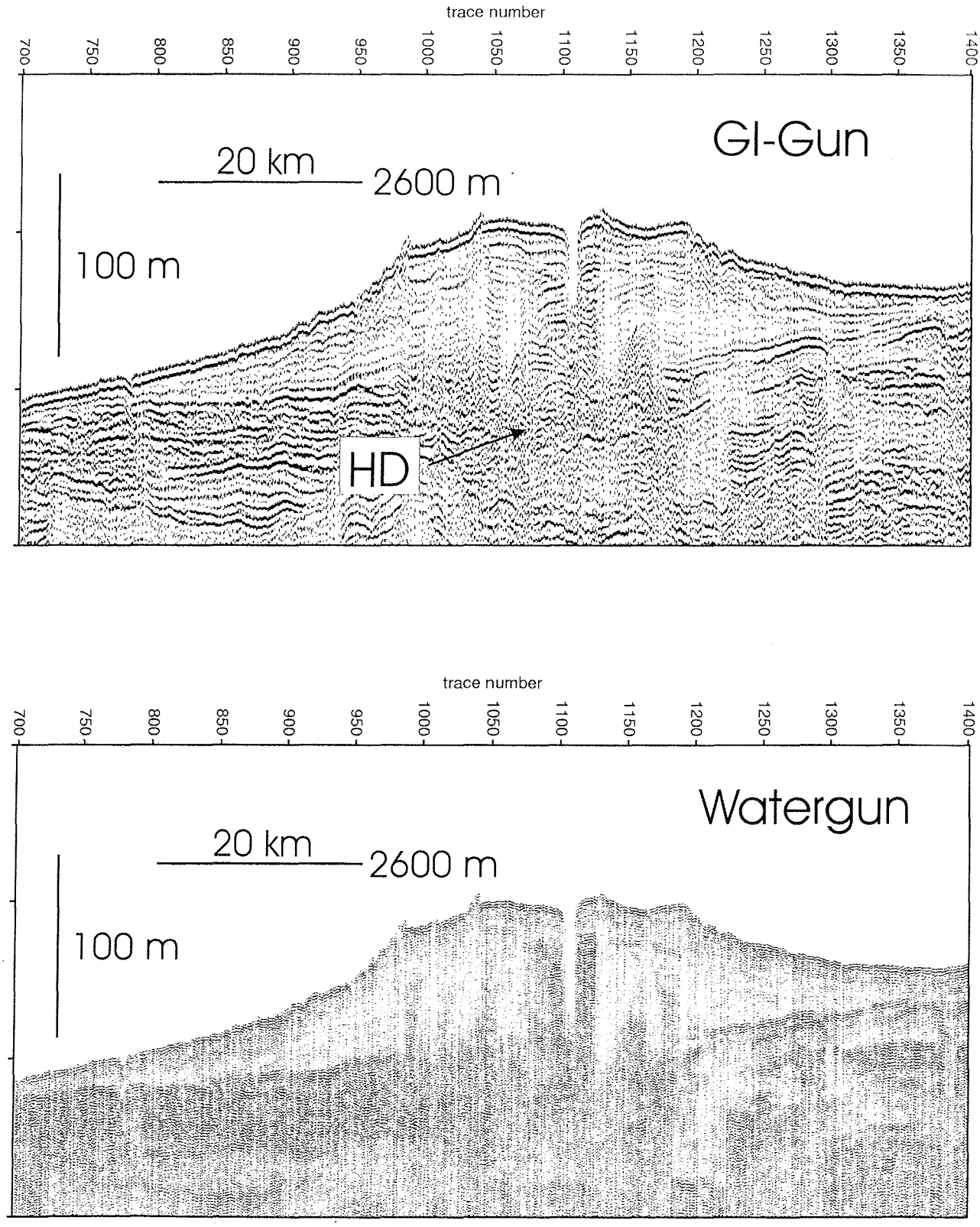

Fig. 21. GI-Gun and watergun data from Line GeoB 97-059, detail study area 'g'.

6. *Track Charts and Seismic Lines*

During R/V SONNE Cruise SO 125 more than 4000 km of multichannel seismic data were collected along 50 seismic lines (GeoB 97-020 - GeoB 97-069). Except for lines GeoB 97-060 - GeoB 97-063, on which only a watergun was used as the seismic source, GI-Gun and watergun were alternating triggered. Altogether 131723 shot gathers have been collected resulting in a total amount of 750 GigaByte of data.

Profile Seis. Sources	Start: Date/Time	Latitude Longitude	End: Date/Time	Latitude Longitude	Shots	Length (km)
GeoB97-020 GI/WG	21.10.97 10:39	8°00.4'N 85°10.5'E	22.10.97 02:04	8°00.5'N 86°25.9'E	10400	139
GeoB97-021 GI/WG	22.10.97 02:20	8°01.6'N 86°25.7'E	22.10.97 04:19	8°08.6'N 86°18.4'E	598	19
GeoB97-022 GI/WG	22.10.97 04:27	8°08.9'N 86°17.9'E	22.10.97 10:05	7°40.0'N 86°16.5'E	1687	54
GeoB97-023 GI/WG	22.10.97 10:08	7°40.0'N 86°16.3'E	22.10.97 22:43	7°41.0'N 85°12.0'E	3562	119
GeoB97-024 GI/WG	22.10.97 22:54	7°41.6'N 85°12.6'E	23.10.97 01:04	7°49.8'N 85°19.0'E	500	19
GeoB97-025 GI/WG	23.10.97 01:23	7°50.0'N 85°20.2'E	23.10.97 14:12	7°51.0'N 86°23.3E	3550	116
GeoB97-026 GI/WG	23.10.97 14:25	7°51.7'N 86°24.0'E	23.10.97 16:03	7°59.8'N 86°24.0'E	456	15
GeoB97-027 GI/WG	23.10.97 16:15	8°00.3'N 86°24.6'E	25.10.97 05:35	8°00.4'N 89°29.3'E	10359	340
GeoB97-028 GI/WG	27.10.97 11:46	10°43.2'N 83°59.6'E	29.10.97 19:28	11°05.5'N 88°40.5'E	15415	515
GeoB97-029 GI/WG	29.10.97 19:28	11°05.5'N 88°40.5'E	29.10.97 21:08	11°12.4'N 88°38.8'E	467	13
GeoB97-030 GI/WG	29.10.97 21:08	11°12.4'N 88°38.8'E	30.10.97 00:50	11°10.6'N 88°20.4'E	1024	34
GeoB97-031 GI/WG	30.10.97 01:07	11°11.3'N 88°20.3'E	30.10.97 02:45	11°12.0'N 88°28.4'E	456	15
GeoB97-032 GI/WG	30.10.97 03:43	11°12.0'N 88°28.4'E	30.10.97 04:09	11°13.6'N 88°26.9'E	135	4
GeoB97-033 GI/WG	30.10.97 04:47	11°13.3'N 88°26.8'E	30.10.97 06:01	11°08.8'N 88°23.2'E	342	11
GeoB97-034 GI/WG	30.10.97 06:35	11°08.8'N 88°24.2'E	30.10.97 07:34	11°13.6'N 88°24.2'E	275	9
GeoB97-035 GI/WG	30.10.97 07:58	11°13.4'N 88°25.2'E	30.10.97 08:54	11°08.8'N 88°25.2'E	261	9
GeoB97-036 GI/WG	30.10.97 09:20	11°08.7'N 88°26.2'E	30.10.97 10:25	11°13.5'N 88°26.2'E	300	9
GeoB97-037 GI/WG	30.10.97 10:30	11°15.0'N 88°25.8'E	30.10.97 12:20	11°23.1'N 88°24.8'E	529	15
GeoB97-038 GI/WG	30.10.97 12:51	11°23.1'N 88°24.7'E	31.10.97 11:55	11°15.1'N 86°28.6'E	6386	212
GeoB97-039 GI/WG	31.10.97 11:55	11°15.1'N 86°28.6'E	31.10.97 17:02	11°39.4'N 86°23.2'E	1416	46
GeoB97-040 GI/WG	31.10.97 17:02	11°39.4'N 86°23.2'E	01.11.97 06:31	11°40.1'N 87°30.2'E	3739	122
GeoB97-041 GI/WG	02.11.97 11:27	14°00.0'N 84°35.0'E	04.11.97 20:34	14°00.1'N 89°24.4'E	15040	522
GeoB97-042 GI/WG	04.11.97 20:47	14°01.0'N 89°24.2'E	05.11.97 05:43	14°30.0'N 88°59.7'E	2571	70
GeoB97-043 GI/WG	05.11.97 05:43	14°30.0'N 88°59.7'E	06.11.97 10:41	14°50.6'N 86°34.6'E	8022	264
GeoB97-044 GI/WG	06.11.97 11:00	14°49.5'N 86°34.6'E	06.11. 13:16	14°38.2'N 86°34.6'E	633	21

Profile	Start: Date/Time	Latitude Longitude	End: Date/Time	Latitude Longitude	Shots	Length (km)
GeoB97-045 GI/WG	06.11.97 13:21	14°38.0'N 86°34.9'E	07.11.97 02:16	14°33.0'N 87°39.8'E	3572	117
GeoB97-046 GI/WG	07.11.97 02:21	14°32.6'N 87°40.0'E	07.11.97 03:15	14°28.2'N 87°39.9'E	248	8
GeoB97-047 GI/WG	07.11.97 03:19	14°28.0'N 87°39.6'E	07.11.97 06:18	14°28.0'N 87°24.6'E	821	27
GeoB97-048 GI/WG	07.11.97 10:23	14°30.5'N 87°15.0'E	07.11.97 12:41	14°30.5'N 87°26.8'E	636	21
GeoB97-049 GI/WG	07.11.97 13:13	14°29.8'N 87°27.0'E	07.11.97 15:36	14°29.8'N 87°15.0'E	660	22
GeoB97-050 GI/WG	07.11.97 16:09	14°30.2'N 87°15.1'E	07.11.97 18:32	14°30.2'N 87°27.0'E	657	21
GeoB97-051 GI/WG	07.11.97 18:54	14°30.8'N 87°26.6'E	07.11.97 21:16	14°30.8'N 87°14.6'E	657	22
GeoB97-052 GI/WG	07.11.97 21:53	14°31.1'N 87°16.5'E	08.11.97 00:11	14°31.1'N 87°28.0'E	636	21
GeoB97-053 GI/WG	08.11.97 00:41	14°32.0'N 87°27.9'E	08.11.97 01:58	14°31.6'N 87°21.6'E	356	11
GeoB97-054 GI/WG	08.11.97 02:04	14°32.0'N 87°21.6'E	08.11.97 07:43	14°55.0'N 87°37.5'E	1563	51
GeoB97-055 GI/WG	08.11.97 07:43	14°55.0'N 87°37.5'E	08.11.97 20:20	15°10.0'N 88°39.9'E	3497	116
GeoB97-056 GI/WG	08.11.97 20:33	15°10.8'N 88°40.0'E	08.11.97 22:24	15°20.0'N 88°39.9'E	516	17
GeoB97-057 GI/WG	08.11.97 22:24	15°20.0'N 88°39.9'E	09.11.97 10:30	15°55.9'N 87°16.0'E	3382	108
GeoB97-058 GI/WG	09.11.97 10:30	15°55.9'N 87°16.0'E	09.11.97 17:44	16°06.8'N 87°16.0'E	1967	68
GeoB97-059 GI/WG	09.11.97 17:52	16°07.4'N 87°16.0'E	10.11.97 06:34	16°48.7N 88°04.4'E	3616	116
GeoB97-060 WG	11.11.97 20:18	16°21.5'N 87°45.2'E	11.11.97 22:48	16°29.4'N 87°55.0'E	1514	23
GeoB97-061 WG	11.11.97 23:20	16°29.7'N 87°54.6'E	12.11.97 02:02	16°21.3'N 87°44.0'E	1618	25
GeoB97-062 WG	12.11.97 03:04	16°21.8'N 87°43.9'E	12.11.97 05:14	16°28.7'N 87°52.5'E	1291	20
GeoB97-063 WG	12.11.97 05:56	16°29.1'N 87°52.2'E	12.11.97 09:23	16°18.2'N 87°38.6'E	2076	32
GeoB97-064 GI/WG	12.11.97 09:56	16°18.6'N 87°38.6'E	12.11.97 15:05	16°34.9'N 87°58.5'E	1429	47
GeoB97-065 GI/WG	12.11.97 15:25	16°35.9'N 87°57.9'E	12.11.97 20:38	16°33.1'N 87°31.5'E	1434	47
GeoB97-066 GI/WG	12.11.97 21:51	16°37.7'N 87°30.3'E	13.11.97 03:34	16°40.8'N 87°59.7'E	1583	53
GeoB97-067 GI/WG	13.11.97 04:24	16°44.5'N 87°58.7'E	13.11.97 09:52	16°41.5'N 87°31.0'E	1512	50
GeoB97-068 GI/WG	13.11.97 10:48	16°45.9'N 87°30.1'E	13.11.97 16:42	16°49.4'N 88°00.1'E	1631	54
GeoB97-069 GI/WG	13.11.97 16:42	16°49.4'N 88°00.1'E	14.11.97 17:01	17°30.0'N 90°10.0'E	6728	243

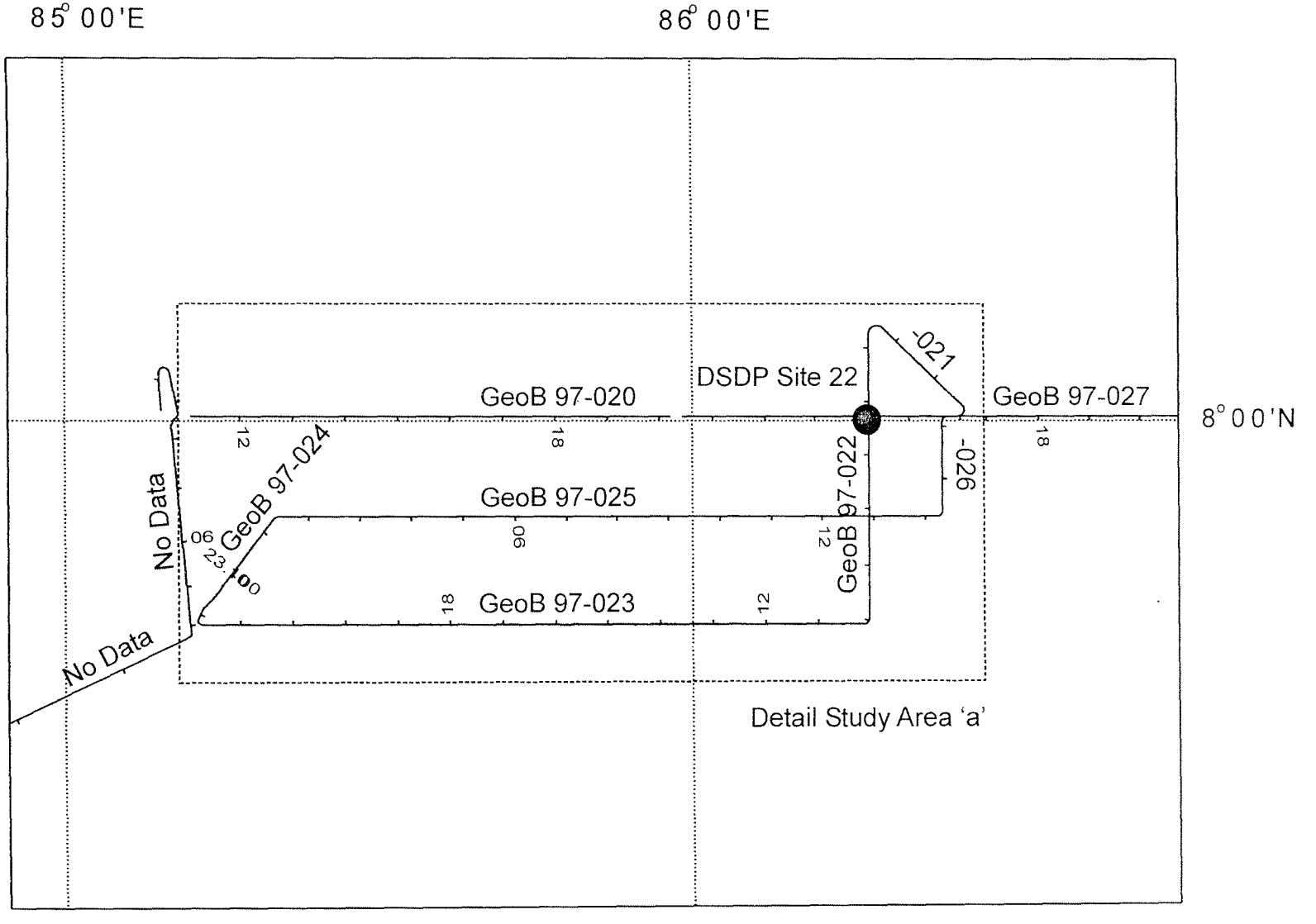

Fig. 22. Southernmost W-E transect and detail study area 'a' of SO125 cruise near DSDP Site 22.

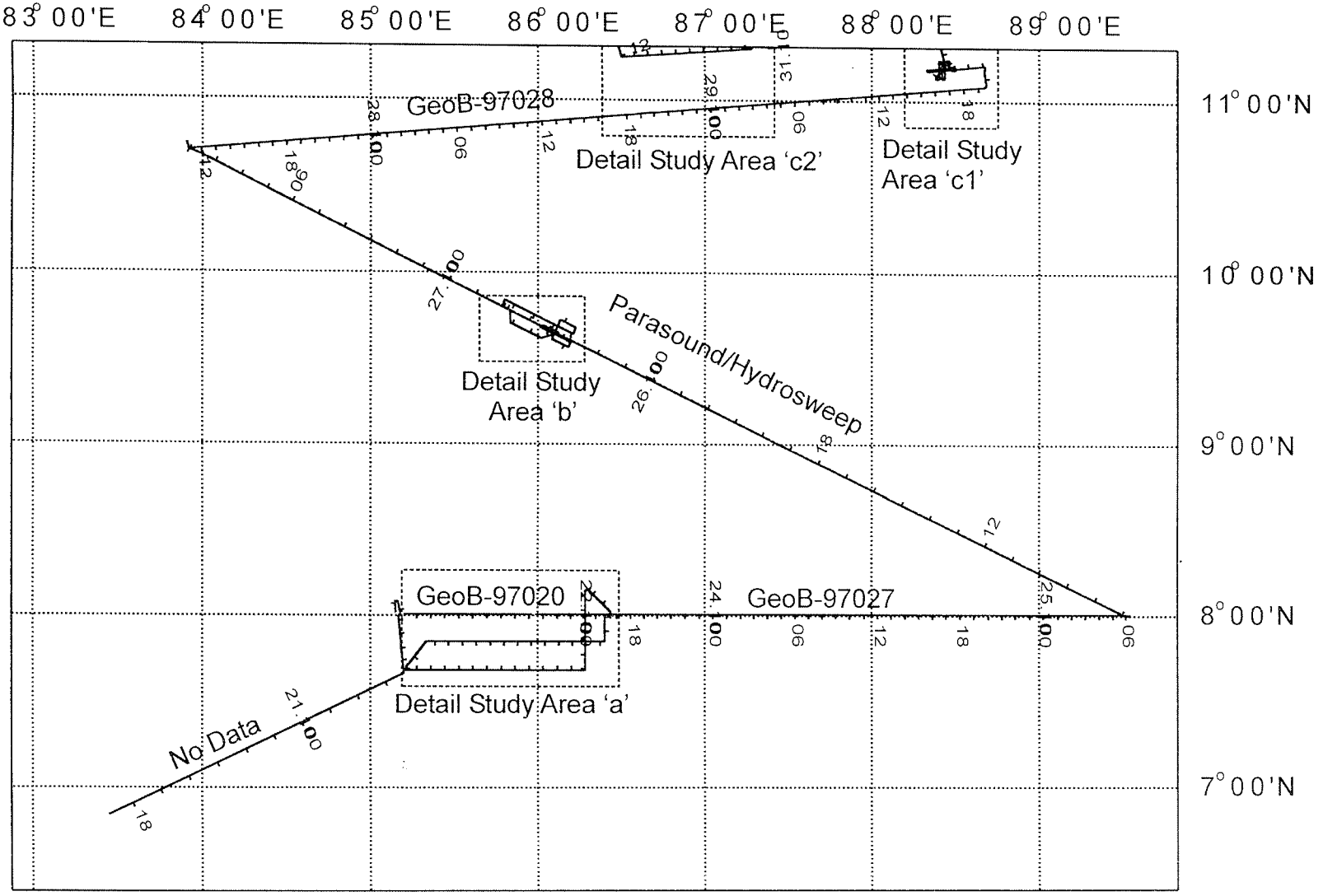

Fig. 23. Southern part of SO125 survey area.

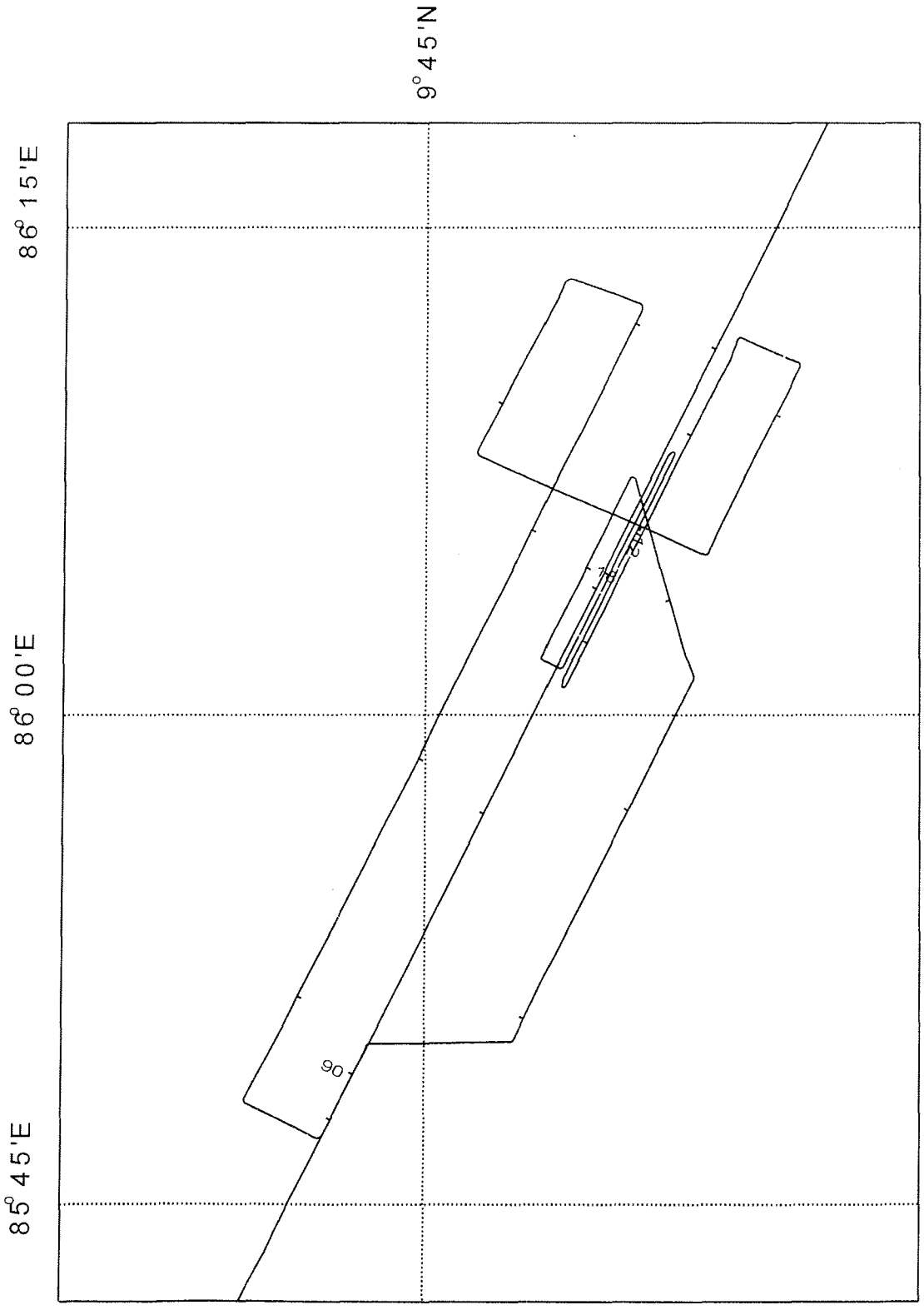

Fig 24. Parasound / Hydrosweep survey at detail study area 'b'.

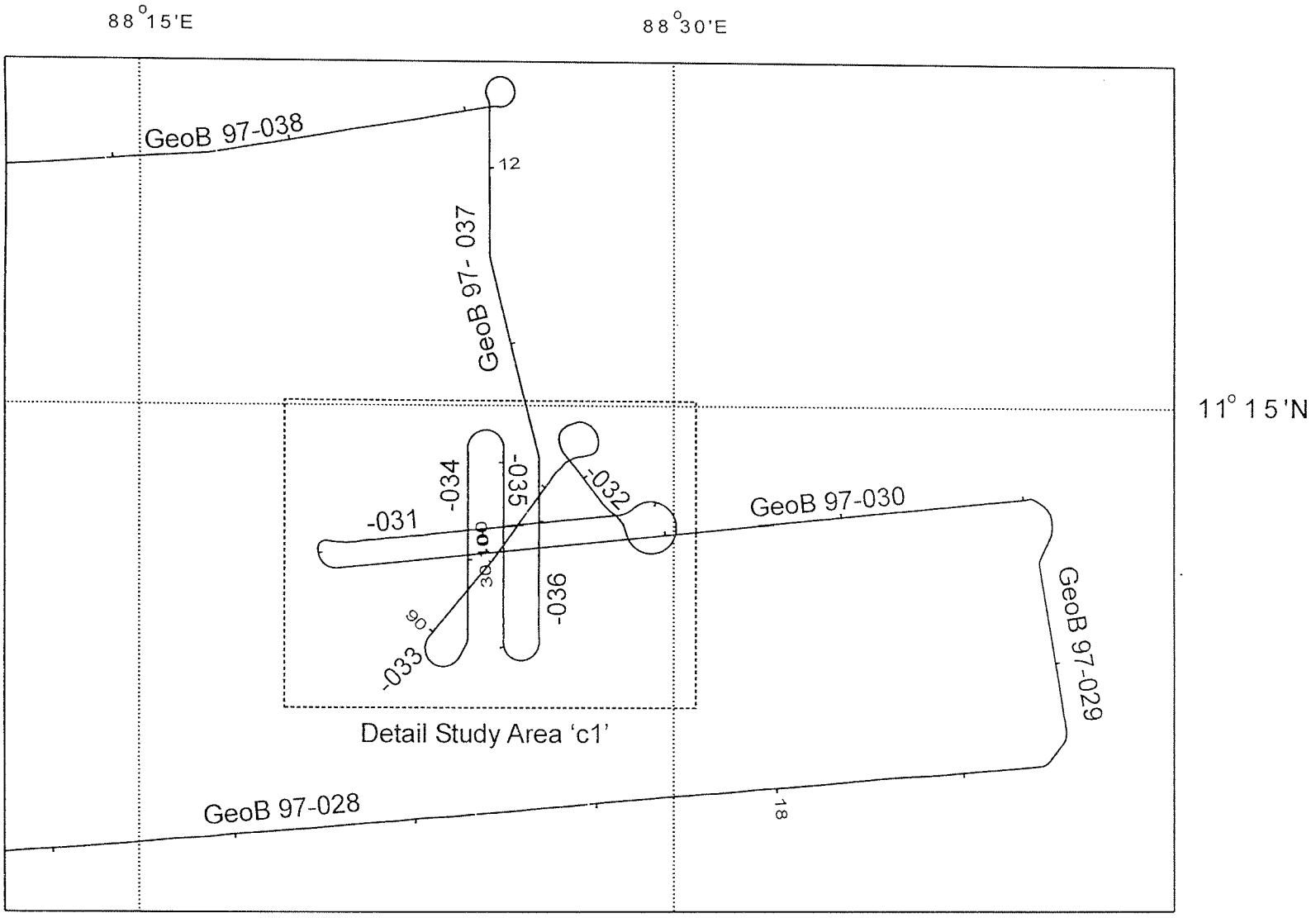

Fig. 25. Area around detail study area 'c1'.

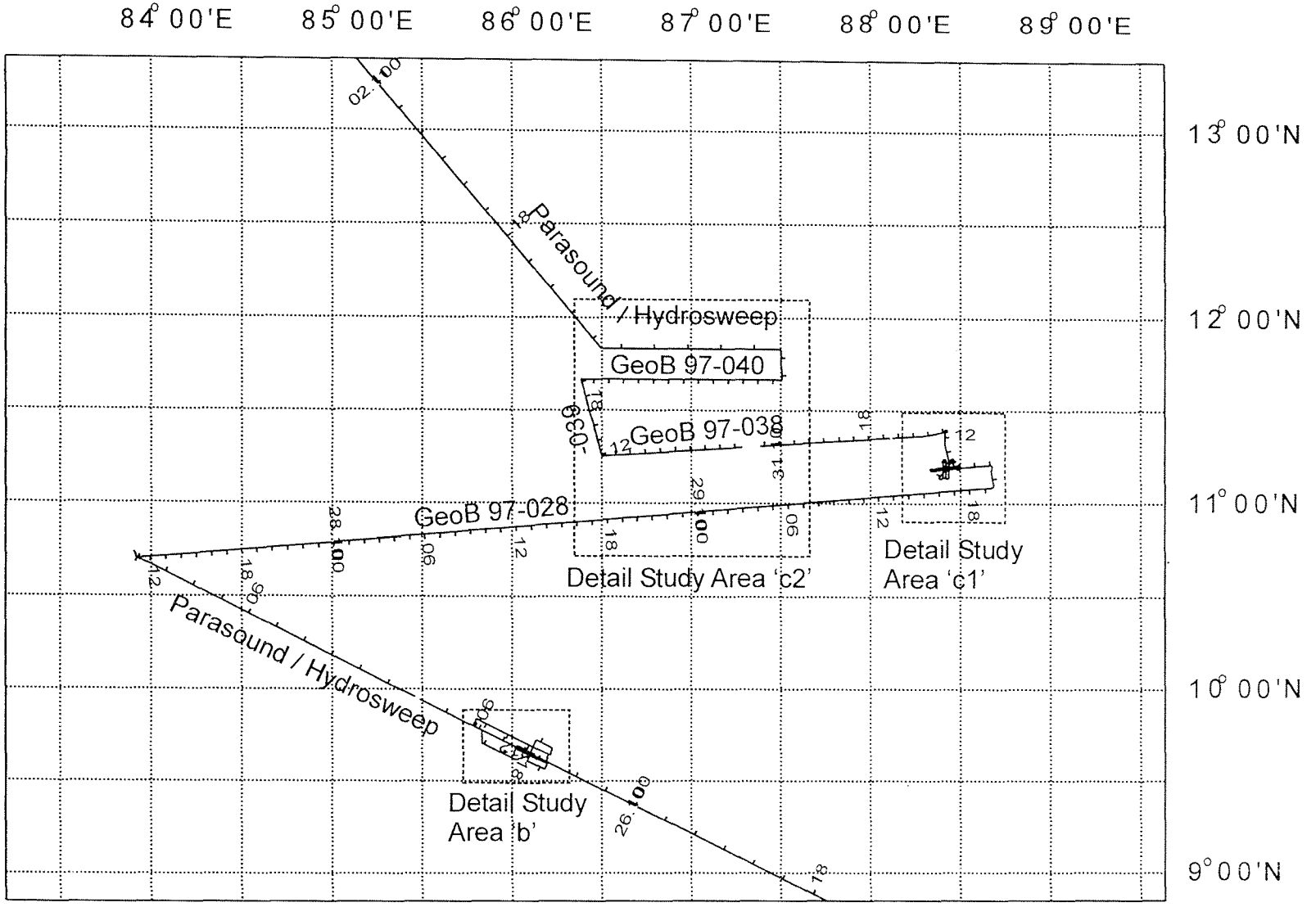

Fig. 26. Middle part of SO125 survey area.

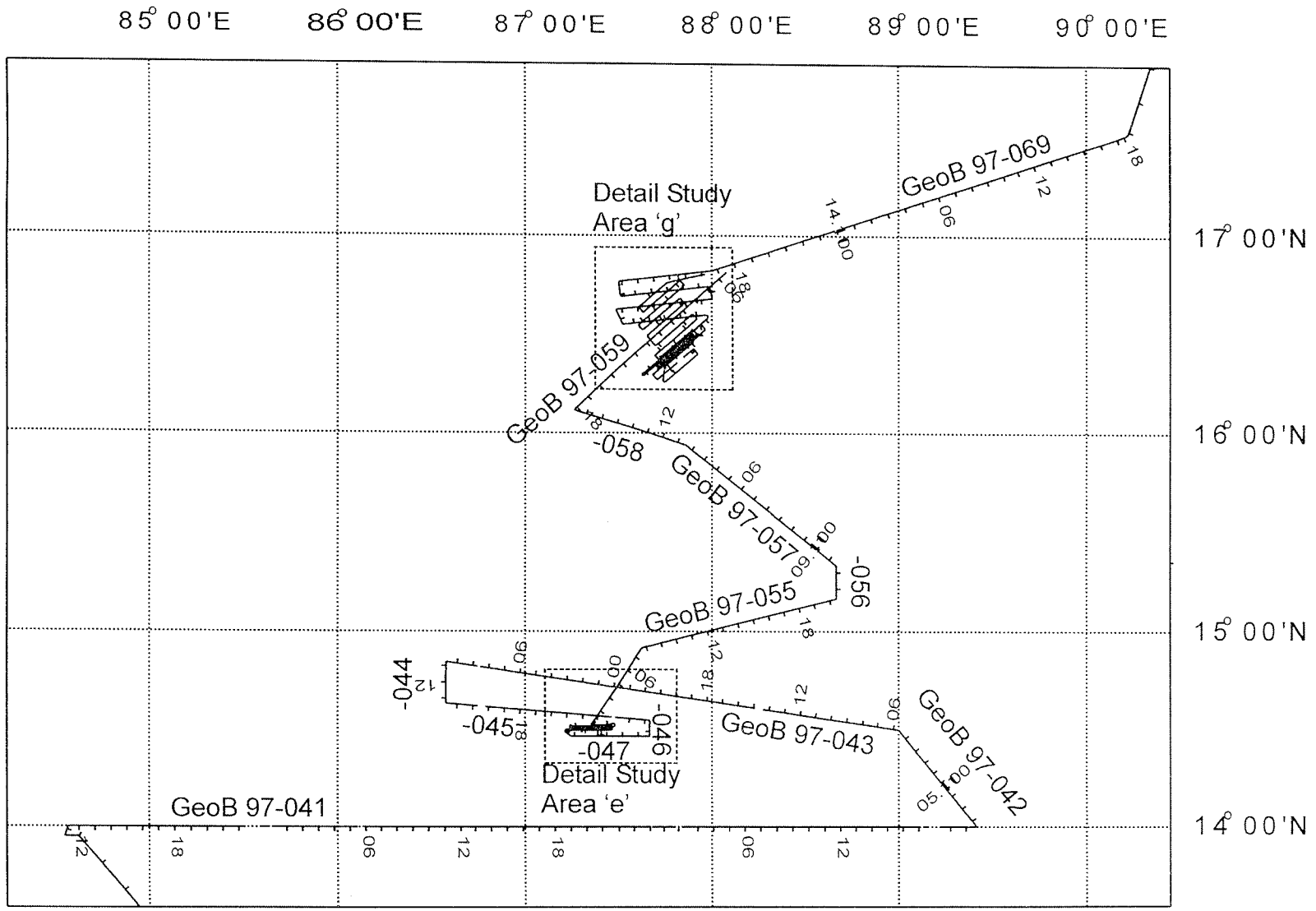

Fig. 27. Northern survey area of cruise SO125 including detail study surveys 'e' and 'g'.

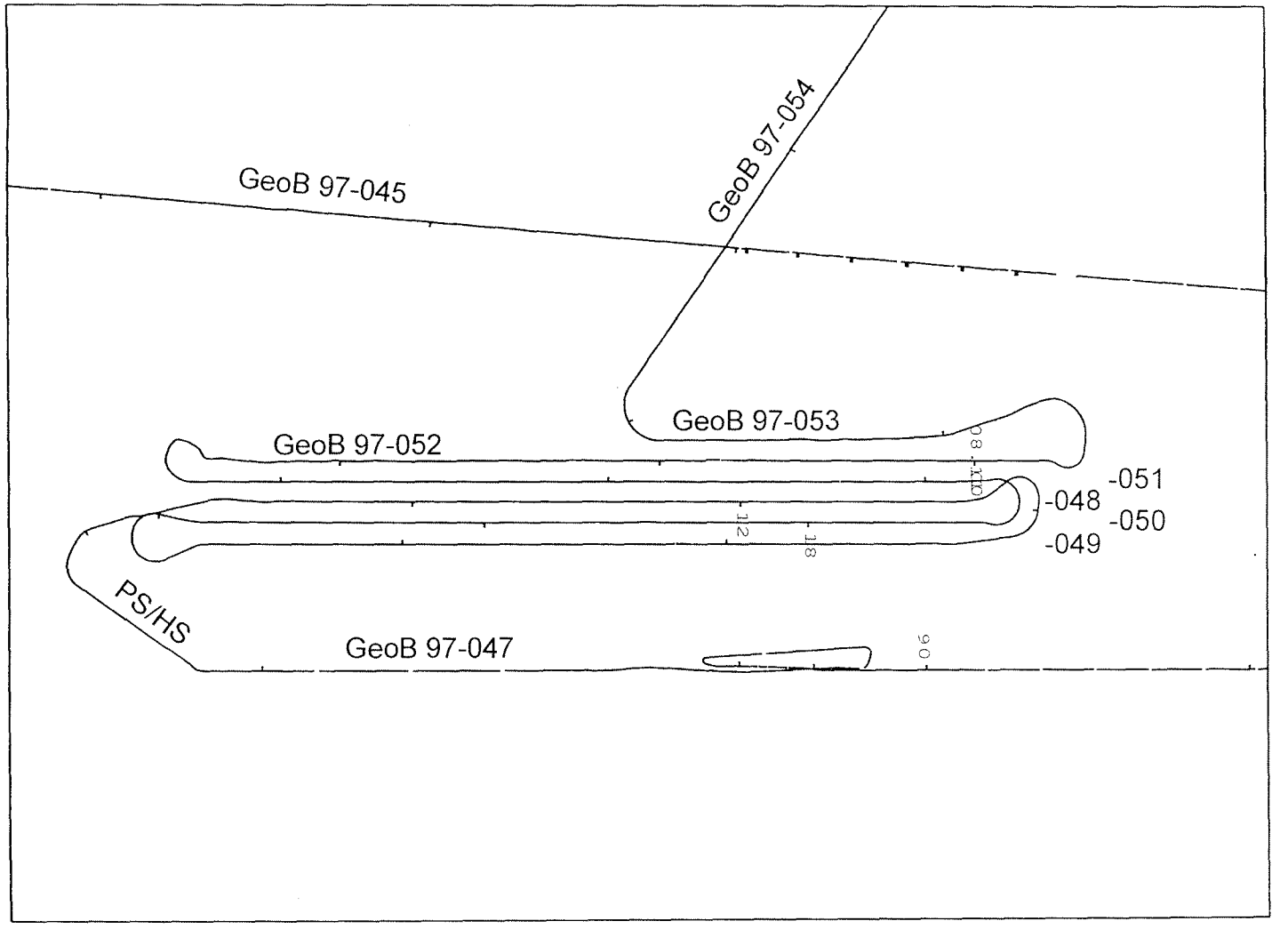

Fig. 28. Detail study area 'e' of SO125 cruise.

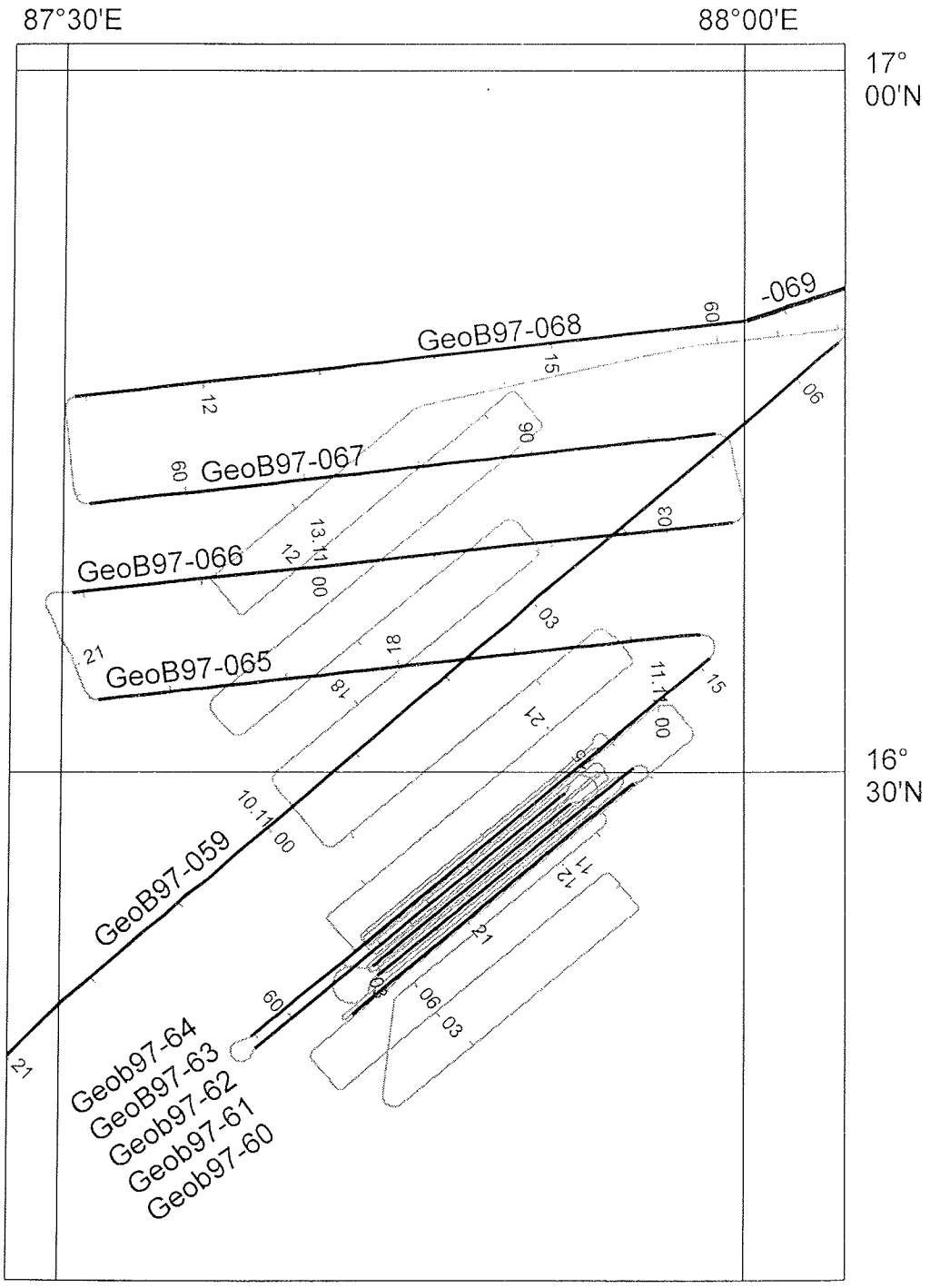

Fig. 29. Detail study area 'g' of SO125 cruise (Seismic lines drawn as black lines).

7. Acknowledgments

The scientific party aboard R/V SONNE during Cruise SO125 gratefully acknowledges the friendly cooperation and efficient technical assistance of Captain Kalthoff, his officers and crew who substantially contributed to the overall scientific success of this expedition.

We also appreciate the most valuable help of the Projektträger BEO, Rostock-Warnemünde, in the planning and realization of the cruise.

The work was funded by the Bundesministerium für Bildung, Wissenschaft, Forschung und Technologie, Förderkennzeichen 03G0125A.

Appendices

A Berichtsblatt

B Wochenberichte

C Cruise report SO 126 - Bengal Shelf, Chapter 8

Parasound and Hydrosweep

(originally published in Kudrass, H.-R., 1998. Cruise Report SO 126)

D Cruise report SO 126 - Bengal Shelf, Chapter 9

Very High-Resolution Multichannel Reflection Seismics

(originally published in Kudrass, H.-R., 1998. Cruise Report SO 126)

E Cruise report SO 126 - Bengal Shelf, Chapter 11.4

Ultrasonic Full Waveform Core Logging

(originally published in Kudrass, H.-R., 1998. Cruise Report SO 126)

Appendix A

Berichtsblatt

Berichtsblatt

1. ISBN oder ISSN 0931-0800	2. Berichtsart Fahrtbericht

3a. Titel des Berichts
SO 125 - BengalSeis

3b. Titel der Publikation
Report and Preliminary Results of R/V Sonne Cruise 125, Cochin - Chittagong, 17.10.-17.11.97

4a. Autoren des Berichts (Name, Vorname(n)) Spieß, V., C. Hübscher, M. Breitzke und Fahrtteilnehmer	5. Abschlußdatum des Vorhabens 31.1.2000
4b. Autoren der Publikation (Name, Vorname(n))	6. Veröffentlichungsdatum August 1998
	7. Form der Publikation
8. Durchführende Institution(en) (Name, Adresse) Fachbereich Geowissenschaften Universität Bremen Klagenfurter Straße 28359 Bremen	9. Ber.Nr. Durchführende Insitution Nr. 123
	10. Förderkennzeichen *) 03G0125A
	11a. Seitenzahl Bericht 128
	11b. Seitenzahl Publikation
13. Fördernde Institution (Name, Adresse) **Bundesministerium für Bildung, Wissenschaft, Forschung und Technologie (BMBF)** **53170 Bonn**	12. Literaturangaben
	14. Tabellen 5
	15. Abbildungen 60

16. Zusätzliche Angaben
Fahrtbericht und erste Ergebnisse, FS Sonne Fahrt 125 - Cochin - chittagong, 17.10.-17.11.97

17. Vorgelegt bei (Titel, Ort, Datum)
Forschungszentrum Jülich - BEO - Rostock - Warnemünde

18. Kurzfassung

In den Berichtszeitraum fällt die Vorbereitung und Durchführung der Meßfahrt SO 125 sowie die Beteiligung an der mit dem Projekt in engem Zusammenhang stehenden Meßfahrt SO 126. Die Arbeiten der SO 125 Reise fanden ausschließlich in internationalen Gewässern zwischen 8°N und 17°N statt. Die geplanten wissenschaftlichen Arbeiten konnten ohne Einschränkungen erfolgreich durchgeführt werden. Die insgesamt 4000 km mehrkanalseismischer Daten verteilen sich auf 4 annähernd West-Ost streichende, lange Meßprofile über den gesamten Bengalfächer sowie auf 5 kleinräumige, flächenhafte Studien. Außerdem wurde während des gesamten Fahrtabschnittes mit den hydroakustischen Bordsystemen Parasound und Hydrosweep kontinuierlich registriert. Damit erfolgte auch die Festlegung von Kolbenlot Beprobungslokationen für den nachfolgenden, thematisch eng verknüpften Fahrtabschnitt SO 126, auf dem speziell für das wissenschaftliche Programm der SO 125 Reise Sedimentkerne genommen werden sollten. Die physikalischen Vermessungen der Sedimentkerne erfolgten in Zusammenarbeit mit der BGR, wobei neben dem Core Logger System der BGR auch die Bremer Ultraschallapparatur zum Einsatz kam.

19. Schlagwörter
Golf von Bengalen. Tiefseefächer, Rinne-Uferwall Systeme, Kanalmäander, Meeresspiegelschwankungen

20. Verlag	21. Preis

*) Auf das Förderkennzeichen des BMBF soll auch in der Veröffentlichung hingewiesen werden

Appendix B

Wochenberichte

Wochenbericht Nr. 1, Sonne-Reise SO 125 - BengalSeis
Cochin - Chittagong
17.10. - 26.10.97

Der Beginn der Charterzeit in einem recht verschlafenen Teil Südindiens wurde durch den Besuch der englischen Königin just am 17.10 etwas durcheinandergebracht, da der ganze Ort in Vorbereitungen und Organisation verstrickt war und für einige Neueinsteiger größere Wartezeiten entstanden. Dennoch konnten, nach intensiven Bemuehungen des Agenten und aller anderen Beteiligten, alle Frachtstücke und Personen rechtzeitig an Bord gebracht werden, so dass die Reise planmäßig am 18.10 gegen 3 Uhr nachmittags beginnen konnte.

Die Anfahrt ins Arbeitsgebiet führte um die Insel Sri Lanka herum nach 7°40'N/85°12'E ausserhalb der 200 sm-Zone, um die Vorbereitungen des seismischen Instrumentariums mit einem Test des Streamers und der Luftkanonen abzuschliessen. Alle Geräte funktionierten einwandfrei und die Messungen begannen unmittelbar im Anschluss mit einem viertägigen Survey.

Das Untersuchungsobjekt der Sonne Fahrt SO 125 ist der Bengalfächer. Dieser größte Sedimentfächer der Erde wird aufgebaut durch die Flüsse Ganges und Brahmaputra über ihre Mündung in Bangladesh. Suspensionsfracht und Turbidite speisen von dort aus einen komplex aufgebauten Kanal, in dem die Sedimente bis in die Tiefsee in mehr als 3000 km Entfernung geleitet werden.

Die seismischen Untersuchungen der Sonne Fahrt SO 125 konzentrieren sich auf einen Abschnitt zwischen 8°N und 18°N geographischer Breite. Dort werden die unterschiedlichen Ausprägungen der mäandrierenden aktiven Hauptrinne detailliert vermessen. Um die vermutlich in enger Beziehung zum Stand des Meeresspiegels stehenden zeitliche Entwicklung der Rinnengeometrie und der Uferwälle zu verstehen, sollen hochauflösend die Sedimentstrukturen mit Echolot, hochfrequenter Watergun und einer GI Luftkanone abgebildet werden. Nur mit diesem spezialisierten Instrumentarium wird es möglich sein, die kleinräumig wechselnden Ablagerungsprozesse an den Mäanderschlaufen zu verstehen und in Beziehung zu setzen.

Der erste Vermessungsabschnitt bestand aus einem langen E-W Profil bei 8°N mit einer Detailvermessung, die in der Umgebung der DSDP Bohrung 218 unweit der aktiven Rinne durchgeführt wurde. Die Eindringung der seismischen Systeme war mit über 1500 m außerordentlich groß, so daß eine Korrelation mit der 780 m tiefen Bohrung möglich sein wird. Aufgrund der besonders günstigen Wetterbedingungen wurde eine sehr hohe Datenqualität erzielt, aus der allerdings erst nach der Bearbeitung der Daten an Land der volle Nutzen gezogen werden kann. Das daran anschließende Parasound/Hydrosweep Profil von 8°N/89°30E nach 10°42N/83°55E, das kurz vor dem Abschluß steht, erbrachte interessante Erkenntnisse über die Terassenbildung innerhalb der aktiven Rinne.

Wochenbericht Nr. 2, Sonne-Reise SO 125 - BengalSeis
Cochin - Chittagong
27.10. - 2.11.97

Die zweite Arbeitswoche der Sonne Fahrt 125 im Golf von Bengalen begann wiederum mit einem langen Seismikprofil von 10°42N/83°55E nach 11°06N/88°40E. Es zeigt eine im Vergleich zum südlicheren Profil deutlich höhere Zahl zugeschütteter Rinnensysteme. Dementsprechend konnten anhand der hochauflösenden Parasound Echolotdaten auch oberflächennah zahlreiche Rinnensysteme wiedergefunden werden, die auf Parallelprofilen schon während der SO 93 Reise überlaufen wurden.

Überraschend war, daß in mehreren Fällen die stark mäandrierenden Kanäle abschnittsweise einen hangparallelen Verlauf und einen deutlichen seitlichen Versatz zeigten. Dadurch wird das Auffinden der jeweils aktiven Rinne und das Zuordnen zu Parallelprofilen erschwert.

An das zweieinhalbtägige Meßprofil schloß sich planmäßig eine kleinräumige seismische Vermessung an, mit der die Entstehung von Mäanderterrassen untersucht werden sollte. Die meisten Rinnen im Fächer werden vermutlich bei einem Meeresspiegeltiefstand - wie zum Beispiel während der letzten Eiszeit - angelegt und besitzen dann ihre größte Breite. Steigt der Meeresspiegel an, so wandert weniger Sediment langsamer durch die Rinnen und es kommt zu terrassierten Sedimentablagerungen, zur sukzessiven Einengung des Querschnitts und zur Ausbildung von Mäandern. Wie auch bei Flüssen bilden sich in Tiefseemäandern Prall- und Gleithänge aus, die mit einer Um- und Ablagerung von Sediment verbunden sind. Diese Terrassen werden von oft akustisch transparenten Zonen unterbrochen, deren Entstehung weitgehend unklar war. Erste Interpretationen der neuen Daten lassen vermuten, daß es sich um Relikte von Uferwällen handelt, die nach Verlagerung des Kanals zugeschüttet wurden.

Die Lebensdauer von Kanalsystemen im Bengal Fächer beträgt nach den Ergebnissen der SO 93 Expedition nur wenige tausend Jahre. Danach verlagert sich der Kanal und sedimentiert oft auf die Randbereiche des zuvor aktiven Systems. So läßt sich auch aus seismischen Daten eine zeitliche Abfolge erkennen. Auf den in der zweiten Wochenhälfte vermessenen seismischen Profilen konnte ein gerade in Entstehung befindliches Kanalsystem untersucht werden. Sehr überraschend war, daß diese offensichtlich zur Zeit aktive Rinne gerade im Meßgebiet endete und einen breiten Schuttfächer mit vielen verzweigten kleinen Erosionsrinnen erzeugt. Je weiter nördlich das System überlaufen wurde, desto besser war der Hauptkanal ausgebildet. Nach unserem Diskussionsstand muß daraus geschlossen werden, daß die Sedimentation durch die aktive Rinne derzeit auf das Untersuchungsgebiet beschränkt ist und sich erst langsam wieder hangabwärts bewegen wird. Über die damit verbundenen Zeitskalen bestehen bislang keine konkreten Vorstellungen, aber die hier gewonnenen seismischen Datensätze versprechen dafür einen ersten Ansatz.

Den Arbeiten sehr zugute kamen uns erneut die günstigen Wetterbedingungen, auch wenn sich die See nicht mehr wie in der ersten Woche spiegelglatt präsentierte. Windgeschwindigkeiten und Wellenhöhen blieben aber sehr gering, so daß alle Systeme fehlerfrei, mit nur geringen akustischen Störungen arbeiten und Datensätze von hoher Qualität gesammelt wurden. Dies hebt natürlich auch die Stimmung aller Beteiligten an Bord. Gelegentlich kündigen jetzt dunklere Wolken am Horizont episodische Regengüsse an, die wir als Ausläufer der Monsunzeit wohl in die zweite Hälfte der Reise mitnehmen müssen.

Alle an Bord sind aber trotzdem guter Dinge, wohlauf und grüßen herzlich.

Die GeoB Seismiker

Wochenbericht Nr. 3, Sonne-Reise SO 125 - BengalSeis
Cochin - Chittagong
3.11. - 9.11.97

In der dritten Arbeitswoche der Sonne Fahrt 125 im Golf von Bengalen wurden die seismischen Arbeiten fortgesetzt. Da alle Systeme einwandfrei funktionierten, gab es nur kurze Unterbrechungen für die Wartung der seismischen Quellen.

Ein dreitägiges Seismikprofil bei 14°N zeigte, daß im Gegensatz zu den südlicheren Arbeitsgebieten die Komplexität der Rinnensysteme deutlich zunimmt. Die Rinnen sind nicht länger nur geprägt durch einen einzigen, mäandrierenden Transportkanal. Offensichtlich kommt, wie bereits von der SO 93 Reise bekannt war, die Existenz eines vormals viel breiteren Hauptkanals hinzu. Dieser bildete sich vermutlich bei einem Meeresspiegeltiefstand, wenn die Menge transportierten Sediments viel größer ist. In der Nacheiszeit verkümmerte dieses System, und es bildeten sich in dem breiten Kanal kleinere Rinne-Uferwall Komplexe aus, die noch dazu stark mäandrieren. Durch die Begrenzung auf den 10-15 km breiten Hauptkanal entwickeln sich Terassen mit charakteristischen internen Störungen, die auf eine dynamische Entwicklung mit zahlreichen Mäanderdurchstichen und -verlagerungen hindeuten.

In der dritten und vierten Arbeitswoche stand auf dem Programm, diese Systeme näher zu untersuchen und einige der Prozesse zu verstehen, die zu ihrer Bildung führen und die Entwicklung steuern. Auf dem langen Seismikprofil bei 14°N sollte zunächst eine Bestandsaufnahme der rezenten und älteren Rinnensysteme erfolgen. Es zeigte sich eine deutlich dichtere Abfolge von Rinnen, die auch besser anhand ihrer seismischen Signatur unterscheidbar waren. Die Ergebnisse der SO 93 Fahrt ließen uns erwarten, daß terassierte Rinne-Uferwall Komplexe mit einfachem internen Aufbau exemplarisch untersucht werden können.

Bei 14°40'N folgte dann für den Rest der Arbeitswoche eine großräumigere Vermessung, auf der auch hangabwärtig eine unerwartet starke Variabilität in Geometrie und interner Struktur der Rinnen zu beobachten war. Es zeigte sich, daß bei Annäherung an die zur Zeit aktive Rinne ältere Systeme rasch bis zur Unkenntlichkeit verschüttet werden können. Dies machte eine Anpassung der ursprünglichen Profilplanung auf Basis der neu gesammelten Daten erforderlich, die dann aber letztlich zu einer Klärung der räumlichen Bezüge zum aktiven Sedimentationszentrum führte. Es konnten eine detaillierte Vermessung eines einfachen terassierten Kanalsystems angeschlossen und wichtige Informationen für die Untersuchungen im nördlichsten Arbeitsgebiet gewonnen werden.

Auch in der dritten Arbeitswoche ließen die äußeren Bedingungen eine ungestörte Fortsetzung der seismischen Messungen zu. Allerdings hatte sich der Taifun Linda im Golf von Bengalen festgesetzt und für eine geraume Zeit mußten wir mit einem Zusammentreffen rechnen. Das Wetter verschlechterte sich allerdings nur leicht. Die häufigeren Regenschauer, die teils geschlossene Wolkendecke und der mäßig aufgebriste Wind waren daher gut zu ertragen. Wie sich danach herausstellte, war unsere Sorge unbegründet und der Taifun wurde schließlich für aufgelöst erklärt. Die seismische und akustische Datenqualität wurde durch die Bedingungen zwar kursabhängig leicht beeinträchtigt, doch können wir in Anbetracht der hochinteressanten Datensätze weiterhin sehr zufrieden sein.

Daher gehen wir auch mit viel Optimismus und guter Stimmung in die letzte Arbeitswoche, die uns mit den Messungen sehr dicht an unser Fahrtziel Chittagong führen wird.

Es grüßen aus dem Golf von Bengalen
die GeoB Seismiker

Wochenbericht Nr. 4, Sonne-Reise SO 125 - BengalSeis
Cochin - Chittagong
10.11. - 16.11.97

In der abschließenden vierten Arbeitswoche der Sonne Fahrt 125 im Golf von Bengalen konzentrierten sich die Arbeiten auf den nördlichsten Teil der aktiven Rinne außerhalb der 200 sm Zone bei 16°30'N / 87°30'E. Dieser Abschnitt des Bengalfächers gehört zu den komplexesten Ablagerungsräumen, die überhaupt in Fächersystemen beobachtet wurden. Eine mehrtägige detaillierte Vermessung mit Hydrosweep, Parasound und verschiedenen, simultan registrierten seismischen Quellen sollte die nach der Expedition SO 93 aufgeworfenen Fragen beantworten helfen.

Wie schon in der vergangenen Woche weiter südlich beobachtet, werden in diesem Teil des Sedimentfächers die Kanalsysteme durch eine meist über 10 km breite Hauptrinne charakterisiert, die wohl zu Zeiten höherer Sedimentanlieferung entstanden ist. Später entwickelten sich innerhalb kleinere Rinne-Uferwall Komplexe, die einem stark mäandrierenden Lauf folgen. Entsprechend sind die Uferwälle aufgrund der Einengung als Terrassen ausgebildet.

Im Untersuchungsgebiet wurden in den früheren Echolotaufzeichnungen gleich mehrere Phasen solcher Rinne-Uferwall Systeme innerhalb des Hauptkanals beobachtet, deren zeitliche Abfolge nun geklärt werden sollte. Insbesondere stellt sich die Frage, ob es sich bei den beobachteten Strukturen um eine sukzessive Einschnürung des vormals breiteren Kanals handelt, die mit einer stetigen Erhöhung des Meeresspiegels beim Übergang von Kalt- zu Warmzeiten einhergeht. Oder ob die wenige bisher verfügbare Seismik Bilder chaotischer, sich schnell verändernder oder verlagernder Mäandersysteme liefert und die Füllung des Hauptkanals viel rascher und vollständig erfolgte.

Eine großflächige Hydrosweep/Parasound Vermessung eines etwa 40 x 50 km großen Areals mit einem Profilabstand von 4 km machte den Anfang. Daran schloß sich auf Grundlage der gewonnenen Daten die Detailvermessung eines kurzen Abschnitts der aktiven Rinne an, die auch bei einem Profilabstand von 1 km noch viele Fragen offen ließ. Nach einer Verdichtung der Parasound Profile erfolgte der Einsatz der seismischen Meßsysteme. Mit diesen wurde zunächst ein drittes Profil zwischen die bestehenden gelegt, diesmal nur mit einer Watergun als Quelle und einer 3-fach höheren Schußrate als zuvor.

Es wurde deutlich, daß erst mit dieser Informationsdichte die Rekonstruktion der Prozesse im Bereich der aktiven Rinne möglich sein wird. Aus den bathymetrischen Daten und einer vorläufigen Auswertung der seismoakustischen Datensätze ergibt sich, daß in vielen Fällen die beobachteten Strukturen, die sich in der Seismik z.T. durch völlige Transparenz auszeichnen, älteren Rinnen repräsentieren, die sich bei Mäanderdurchstichen in Totarme verwandelten und rasch zusedimentiert wurden. Nach dem kleinräumigen Survey wurden noch mehrere längere Seismikprofile vermessen, die wie schon zuvor eine starke Variabilität hangabwärts dokumentierten.

Alles weist darauf hin, daß der Bengalfächer in diesem Abschnitt auch im Holozän eine sehr dynamische Entwicklung erfährt. Viele der beobachteten Strukturen im letzten Arbeitsgebiet weisen Ähnlichkeiten mit Flußsystemen an Land auf und es wird eine spannende Aufgabe werden, nach Auswertung unserer Daten einen Vergleich zu ziehen, um die physikalischen Prozesse besser zu verstehen.

Nach dem Ablaufen aus dem Vermessungsgebiet erfolgt ein letztes längeres Meßprofil, bevor am 14.11. gegen 23 Uhr Bordzeit alle Systeme eingeholt und für den Flachwassereinsatz auf der nächsten Reise präpariert wurden. Während der gesamten letzten

Woche präsentierte sich das Wetter von seiner allerbesten Seite mit Sonnenschein und teils spiegelglatter See - also beste Bedingungen für sehr hochauflösende seismische Untersuchungen. Inzwischen haben wir Kurs auf Chittagong genommen, wo wir am 16. gegen 8 Uhr auf der Außenreede den Lotsen erwarten werden. Dann geht eine sehr erfolgreiche Forschungsreise zu Ende, die wir auch als Verpflichtung für die nachfolgenden wissenschaftlichen Arbeiten ansehen. Eine Fortsetzung des wissenschaftlichen Programms erfährt diese Reise auf SO 126, wenn im gleichen Arbeitsgebiet Sedimentkerne gezogen werden. Dann wird es für ausgesuchte Lokationen möglich sein, ein besseres Verständnis der physikalischen Strukturen im Sediment und zeitliche Abfolgen zu gewinnen.

Mit diesem Bericht verabschiedet sich die wissenschaftliche Crew auch mit einem Dank für die in jeder Hinsicht freundliche Zusammenarbeit und die kompetente Unterstützung von der Schiffsbesatzung unter Kapitän Kalthoff.

Es grüßen aus dem sommerlich sonnigen Golf von Bengalen
die GeoB Seismiker

Appendix C

Cruise report SO 126 - Bengal Shelf,

Chapter 8

(originally published in Kudrass, H.-R., 1998. Cruise Report SO 126, p. 29-60)

8 Parasound and Hydrosweep

C. Hübscher, M. Breitzke, L. Kruse, G. Mollenhauer

8.1 Introduction

The hydroacoustical systems of R/V Sonne Cruise SO126 were continuously operated to collect sediment echosounder and swath sounder data from late Quaternary deposits on the Bengal Shelf. The particular scientific targets were the

- prograding foreset beds,
- acoustic voids within topset and foreset beds,
- gassy sediments within topset beds,
- sub-aerial river delta on the late Pleistocene land surface on the outer shelf,
- lowstand wedge at the outer shelf,
- erosional structures at the shelf break,
- sedimentary deposits in the Swatch of No Ground.

Working areas on the shelf are located in the national waters of Bangladesh between 89°30'E and 92°E (Fig. 8.1). The Hydrosweep swath sounder and the Parasound sediment echosounder are permanently installed on R/V Sonne. The Hydrosweep system provides topographic information of a width of twice the water depth. The Parasound sediment echosounder uses frequencies around 4 kHz, which allow signal penetration between 10 and 100 m depending on sediment composition and grain size. Digital echosounder data were routinely collected with the help of all scientists onboard by participating in the 24-hour watch keeping duties.

8.2 Instruments

8.2.1 PARASOUND

The PARASOUND system works both as a low-frequency sediment echosounder and as high-frequency narrow beam sounder to determine the water depth. It makes use of the parametric effect, which produces additional frequencies through nonlinear acoustic interaction of finite amplitude waves. If two sound waves of similar

frequencies (here 18 kHz and e.g. 22 kHz) are emitted simultaneously, a signal of the difference frequency (e.g. 4 kHz) is generated for sufficiently high primary amplitudes. The new component is traveling within the emission cone of the original high frequency waves, which are limited to an angle of only 4° for the equipment used. Therefore, the footprint size of 7% of the water depth is much smaller than for conventional systems and both vertical and lateral resolution are significantly improved.

The PARASOUND system is permanently installed on the ship. The hull-mounted transducer array has 128 elements on an area of ~1 m^2. It requires up to 70 kW of electric power due to the low degree of efficiency of the parametric effect. In 2 electronic cabinets, beam forming, signal generation and the separation of primary (18, 22 kHz) and secondary frequencies (4 kHz) is carried out. With the third electronic cabinet in the echosounder control room the system is operated on a 24 hour watch schedule.

Since the two-way travel time in the deep sea is long compared to the length of the reception window of up to 266 ms, the PARASOUND System sends out a burst of pulses at 400 ms intervals, until the first echo returns. The coverage of this discontinuous mode depends on the water depth and produces non-equidistant shot distances between bursts. On average, one seismogram is recorded about every second providing a spatial resolution on the order of a few meters on seismic profiles at 4.9 knots.

The main tasks of the operators are system and quality control and the adjustment of the start of the reception window. Because of the limited penetration of the echosounder signal into the sediment, only a short window close to the sea floor is recorded.

Beyond the analog recording features with the b/w DESO 25 device, the PARASOUND System was equipped with the digital data acquisition system ParaDigMA, which was developed at the University of Bremen (Spieß, 1993). The data were stored directly on 6250 bpi, 1/2" magnetic tapes using the standard, industry-compatible SEGY-format. The 486-processor based PC allows the buffering, transfer and storage of the digital seismograms at very high repetition rates. From the emitted series of pulses usually every second pulse could be digitized and stored, resulting in recording intervals of 800 ms within a pulse

sequence. The seismograms were sampled at a frequency of 40 kHz, with a typical registration length of 266 ms for a depth window of ~200 m. The source signal was a band limited, 2-6 kHz sinusoidal wavelet of 4 kHz dominant frequency with a duration of 1 periods (~250 μs total length).

Already during the acquisition of the data an online processing was carried out. For all profiles Parasound sections were plotted with a vertical scale of several hundred meters. Most of the changes in window depth could thereby be eliminated. From these plots a first impression of variations in sea floor morphology, sediment coverage and sedimentation patterns along the ships track could be gained. To improve the signal-to-noise ratio, the echogram sections were filtered with a wide band pass filter. In addition the data were normalized to a constant value much smaller than the maximum average amplitude, to amplify in particular deeper and weaker reflections.

To study the influence of frequency and length of the source signal on the reflection pattern, these parameters were systematically varied at sites, where gravity or piston cores were recovered ('source signal test'). The frequency of the source signal was changed in 0.5 kHz steps over the available frequency range from 2.5 to 5.5 kHz, while the pulse length was set to 1, 2, and 4 sinus periods. The setting was kept for a time span of 2 minutes to enable later signal stacking and an evaluation of the variability of seismograms from the same location. In order to quantify interference phenomena, seismograms recorded with different frequencies will be studied in more detailed, shore based analyses in comparison with physical property logs from the cores.

8.2.2 HYDROSWEEP

The multibeam echosounder HYDROSWEEP on R/V SONNE was routinely used during the cruise and serviced by the system operator and the electronics engineers. During a 24 hour watch the scientific crew operated continuously both the HYDROSWEEP and the PARASOUND echosounder systems in parallel. The HYDROSWEEP System worked without major technical problems. The multi-beam sounder provided a complete coverage of the sea floor topography with a swath

width of twice the water depth. The data quality was generally good with data losses at higher speeds and due to high sea states.

8.3 First Results

A Parasound section crossing the western survey area exhibits the foreset and bottomset beds, the outer continental shelf, and the shelf break (Fig. 8.2). Within the upper foreset acoustic voids are present. The prograding clinoforms beneath the outer shelf have been interpreted as a regressive lowstand wedge by Hübscher et al. (1998). Wiedicke et al. (submitted) identified the pinnacles on top of the wedge as oolitic beach barriers of late Pleistocene age. Clinoforms prograding towards the shelf break are visible beneath the lowstand wedge.

A Parasound section from the topset beds in the western survey (Fig. 8.3) area shows the differences in the acoustic characteristics of gassy and mobilized sediments (acoustic voids). The acoustic voids do not attenuate seismic energy. They have linear boundaries, the upper and lower boundaries show no increased reflection coefficient compared to the reflections beside the acoustic voids. In opposite, the top of the gassy sediments is an irregular strong reflection that prevents deeper signal penetration.

An app. 50 km long Parasound section parallel to the foreset beds was plotted in order to study lateral variations in bed thickness and growth patterns of the prograding subaqueous delta (Fig. 8.4). Most of the sub-parallel reflections run continuously from West to the East without significant variations in bed thickness.

Fluvial incised valley fill deposits characterize the late Pleistocene land surface, an almost 10 km wide and up to 10 m thick example with complex reflection patterns is presented in Fig. 8.5. The covering transgressive veneer exhibits erosional structures.

An intricate pattern of erosional and downlapping unconformities of sea-floor near sedimentary units close to the shelf break shows the Parasound section in Fig. 8.6. The strong erosion indicates a shallow marine environment as it was present during the last glacial maximum.

Canyon deposits from the Swatch of No Ground include well layered deposits with intercalated slumps (Fig. 8.7). The profile strikes parallel to the canyon axis.

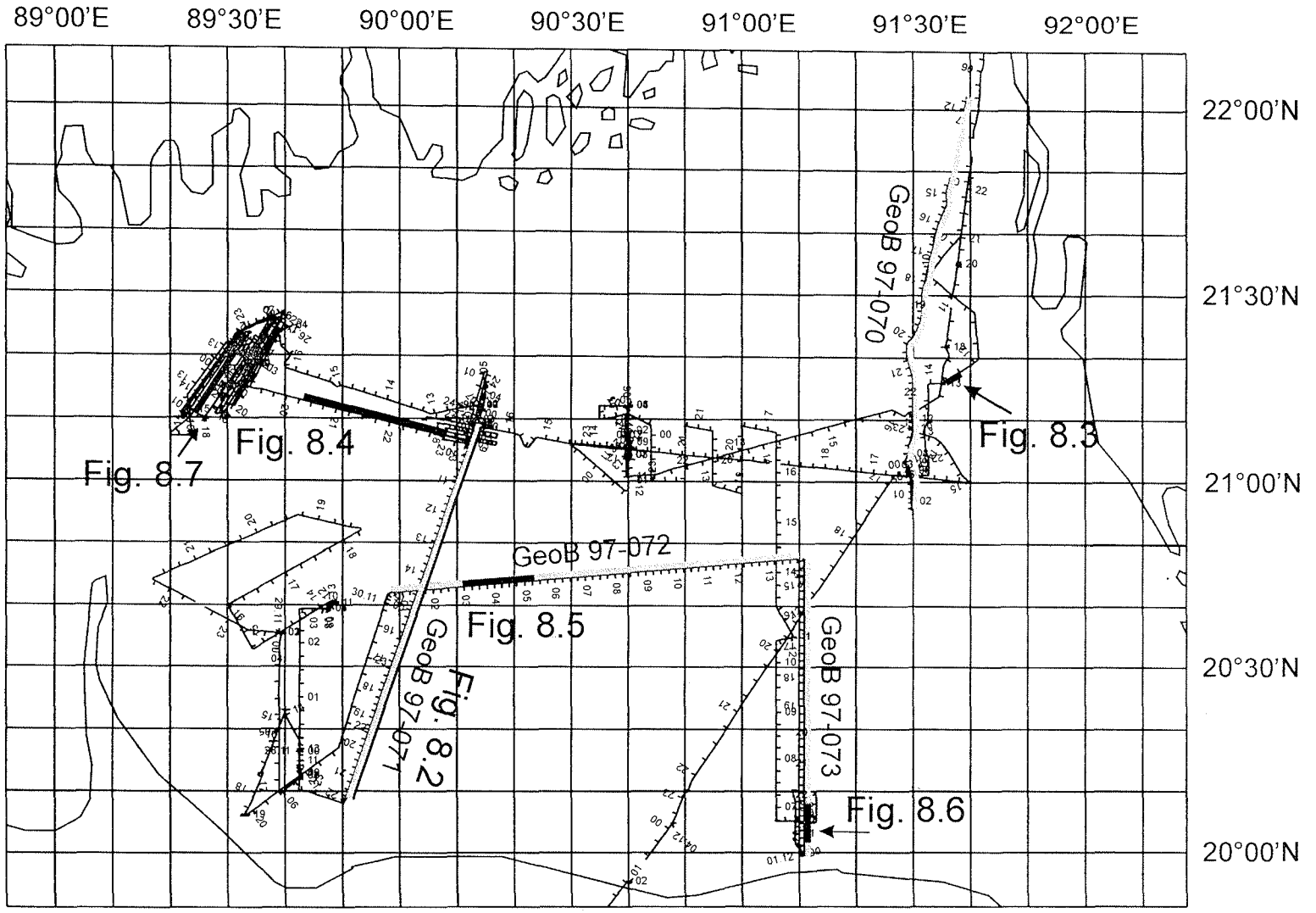

Fig. 8.1: Track chart SO126 on the Bengal Shelf. Seismic lines are marked with grey bars, figures with black bars.

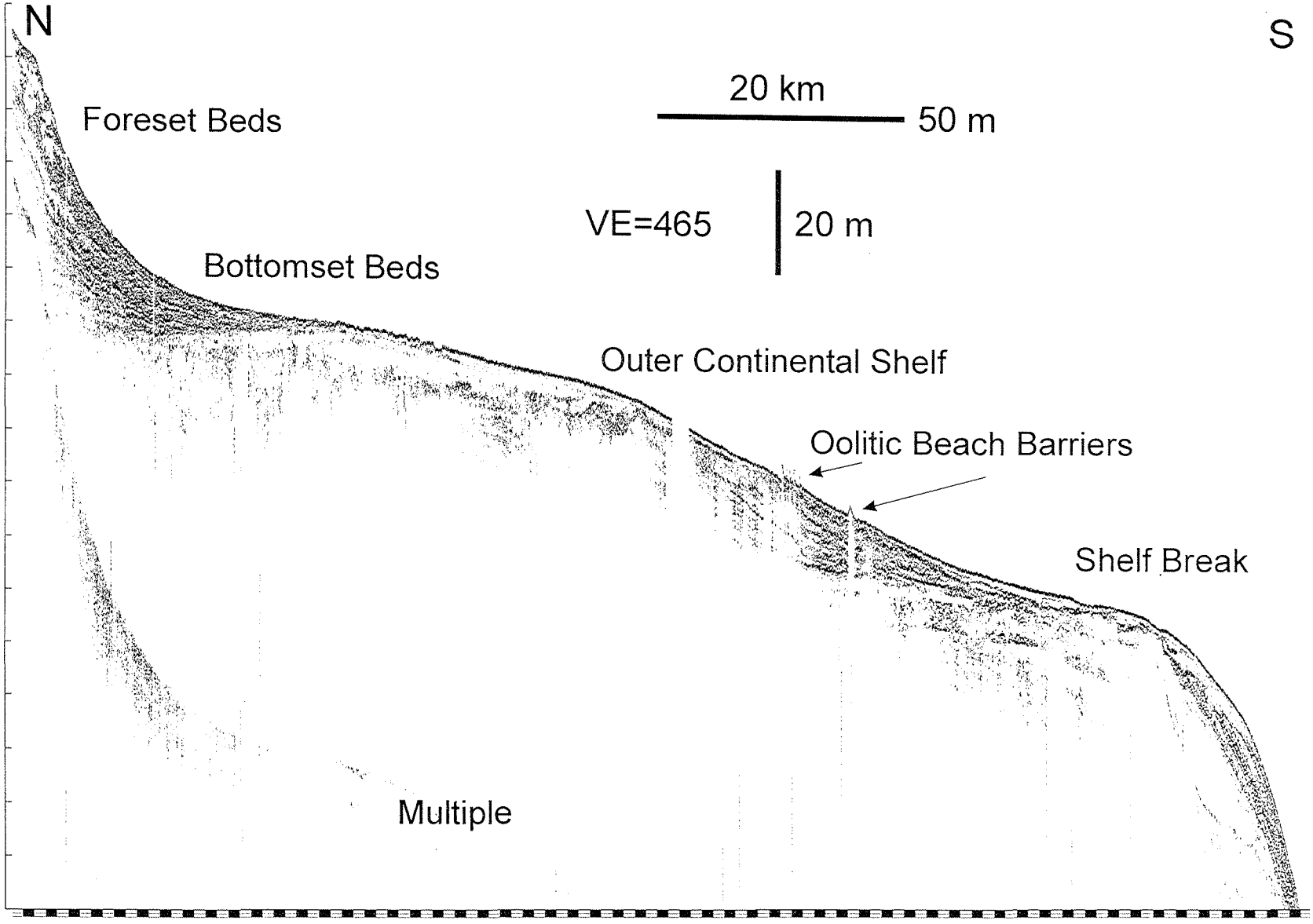

Fig. 8.2: Parasound section crossing foreset, continental shelf and shelf break.

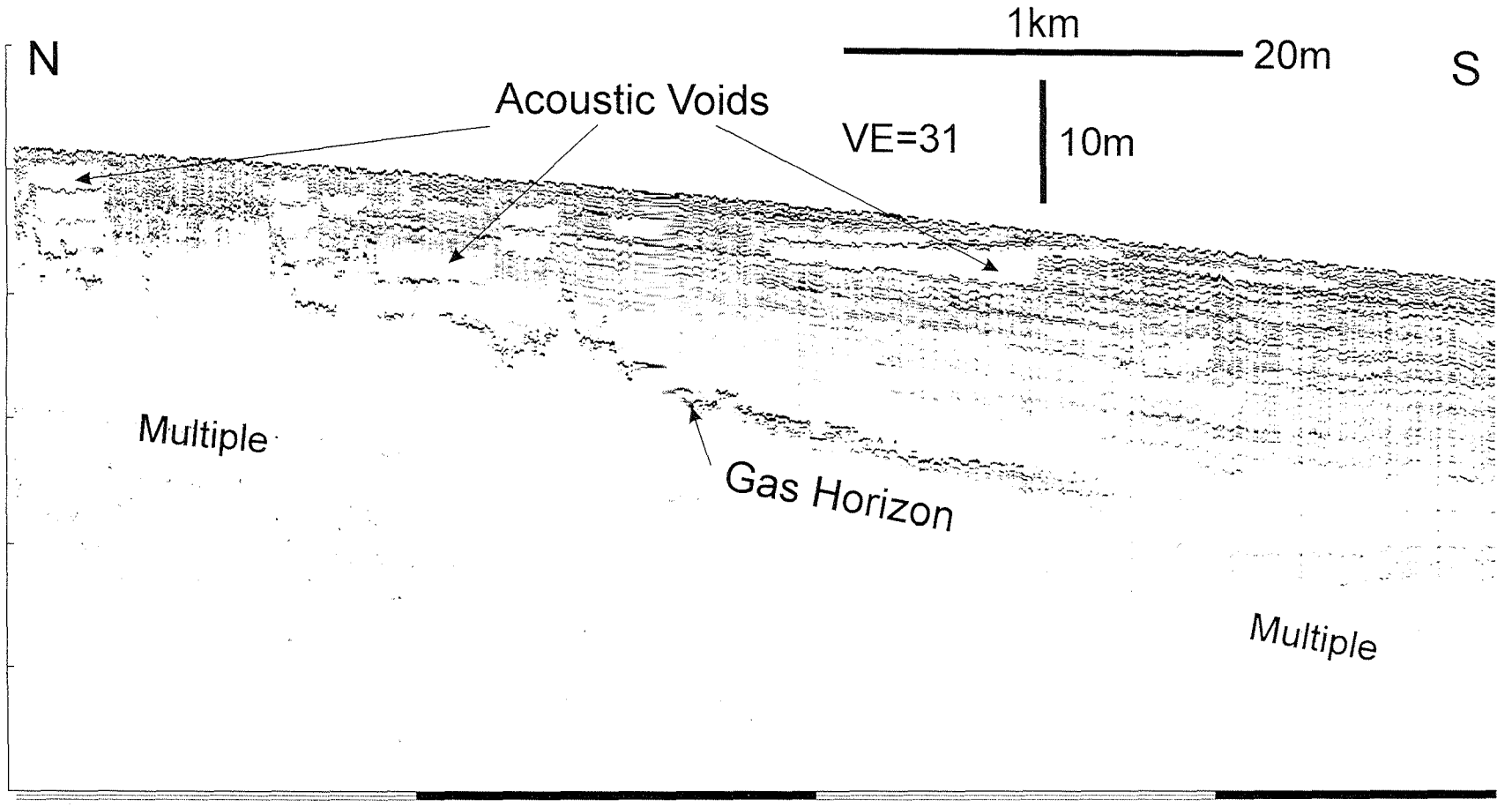

Fig. 8.3: Gassy sediments and acoustic voids within topset beds.

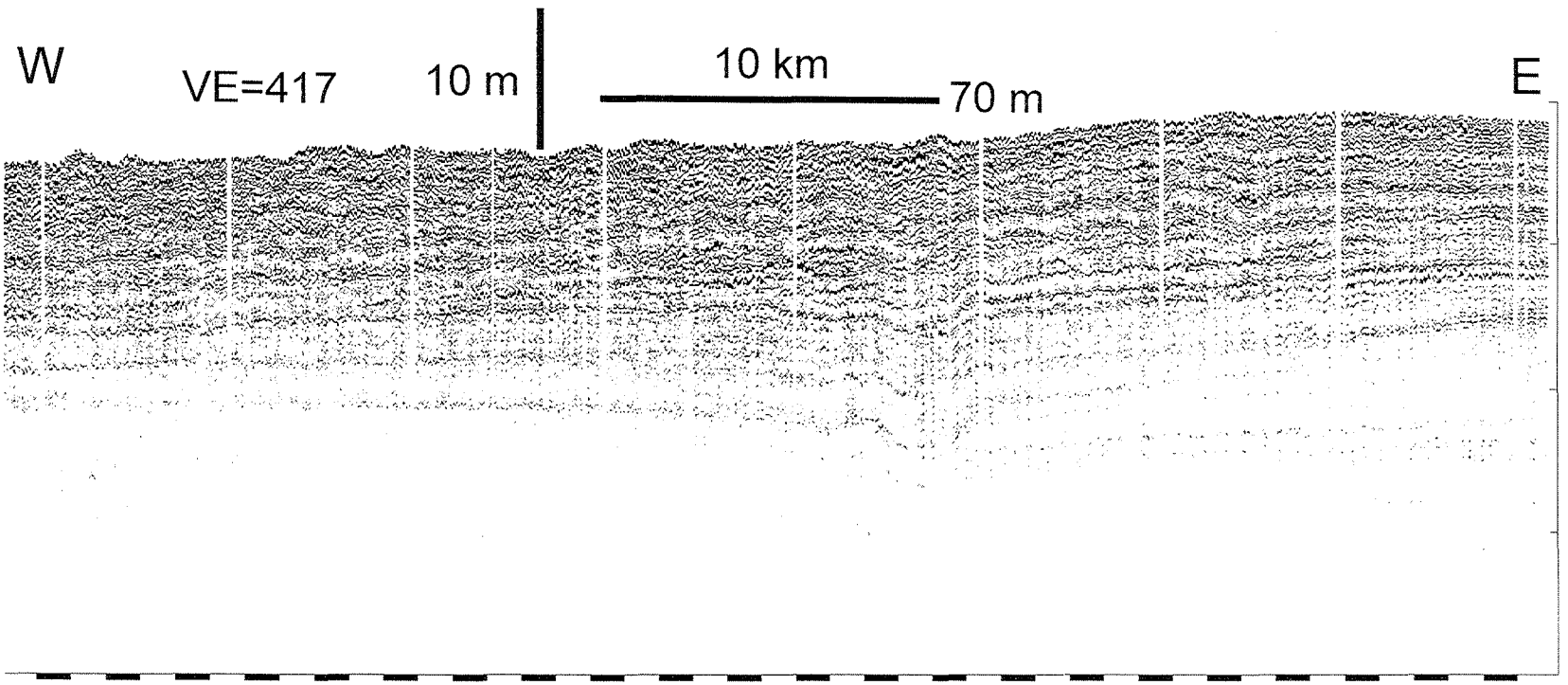

Fig. 8.4: Parasound section parallel to foreset beds.

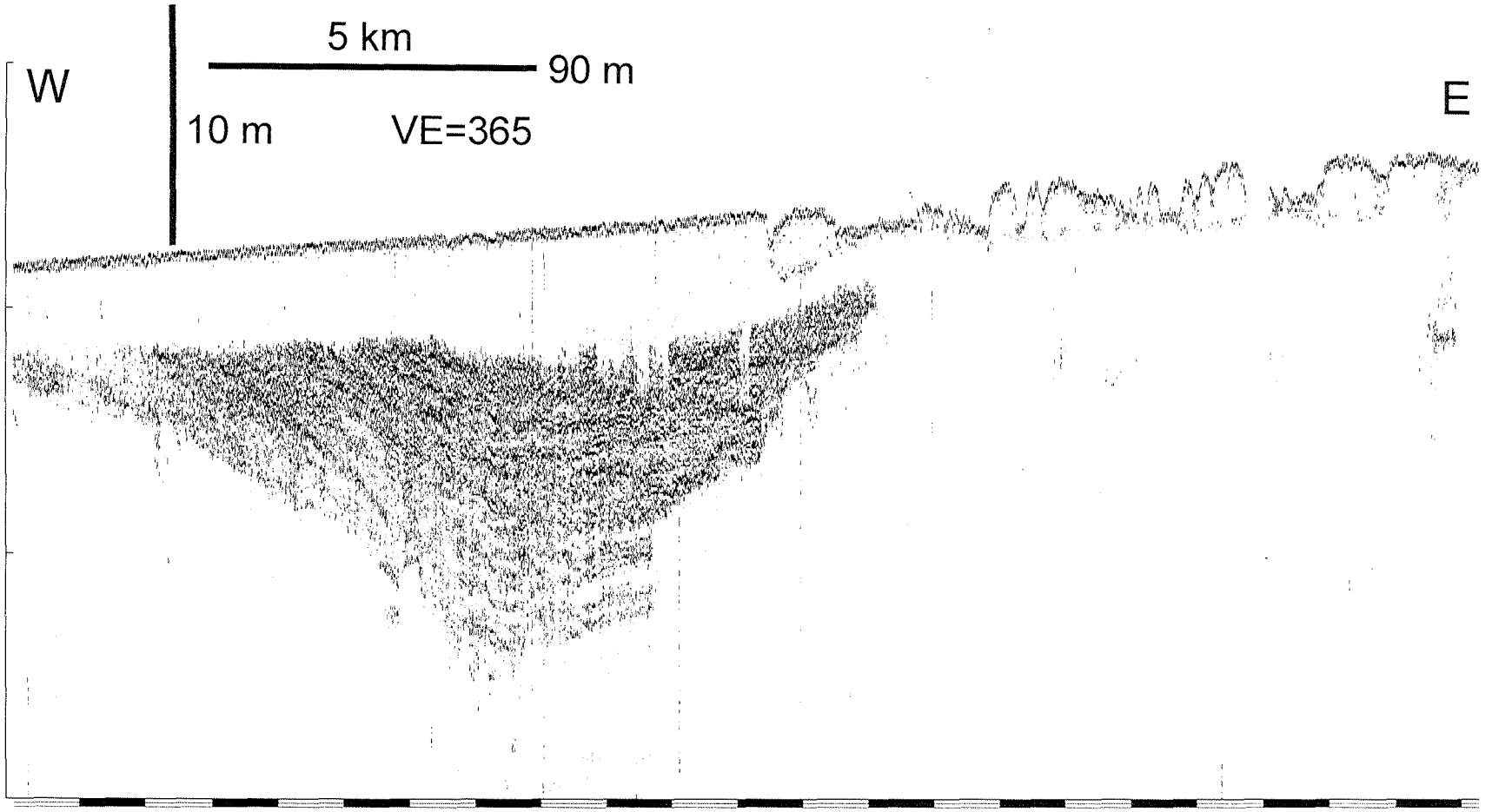

Fig. 8.5: Incised valley fill deposits and eroded late Pleistocene land surface.

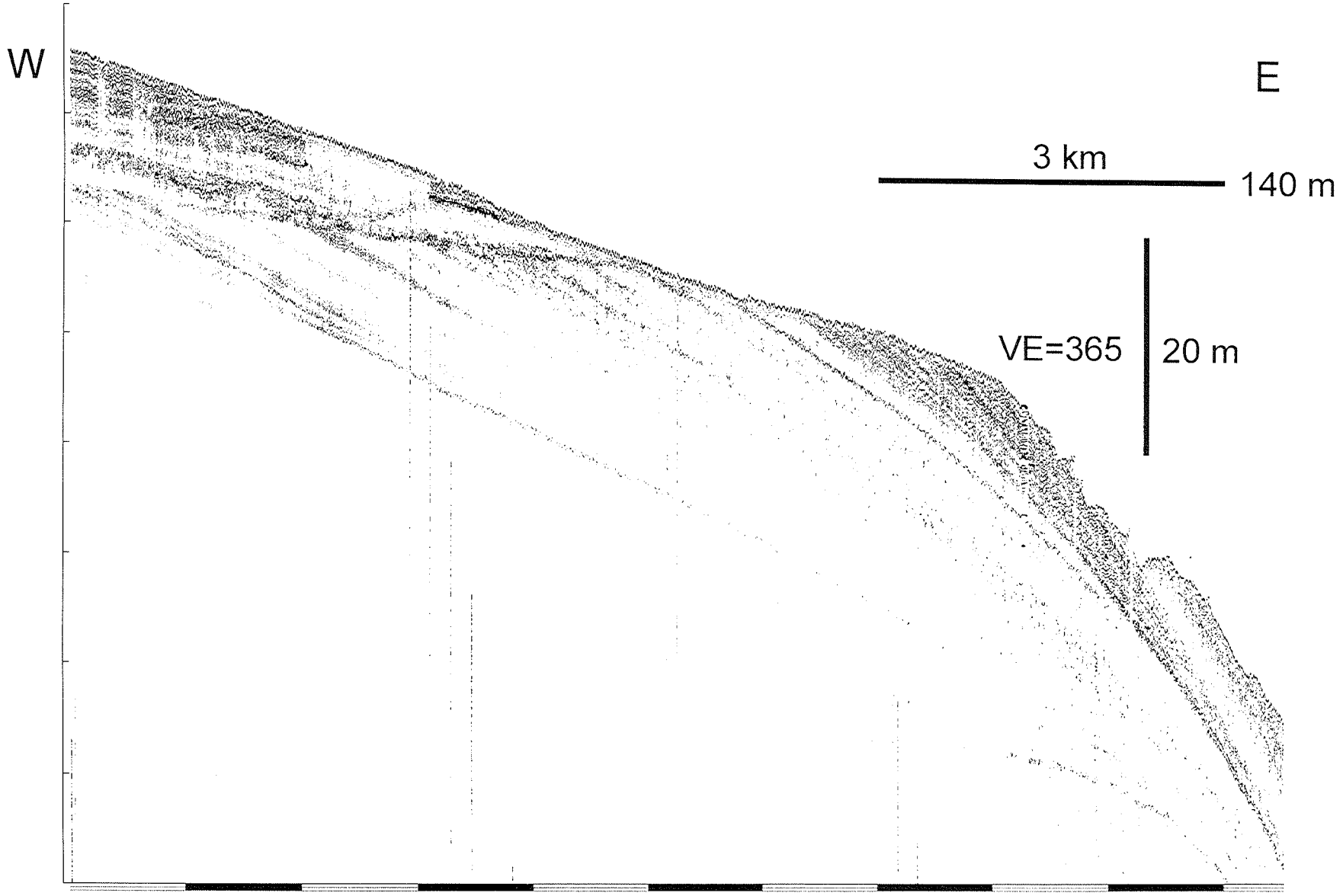

Fig. 8.6: Erosional unconformities of sea-floor near sedimentary units close to the shelf break.

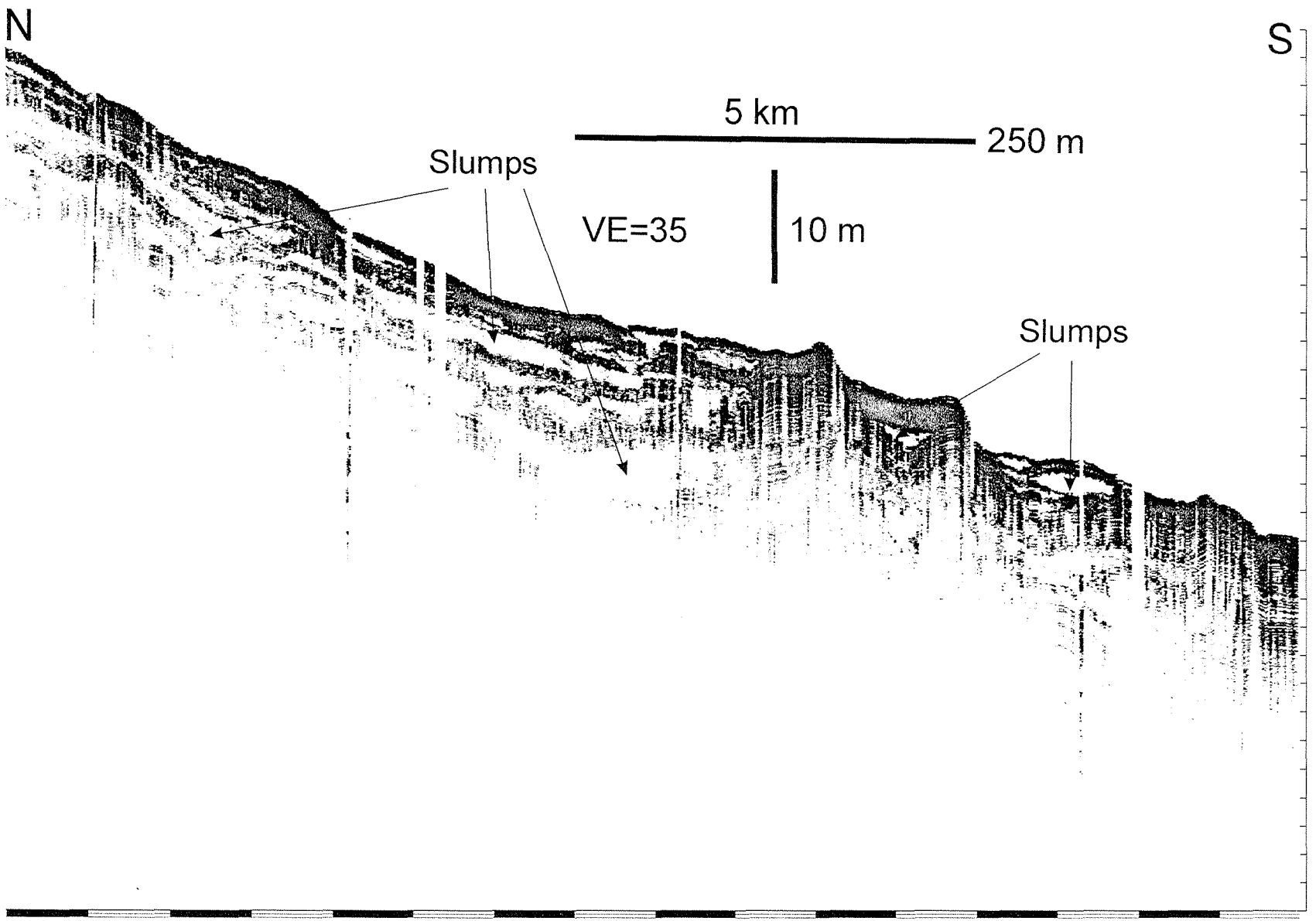

Fig. 8.7: Slumps and well layered deposits characterize the deposits on the floor of the Swatch of No Ground.

Appendix D

Cruise report SO 126 - Bengal Shelf,

Chapter 9

(originally published in Kudrass, H.-R., 1998. Cruise Report SO 126, p. 61-66)

9 Very High-Resolution Multichannel Reflection Seismics

C. Hübscher, M. Breitzke, L. Kruse, G. Mollenhauer

9.1 Introduction

Multichannel seismic measurements were carried out with a new instrumentation of the Department of Earth Sciences, Bremen University, utilizing two seismic sources of different volume in an alternating mode (Fig. 9.1). A SODERA Inc. S-15 water gun with a frequency range from 200 to 2000 Hz provides information of the upper 100 to 300 m of the sediment column, whereas a GI-Gun (Generator-Injector Gun; SODERA Inc.) with signal energy up to 500 Hz allows seismic imaging of sedimentary layers down to 1000-2000 m below sea-floor. A total of 470 km of multichannel data were collected along 4 seismic lines (Fig. 8.1; Tab. 9.1).

Profile Seis. Sources	Start: Date/Time	Latitude Longitude	End: Date/Time	Latitude Longitude	Shots	Length (km)
GeoB97-070 WG	21.11.97 11:04	22°04.6'N 91°40.1'E	22.11.97 01:01	20°58.2'N 91°30.9'E	15400	125
GeoB97-071 GI/WG	27.11.97 09:00	21°08.6'N 90°13.2'E	27.11.97 22:24	20°00.8'N 89°49.7'E	6700	133
GeoB97-072 GI/WG	29.11.97 04:20	20°42.0'N 89°58.5'E	29.11.97 14:07	20°47.5N 91°10.5'E	6943	126
GeoB97-073 GI/WG	29.11.97 14:21	20°46.8N 91°10.8'E	29.11.97 23:46	19°59.9'N 91°10.9'E	4800	87

Tab. 9.1. Seismic profiles during SO126. For location see Fig. 8.1.

9.2 Instruments

9.2.1 Trigger Unit

The custom trigger unit controls seismic sources, seismograph, MultiTrak Controller, online-plotter and digital scope (near-field hydrophones). The primary building blocks are an IBM compatible PC, an amplifier unit and a gun amplifier unit. The PC runs a custom software, which controls a real-time controller interface card (SORCUS) with 16 I/O channels, synchronized by an internal clock. The program user interface enables the operator to change trigger times of each device online.

The amplifier unit converts the controller output to TTL levels, which have to be negative for most of the devices. The gun amplifier unit was placed in the pulser station to avoid electronic noise in the seismic lab. It generates the required 60V/8 Amp. trigger level for the magnetic valves of the individual seismic sources.

9.2.2 Seismic sources and compressor

During seismic surveying two different seismic sources, a GI-Gun and a watergun, were triggered in an alternating mode at a time interval of 8 s between sources. However, for Line GeoB 97-070 only the watergun was used. Owing to an average ship speed of 4.9 kn a shot distance of ≈20 m between sources and ≈40 m between the same source were obtained. Both sources were operated with an air pressure of 145 bar. Broken welds at the air exhausting pipes of the watergun had no impact on the source signature. Ship velocity during deployment and retrieval was 3 kn and 2 kn, respectively.

High-pressure air for gun operation was provided by a Junkers compressor which is permanently installed on R/V Sonne and which was maintained by the ship's crew. The compressors were operated according to the requirements of the chosen gun volumes.

The volume of a standard GI-Gun was reduced to 2 x 0.41 l by two special titanium volume reducers. It was towed starboard by a wire from the side crane 26 m behind the ship stern with a lateral offset of 6.3 m on the left hand side of the streamer. The towing wire was connected to a bow with the GI-Gun hanging on two chains 56 cm beneath. An elongated buoy , which stabilized the gun in a horizontal position in a water depth of ~1.4 m, was connected to the bow by two rope loops. The Injector was triggered with a delay of 31 ms with respect to the Generator signal, which basically eliminated the bubble signal.

The second source type was a S15 watergun (Sodera) with a volume of 0.16 l. The waterguns was towed by a Meteor rope, that was fixed to the umbilicals of the waterguns, 26 m behind the ship's stern and at an offset of 4.4 m port side of the streamer. A steel frame held the watergun in a tight position parallel to the elongated buoy in a depth of approximately 0.7 m.

9.2.3 Streamer

For operation in the shallow water environment of the Bengal Shelf only 300 m of the 600 m long streamer were used. The multichannel seismic streamer (SYNTRON) consisted of a tow-lead, one 50 m long stretch section and three active sections of 100 m length each. A 100 m long Meteor rope with a buoy at the end was connected to the tail swivel. A 30 m long deck cable connected the streamer to the recording system. During operations the streamer (tow lead) was fixed with two Meteor ropes. The distance from the ship's stern to the beginning of the stretch section was 40 m.

In order to optimize the frequency response character of the streamer in shallow water and therefore large reflection angles, hydrophone groups consisting of only 2 hydrophones at a distance of 0.32 m were chosen. 24 channels with a midpoint distance of 12.5 m have been recorded.

Ship's speed during deployment and retrieval was 3 kn and 2 kn, respectively. Deployment and retrieval lasted around 30 minutes including installation of the 4 Remote Bird Units (RUs; see below).

9.2.4 Multitrak Bird Controller

In operation 4 MultiTrak Remote Units (RU) were attached to the streamer. The position of RUs is listed in Tab. 9.2. Each RU includes a depth and a heading sensor as well as adjustable wings. The RUs are controlled by the MultiTrak controller in the seismic lab. Controller and RUs communicate via communication coils nested within the streamer. A twisted pair wire within the deck cable connects controller and coils. One wire had to be grounded to avoid communication errors. Each shot trigger started a scan (delay 0.5 s, duration 0.2 s) to retrieve values for water depth, heading, water temperature, and battery voltage. The current location of the streamer (depth or heading versus offset) can be displayed on a monitor. All parameters are digitally stored on the controller PC together with shot number, date, and time.

There are two ways of controlling the streamer depth. The most common way is to define an operating depth for the RUs, which was in most cases 2 m allowing a deviation of up to 1 m in both directions. The RUs adjust wing angles to force the streamer to the chosen depth. Another option is to set a constant wing angle. Depth and wing angle statistics help to find and set appropriate parameters.

streamer to the chosen depth. Another option is to set a constant wing angle. Depth and wing angle statistics help to find and set appropriate parameters.

RU (No.)	Position	Distance to Tow-Lead
1	End of Stretch Section	39 m
2	End of Active Section No. 1	139 m
3	End of Active Section No. 2	239 m
4	End of Active Section No. 3	339 m

Tab. 9.2: RU positions along seismic streamer.

9.2.5 Data acquisition system

The recording unit includes a switch box, a seismograph and a single channel recording unit for online plotting. The switch box connects the streamer via deck cable with the seismograph and allows the assignment and optional stacking of streamer hydrophone subgroups to individual recording channels. The configuration during the cruise remained unchanged.

The 48 channel seismograph (BISON) was specially designed for the University of Bremen, which allows a continuous operation mode for very high resolution seismic data. The seismograph allows online data display, online demultiplexing and storing in SEG-Y format. Analog filters were set to 8 Hz (low-cut) and 4000 Hz (high-cut). The sample rate was 0.1 ms for a recording length of 4000 ms. All channels were pre-amplified by a factor of 1000 (60 dB) to keep the incoming signal within the optimum operation voltage. The data were stored on 2 DLT4000 cartridge tapes with 20 GByte uncompressed capacity. The recording delay had to be adjusted according to the current water depth.

For online immediate graphic information about the acquired seismic data, quality control and storing navigation data, the ParaDigMA acquisition system (see chapter 8) with a Hewlett Packard HP 3852 Data Acquisition Unit (DAU) and a PC was modified to display variable area seismic plots on a DesignJet 350 A1 roll paper plotter.

9.3 First Results

An example of the GI-Gun multi-channel seismic data (Line GeoB 97-071) is shown in Fig. 9.2. The profile covers the seaward part of the digital Parasound section in Fig. 8.2. The data reveal different prograding oblique-tangential reflection patterns, subdivided by unconformities. The different units constitute the primary building blocks of the continental shelf. The upper unit boundaries and the succession of the offlap breaks allow to divide the units in aggrading, prograding, and retrograding units.

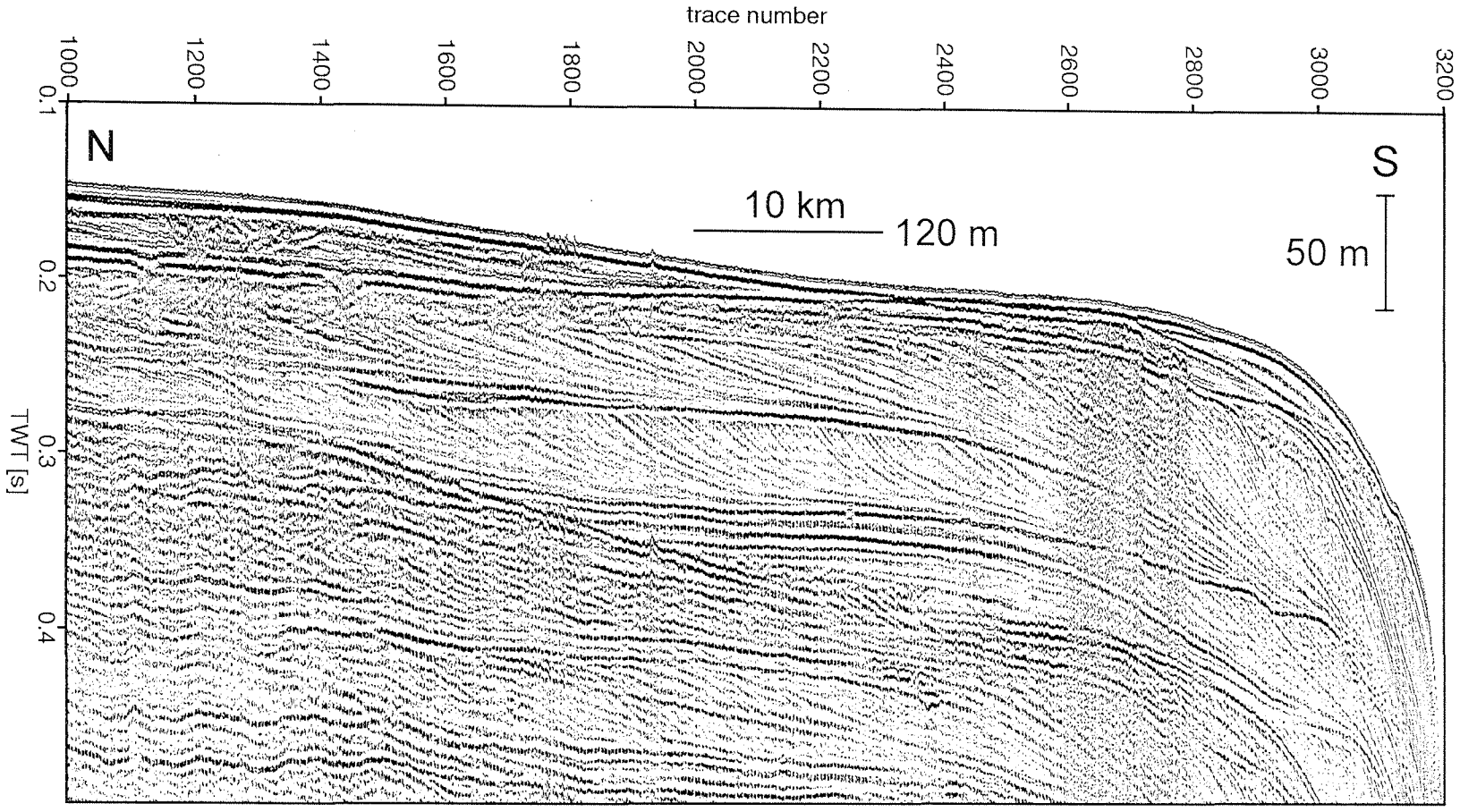

Fig. 9.2: GI-Gun seismic section of the seaward part of Fig. 8.2 (Line GeoB 97-071). For location see Fig. 8.1. Distinctunconformities separate prograding and aggrading reflection units.

Appendix E

Cruise report SO 126 - Bengal Shelf,

Chapter 11.4

(originally published in Kudrass, H.-R., 1998. Cruise Report SO 126, p. 129-160)

11.4 Ultrasonic Full Waveform Core Logging

M. Breitzke, C. Hübscher, L. Kruse, G. Mollenhauer

11.4.1 Introduction

Full waveform ultrasonic transmission seismograms were recorded quasi-continuously on all retrieved sediment cores. The physical background for this method is based on Biot-Stoll's viscoelastic sediment model (Biot, 1956a, b; Stoll, 1989). It considers the unconsolidated, porous, water-saturated sediment as an arrangement of particles which enclose the pore space filled with interstitial pore water. Welded sediment particles and grains in close contact build an elastic frame. Due to the different elastic properties of the solid and fluid components acoustic wave transmission causes a viscous pore water flow relative to the frame as dominant, frequency-dependent damping mechanism. It depends on the size and distribution of the pore space and the stiffness of the frame and affects the P-wave velocity and attenuation as physical parameters. Attenuation is particularly obvious for wavelengths on the order of the microstructure of the sediment, i. e. for wavelengths of few millimeters and frequencies of several hundred Kilohertz. Thus, recording and analysis of ultrasonic P-wave velocities and attenuations provide additional information on fine-scale variations in structure and composition of the sediment which are often primarily controlled by variations in the grain size distribution. Additionally, it allows a visual control of the automated first arrival detection and thus ensures very accurate high-resolution P-wave velocity logs even in coarse-grained sandy layers where attenuation is usually very high and standard first arrival detectors often fail or pick noisy arrivals as first arrivals.

11.4.2 Method

The instruments and laboratory equipment incorporated in the full waveform logging system were described in detail by Breitzke & Spieß (1993) and in the cruise

reports of RV SONNE expeditions SO93/1-3 to the Bengal Fan (Kudrass & Shipboard Scientific Party, 1994). Here, we only summarize the main aspects.

The manufacturer-given dominant frequency of the ultrasonic transducers is 375 kHz, and spectral analysis of reference signals transmitted across a water-filled liner exhibits significant energy between 50 - 500 kHz. This broad frequency band can be used for an attenuation analysis. Radially transmitted ultrasonic signals are digitally recorded by an oscilloscope and stored to a PC's hard disk, so that post-processing methods can later be applied. Transducer transport along the sediment core, distance and diameter measurements and the power with which the transducers are pressed to the core liner by a spring-loaded jig are automatically controlled by a menu-driven FORTRAN program running on the PC. Core diameters are measured at each depth position with an accuracy of 0.01 mm, and power variations of 0.1 N within the spring loaded jig can be resolved.

First arrivals are automatically detected online by a cross-correlation algorithm. It evaluates the travel time difference between the transmitted and a 'zero-offset' signal measured if source and receiver transducer are close together without any core liner in-between. From the travel time t of the first significant maximum of the cross-correlogram and the measured outer core diameter d the P-wave velocity v_P is computed with a relative and absolute precision of 1 - 3 m/s

$$v_P = \frac{d - d_L}{t - t_L}$$

d_L is the double liner wall thickness and t_L the travel time across both liner walls. They amount to 6 mm and 2.4 µs, respectively. Though core logging is only performed if sediment cores reached ambient temperature, laboratory temperature variations between about 20 - 30°C strongly affect P-wave velocity measurements due to the temperature dependence of sound velocity in pore (sea) water. Hence, a temperature correction to 20°C, which accounts for a sound velocity increase of

3 m/s per °C in standard sea water (salinity S=0.035), is additionally applied (Schultheiss & McPhail, 1989)

$$v_{20} = v_P + 3 \cdot (20 - T)$$

v_{20} is the P-wave velocity at 20°C (in m/s), v_P the measured laboratory value of the P-wave velocity at T°C (in m/s) and T the temperature in the sediment core (in °C) measured manually once per core segment with an accuracy of 0.1°C.

As the computation of cross-correlograms implicitly implies bandpass filtering of the data and thus significantly improves the signal-to-noise ratio, very accurate and high resolution P-wave velocity logs can be evaluated online from these transmission seismograms. Compared to P-wave velocity logs derived by GEOTEK's logger having used a zero-crossing method for first arrival detection these P-wave velocity logs are significantly less contaminated by mis-detections of first arrivals particularly in strongly attenuating sandy layers.

Preliminary information on the attenuation of the transmitted signals can online only be derived from their maximum peak-to-peak amplitudes. They neglect any frequency dependence of the signals and are not corrected for a varying power with which both transducers are pressed to the liner wall. A careful, detailed analysis of the frequency-dependent attenuation coefficient by a spectral ratio technique requires much processing time and interactive work and is subject of a later post-processing step (Breitzke et al., 1996).

11.4.3 Shipboard Results

Transmission seismograms were digitally recorded on all gravity, piston and hammer cores with a sampling rate of 20 MHz and a duration of 200 µs starting at a delay of 50 µs. The depth increment of the recordings was 1 cm for all cores retrieved on the Bengal Shelf (03 SL - 47 HL) and for piston core 90 KL from the Lower Bengal Fan. For piston cores 73 KL - 79 KL from the Middle Bengal Fan the

vertical resolution was decreased to 0.5 cm increment. To avoid deteriorations due to the liner caps core logging started and stopped 3 cm apart from both ends of each segment.

The results of full waveform ultrasonic core logging are discussed in detail for piston core 30KL. For the other cores the main, remarkable features of the logging data are summarized with respect to the different coring areas, i. e. for the cores

- 03 SL, 04 SL, 07 SL, 08 SL, 58 KL retrieved from the northeastern shelf,
- 22 KL, 23 KL, 30 KL retrieved from the *Swatch of no Ground,*
- 38 HL, 39KL, 40KL, 41 KL retrieved from the western shelf break,
- 46 HL, 47 HL retrieved from the outer continental shelf,
- 73 KL, 74 KL, 77 KL, 79 KL from the Middle Bengal Fan,
- 90 KL from the Lower Bengal Fan.

Piston Core 30KL: Transmission Seismograms, Amplitude Spectra and Grey-Shaded Full Waveform Core Logs

Piston core 30KL was retrieved from the main active channel of the Bengal Fan, the *Swatch of no Ground*, on top of a well stratified slump sequence in 306 m water depth. After multi-sensor and full waveform logging the core was split. A visual inspection and description of the sediment yields a series of cyclic turbidite events with graded, upward-fining sequences probably correlated with the cyclone history in the study area (Michels et al., 1998).

Figure 11.4.1 presents the full waveform transmission seismograms collected on segment no. 6 between 454 and 554 cm depth. They are normalized to their maximum values in order to facilitate a comparison between different, highly and weakly attenuated signal shapes. The dashed line at the onsets indicate automatically picked first arrivals. Resulting P-wave velocities (without temperature correction, in m/s) and maximum peak-to-peak amplitudes (in mV) are shown on the right-hand side.

The transmission seismograms show distinct changes in their waveform which obviously correlate with variations in the lithology described by the visual core inspection. High-frequency signals indicate fine-grained clayey sediments while low-frequency signals appear at the coarse-grained base of turbiditic events. P-wave velocities and maximum peak-to-peak amplitudes are inversely correlated. High P-wave velocities of maximum 1600 m/s and low amplitude values occur at coarse-grained turbidite bases while low P-wave velocities and high amplitude values indicate fine-grained sediments. Gradually decreasing P-wave velocities (increasing first arrival times) and increasing peak-to-peak amplitudes clearly reflect upward-fining sediment compositions above the turbidite bases.

The amplitude spectra computed from the dominant wavegroup between 50 - 150 µs show the general frequency content of the transmission seismograms and provide further insight in the relation between frequency-dependent attenuation and lithological variations, particularly in the grain size distribution of the sediment (Fig. 11.4.2). They are also normalized to their maximum values in order to illustrate the energy shift from high- to low-frequency components. Informations on spectral amplitude variations of the 375 kHz component and on the dominant frequency of the spectra are displayed in both logs on the right-hand side.

Generally, the spectra contain several frequency bands between 50 - 500 kHz, resulting from internal reflections and resonance characteristics of the ultrasonic transducers (wheel probes). Usually, in weakly attenuating sediments the energy is concentrated in a frequency band between about 350 - 450 kHz. The dominant frequency is 375 kHz, and its spectral amplitude is high. An increasing amount of coarse-grained particles within a graded bedding causes an enhanced attenuation of the high-frequency components so that the lower frequency bands become more significant. At sandy turbidite bases the spectral components around 80 kHz prevail and cause a shift in the dominant frequency from 375 to 80 kHz.

In order to display the complete information of full waveform ultrasonic core logging on a handy scale the transmission seismogram amplitudes are converted to a grey-shaded pixel graphic. Together with the P-wave velocity (after temperature

correction) and maximum peak-to-peak amplitude logs this graphic display provides an ultrasonic image of the sediment core lithology already onboard. For piston core 30 KL it yields a lot of fine-scale turbidite events (Fig. 11.4.3). P-wave velocities generally reveal a slightly increasing trend from 1470 to 1490 m/s in the fine-grained parts. At the coarse-grained turbidite bases they vary between 1510 and 1600 m/s and thus probably indicate finer or coarser grain sizes. Maximum peak-to-peak amplitudes are generally inversely correlated. Unfortunately, probably due to the new piston corer technique used on this cruise and probably due to the large piston core diameter (≈125 mm) amplitudes periodically increase at both ends of each segment due to a slightly increased core diameter. These larger diameters cause a slightly increased power with which the ultrasonic transducers are pressed to the liner walls and, thus simultaneously enhanced signal amplitudes. They have to be corrected to a constant power prior to a frequency-dependent attenuation analysis.

Summary for all sediment cores

The grey shaded display of the transmission seismograms combined with the P-wave velocity and maximum peak-to-peak amplitude logs is used to give an overview on the full waveform logging data collected on all sediment cores and on the lithology imaged by these recordings (Figs. 11.4.5 - 11.4.23). Additionally, mean values and standard deviations are computed for the P-wave velocity and amplitude log of each core and are displayed in Figure 11.4.4 together with the recovered core lengths and the water depths of each coring site. While the mean values approximately indicate different trends and illustrate the average P-wave velocity and amplitude of the ultrasonic signals recorded on each core, the standard deviations roughly reflect both the amount and the maximum difference between the highest and lowest values of downcore variations. For instance, a large number of sandy layers embedded in clayey sediments and a large difference between maximum and minimum P-wave velocity will cause a large standard deviation.

Northeastern shelf (03 SL, 04 SL, 07 SL, 08 SL, 58 KL)

The sediments of the northeastern shelf were sampled by gravity cores 03 SL, 04 SL, 07 SL, 08 SL and by piston core 58 KL. They were retrieved from water depths between 28 and 61 m with core lengths of 3.78 and 5.28 m recovery.

The high-frequency character of the transmission seismograms and the low P-wave velocity values of 1480 - 1490 m/s indicate very fine-grained sediments in core 03 SL (Fig. 11.4.5). Thin beds of coarser grain sizes and less than 10 cm thickness are embedded in these sediments and can easily be identified from higher P-wave velocities of 1510 - 1540 m/s and very low amplitudes of less than 10 mV, in some layers even less than 1 mV. Generally, the amplitudes of the transmitted ultrasonic signals are unusually low for fine-grained sediments (mean amplitude < 10 mV, Fig. 11.4.4) and might either be interpreted by an unusual microstructure or sediment frame or might indicate a very low amount of gas captured in the pore space.

Cores 04 SL and 58 KL are composed of an interlayering of fine- and coarse grained sediments which can be identified from downcore varying high- and low-frequency waveforms, low- and higher P-wave velocities and inversely correlated amplitudes (Figs. 11.4.6 and 11.4.18). Rather high P-wave velocities characterize core 04 SL, particularly in obviously fine-grained parts, e. g. between 1.10 - 1.90 m depth. Here, P-wave velocities of about 1540 m/s - derived from high-frequency signals - are positively correlated with increased amplitude values of 100 - 200 mV. In contrast, waveforms of a similar shape only reveal P-wave velocities of about 1510 m/s in core 58 KL, accompanied by similar amplitude values of 100 - 200 mV.

These unusually high P-wave velocities and the positively correlated high amplitudes possibly result from a significant shear modulus of the sediment which increases the P-wave velocity but leaves the attenuation coefficient unchanged. This is obviously also valid for core 08 SL (Fig. 11.4.8) which sampled two successive acoustic voids. They appear as transparent intervals in the PARASOUND recordings (compare Fig. 8.3) and correlate with almost homogeneous sediments between 1.00 - 2.05 m and 2.15 - 3.5 m depth. Almost constant P-wave velocities of about

1550 m/s were measured in the upper and of 1550 - 1600 m/s in the lower part. A significant velocity decrease to 1500 m/s at 2.1 m depth can obviously be associated with a reflection horizon in the PARASOUND recordings between both acoustic voids.

The gas horizon appearing below the acoustic voids in the PARASOUND seismogram section in Figure 8.3 moves close to the sea floor nearby the coring site of 08 SL. Core 07 SL was retrieved from such gassy sediments (Fig. 11.4.7). A few amount of gas bubbles enclosed in the pore water cause the noisy, highly scattered transmission signals.

Swatch of no Ground (22 KL, 23 KL, 30 KL)

Piston cores 22 KL, 23 KL and 30 KL sampled the sediments on top of well stratified slump sequences in the main active channel of the Bengal Fan, the *Swatch of no Ground* (Figs. 11.4.9 - 11.4.11). Water depths vary between 306 and 564 m and cores were retrieved with 14.65 to 17.17 m recovery. All cores reveal a series of cyclic turbidite events which might be associated with the cyclone history of the Bengal Shelf and cause very high sedimentation rates (Michels et al., 1998). They are characterized by graded upward-fining sediment compositions already discussed above for core 30 KL. Their thickness ranges from few centimetres to several decimetres. P-wave velocities are low and on the average range between 1480 - 1500 m/s (Fig. 11.4.4), values typical for fine-grained, high-porosity sediments. Accordingly, maximum amplitudes of the transmitted ultrasonic signals are high and on the average amount to 150 mV.

Western shelf break (38 HL, 39 KL, 40 KL, 41 KL)

Hammer core 38 HL was retrieved close to the western shelf break from 131 m water depth (Fig. 11.4.12). Recovery was 5.50 m but the upper 50 cm of the core top are destroyed and could not be logged. Sediments are rather fine-grained and reveal P-wave velocities of about 1500 m/s and amplitudes of 100 - 200 mV.

Piston cores 39 KL, 40 KL and 41 KL were retrieved from successively decreasing water depths (318 - 180 m) along the shelf break in order to sample different depth intervals of an outcropping layer sequence (Figs. 11.4.13 -11.4.15). Recoveries ranged between 6.22 m for the shallow (41 KL) and 10.41 m for the deepest site (39 KL). Ultrasonic core logging is significantly affected by gas in the lower parts of cores 39 KL and 40 KL. Transmitted signals were strongly attenuated so that P-wave velocities could not be evaluated. Only in core 41 KL there was no evidence for gas. It mainly consists of clayey to silty sediments with average P-wave velocities of 1540 m/s and amplitudes of 100 mV (Fig. 11.4.4). Some sandy layers below 3.5 m depth can be identified from high P-wave velocities of maximum 1650 m/s.

Outer continental shelf (46 HL, 47 HL)

The hammer cores 46 HL and 47 HL sampled the sediments of the outer continental shelf in water depths of 86 - 148 m (Figs. 11.4.16 - 11.4.17). Recoveries in this silty and sandy sediments were 4.65 and 5.30 m. Changes in the ultrasonic signal shape and variations in P-wave velocities and maximum amplitudes between 1500 - 1700 m/s and 2 - 200 mV clearly reflect lithological changes.

Middle Bengal Fan (73 KL, 74 KL, 77 KL, 79 KL)

Piston cores 73 KL, 74 KL, 77 KL and 79 KL were retrieved from different parts of the segmented structure of the channel levee system built up during the holocene by the main active channel (Hübscher et al., 1997). These cores support the seismic and PARASOUND echosounder surveys of the preceding RV SONNE cruise SO125. Piston core 74 KL was imploded so that 77 KL was recovered from almost the same coring site. Water depths varied between 2565 - 2571 m and recoveries ranged from 13.84 - 14.74 m. The sediments are almost homogeneous and very fine-grained and show low P-wave velocities of 1480 - 1500 m/s and high amplitudes of 100 - 200 mV. Only very fine-scale, few centimetres thin beds of probably slightly coarser grain sizes can be identified from peaks of slightly increased P-wave velocities (up to

1530 m/s) in core 73 KL and particularly in the lower part of 79 KL. Only core 77 KL reveals a thick silty to sandy layer between 8.3 to 9.5 m depth, with maximum P-velocities of 1600 m/s, and a series of graded beddings with clayey to silty sediment compositions below 9.5 m depth.

Maximum amplitude logs are deteriorated by increased amplitudes at both ends of each segment. They result from an increased power with which the ultrasonic wheel probes are pressed to the liner wall due to slightly increased core diameters at both ends of each segment. Corrections to a constant power are necessary during post-processing prior to a detailed attenuation analysis.

Lower Bengal Fan (90 KL)

Piston core 90 KL sampled the sediments on top of a levee of the active channel in the Lower Bengal Fan and also supports the seismic and PARASOUND echosounder studies of RV SONNE cruise SO125. It was retrieved from 3269 m water depth with 12.33 m recovery. It is composed of an interlayering of fine- and very coarse-grained sediments which yield P-wave velocities and amplitudes of 1490 - 1500 m/s and about 150 mV in fine-grained parts and of maximum 1680 m/s and less than 5 mV in coarse-grained parts, particularly below 9.5 m depth.

11.4.4 References

Biot M. A. (1956a). Theory of wave propagation of elastic waves in a fluid-saturated porous solid. I. Low-frequency range. Journal of the Acoustical Society of America, 28, 168 - 178

Biot M. A. (1956b). Theory of propagation of elastic waves in a fluid-saturated porous solid. II. Higher frequency range: Journal of the Acoustical Society of America, 28, 179 - 191.

Breitzke M., Spieß V. (1993). An automated full waveform logging system for high-resolution P-wave profiles in marine sediments. Marine Geophysical Researches, 15, 297 - 321

Breitzke M., Grobe H., Kuhn G., Müller P. (1996). Full waveform ultrasonic transmission seismograms - a fast new method for the determination of physical and sedimentological parameters in marine sediment cores. Journal of Geophysical Research, 101, 22123 - 22141

Hübscher, C., Spieß, V. Breitzke, M. & Weber, M. (1997). The youngest channel levee system of the Bengal Fan from digital sediment echosounder data, Marine Geology, 141, 125 - 145

Kudrass, H. R. & Shipboard Scientific Party (1994). SO93/1-3 Bengal Fan - Cruise Report. Federal Institute for Geosciences and Natural Resources, BGR, Hannover.

Michels, K. H., Kudrass, H. R., Hübscher, C., Suckow, A. & Wiedicke, M. (1998). The submarine delta of the Ganges-Brahmaputra: Cyclone-dominated sedimentation patterns. Marine Geology, in press

Schultheiss, P. J., McPhail, S. D. (1989) An automated P-wave logger for recording fine-scale compressional wave velocity structures in sediments. *in* W. Ruddiman, M. Sarnthein et al. (Eds.), Proceedings of the Ocean Drilling Program, Scientific Results, 108, College Station TX (Ocean Drilling Program), 407 - 413

Stoll R. D. (1989) Sediment Acoustics. Springer Verlag, Berlin, 149 pp.

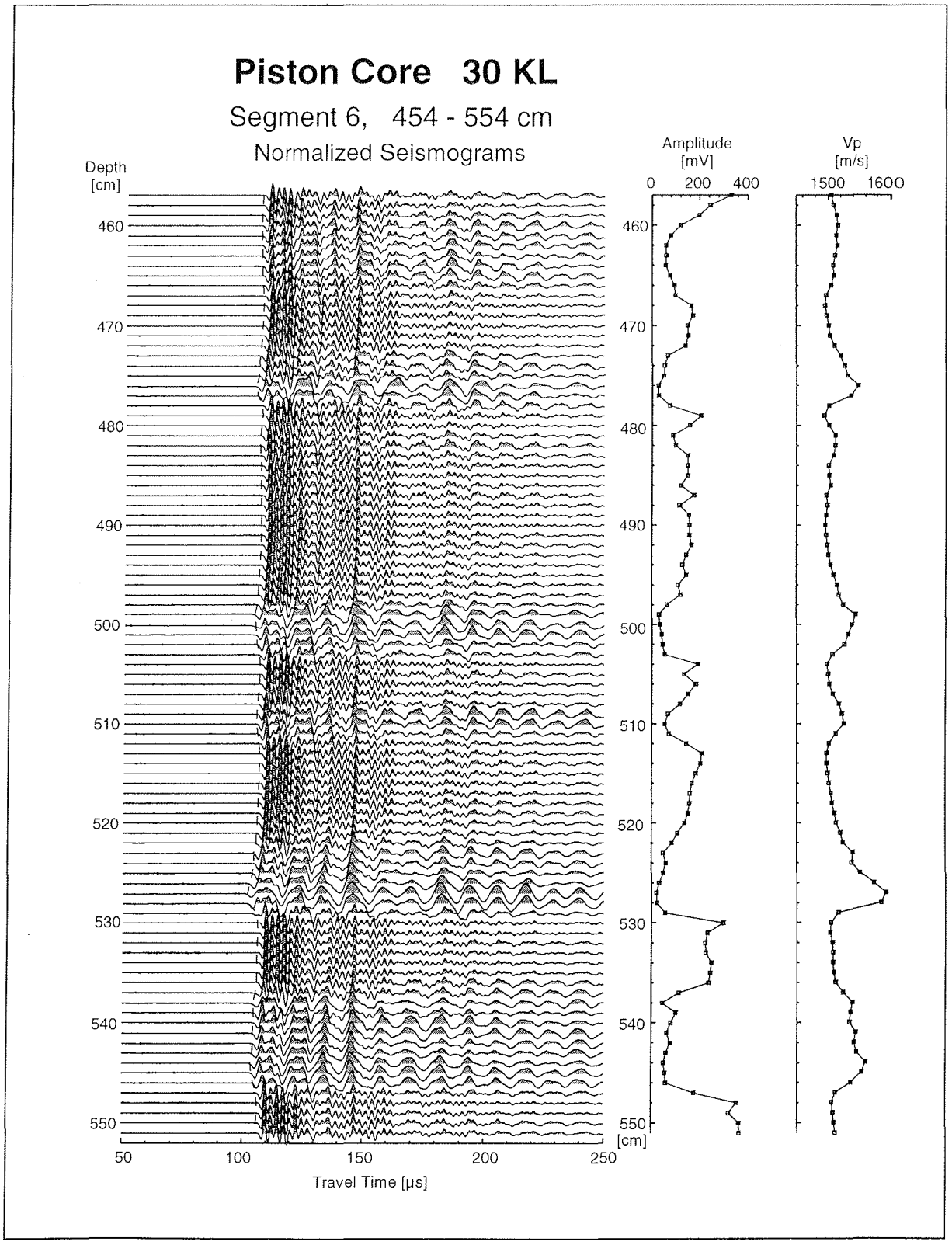

Figure 11.4.1: Normalized transmission seismograms recorded on segment no.6 of core 30KL between 454 - 554 cm depth. The dashed line at the onsets indicates automatically picked first arrivals. The logs on the right-hand side reveal the P-wave velocities (without temperature correction) and maximum peak-to-peak amplitudes evaluated from the transmission seismograms.

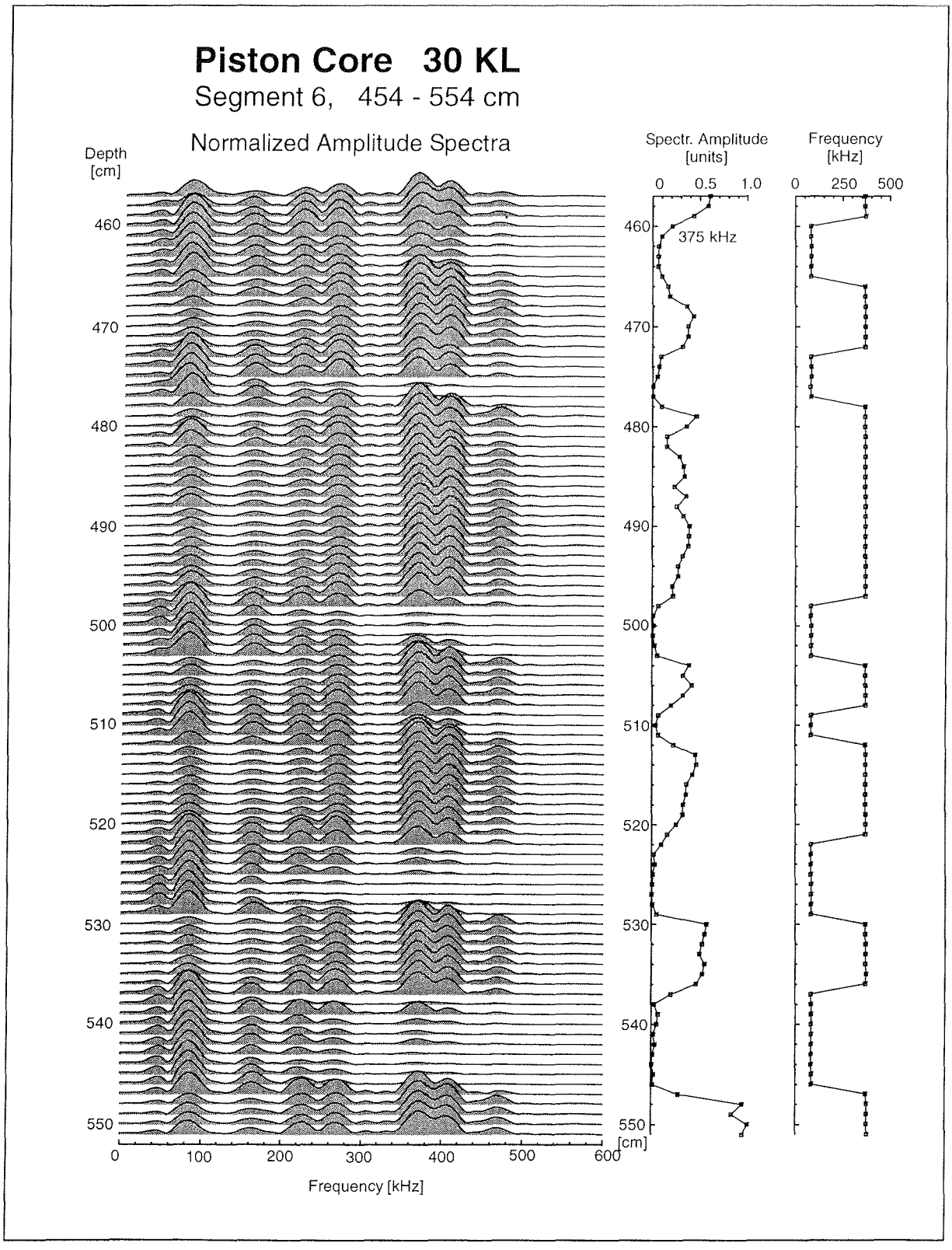

Figure 11.4.2: Normalized amplitude spectra of the transmission seismograms displayed in Figure 11.4.1. The logs on the right-hand side indicate the spectral amplitude of the 375 kHz component, normalized to 1, and the dominant frequency of the amplitude spectra.

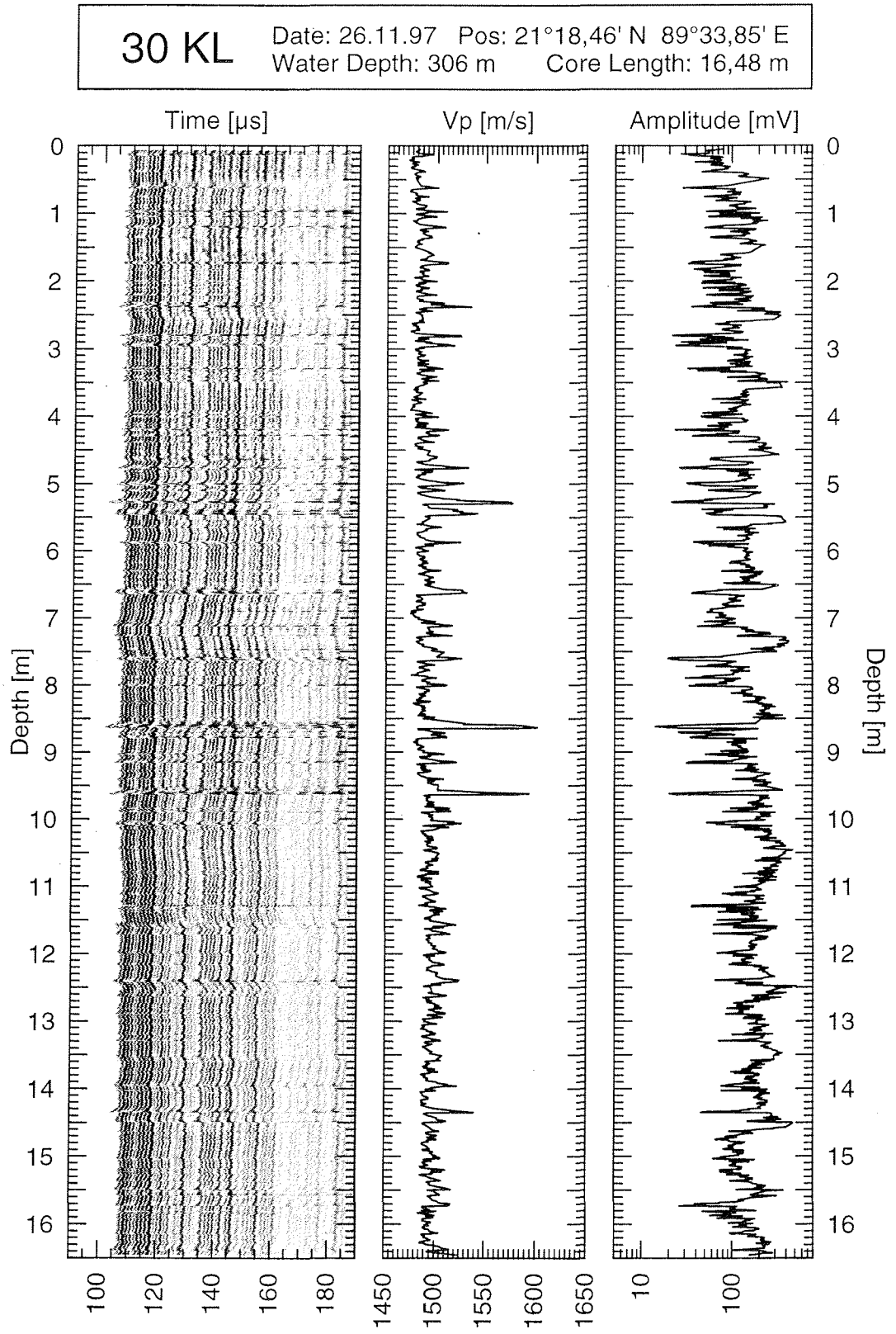

Figure 11.4.3: Grey-shaded full wavefrom transmission seismogram log, combined with the P-wave velocity and maximum peak-to-peak amplitude log of core 30 KL. P-wave velocities are reduced to 20°C, but no corrections for varying power are applied to the amplitude data.

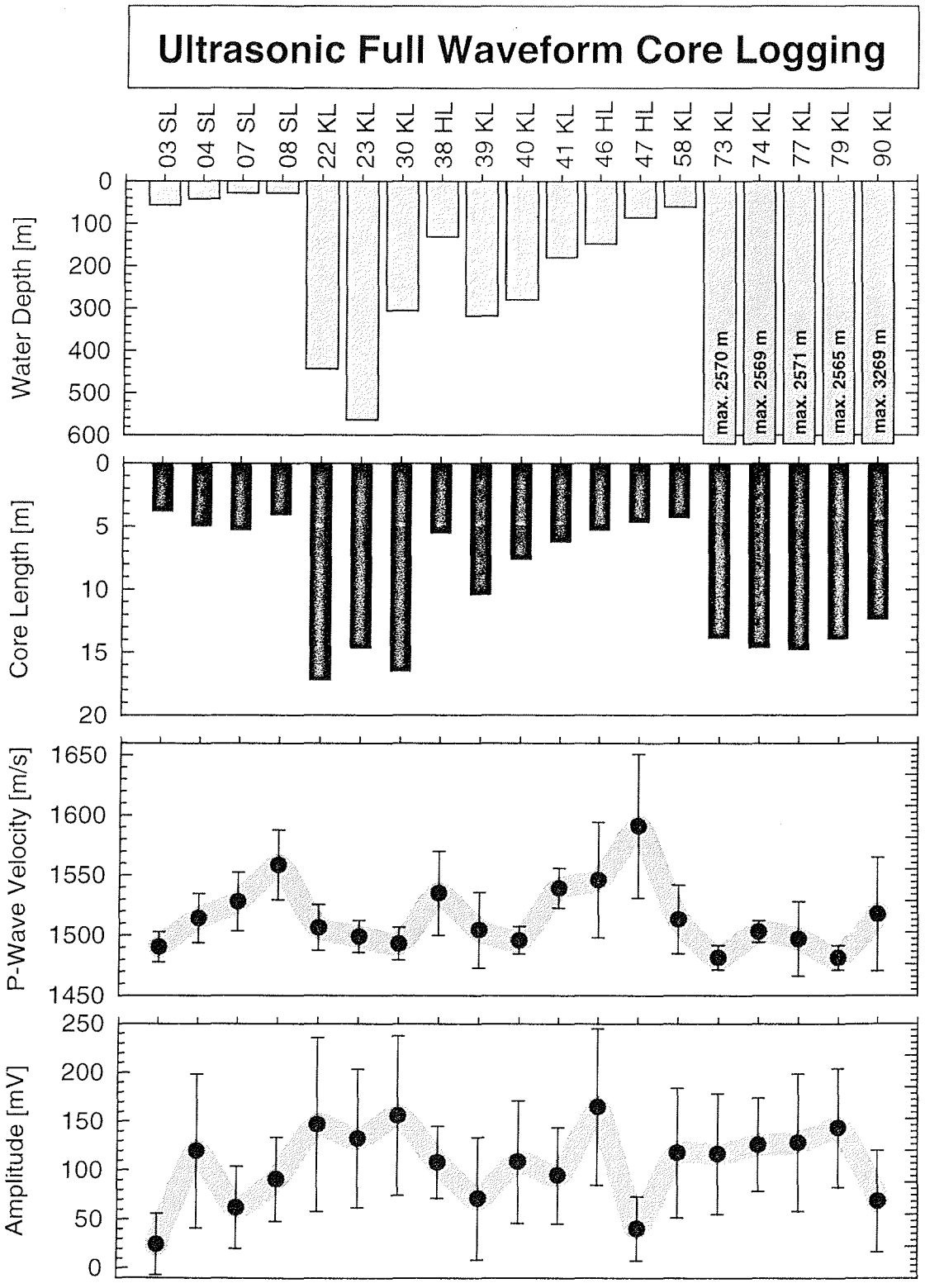

Figure 11.4.4: Mean values of the P-wave velocity and maximum peak-to-peak amplitude logs of all sediment cores retrieved during RV SONNE cruise SO126, in comparison to the recovered core lengths and water depths at the coring sites. The vertical bars denote the standard deviations.

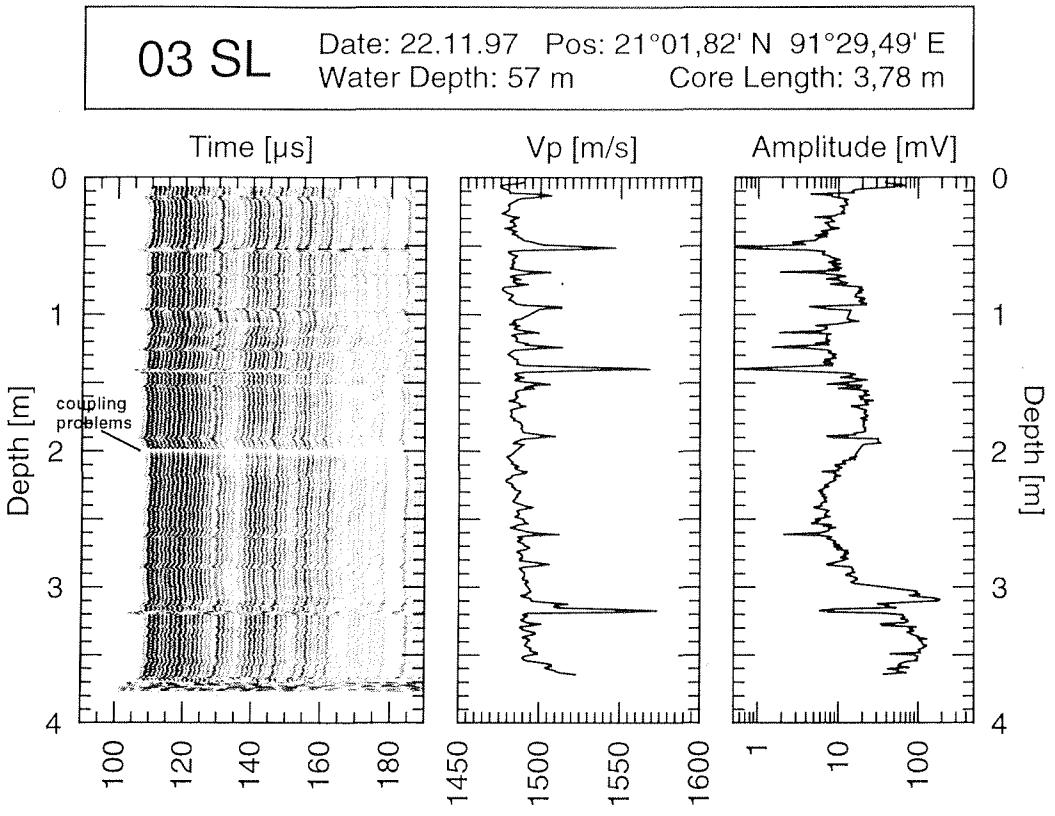

Figure 11.4.5: Grey-shaded full wavefrom transmission seismogram log and P-wave velocity and maximum peak-to-peak amplitude log of gravity core 03 SL. P-wave velocities are reduced to 20°C, no corrections are applied to the amplitude data.

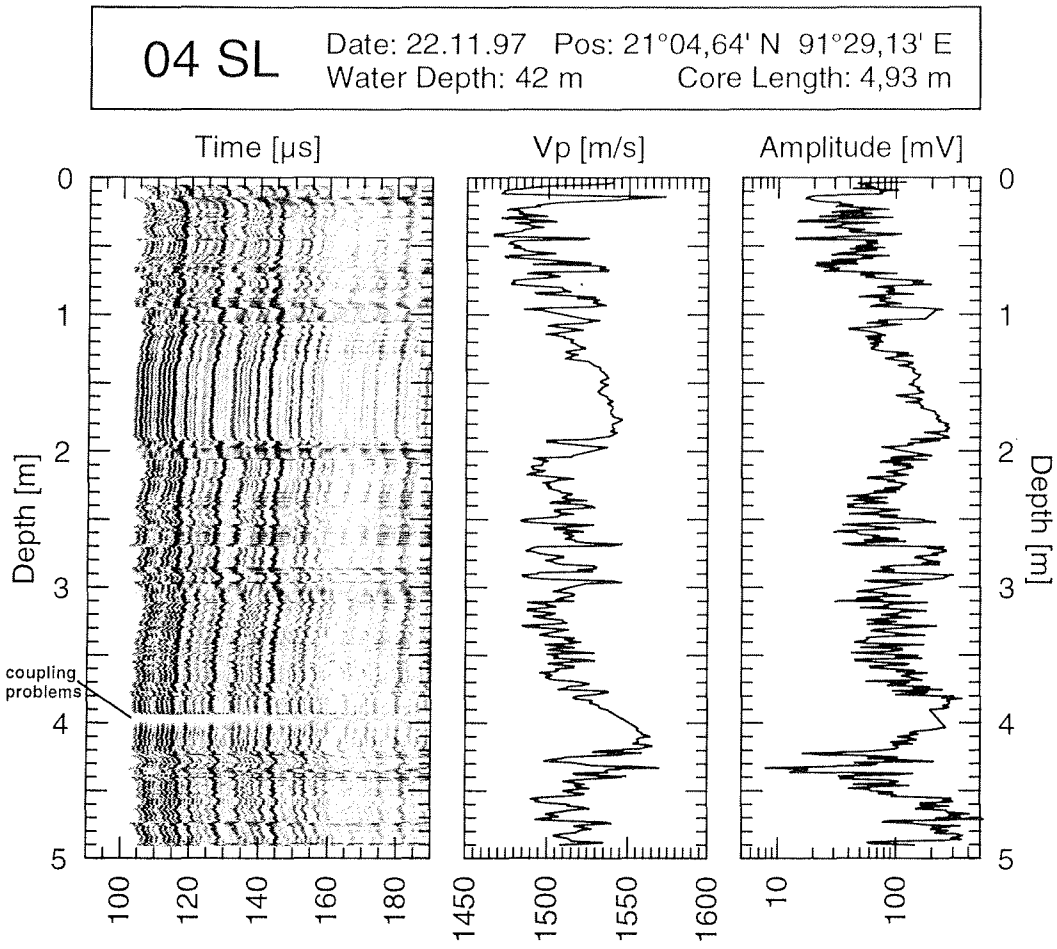

Figure 11.4.6: Grey-shaded full wavefrom transmission seismogram log and P-wave velocity and maximum peak-to-peak amplitude log of gravity core 04 SL. P-wave velocities are reduced to 20°C, no corrections are applied to the amplitude data.

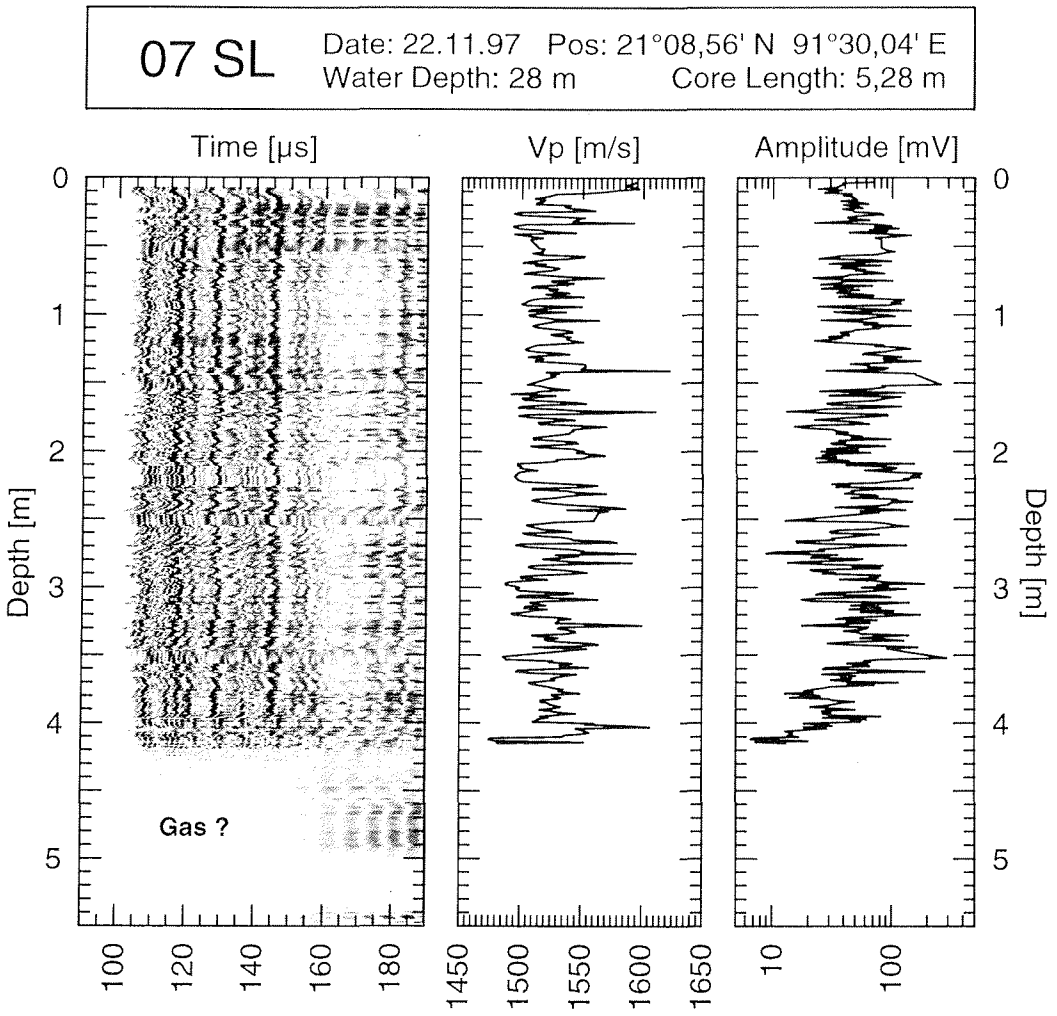

Figure 11.4.7: Grey-shaded full wavefrom transmission seismogram log and P-wave velocity and maximum peak-to-peak amplitude log of gravity core 07 SL. P-wave velocities are reduced to 20°C, no corrections are applied to the amplitude data.

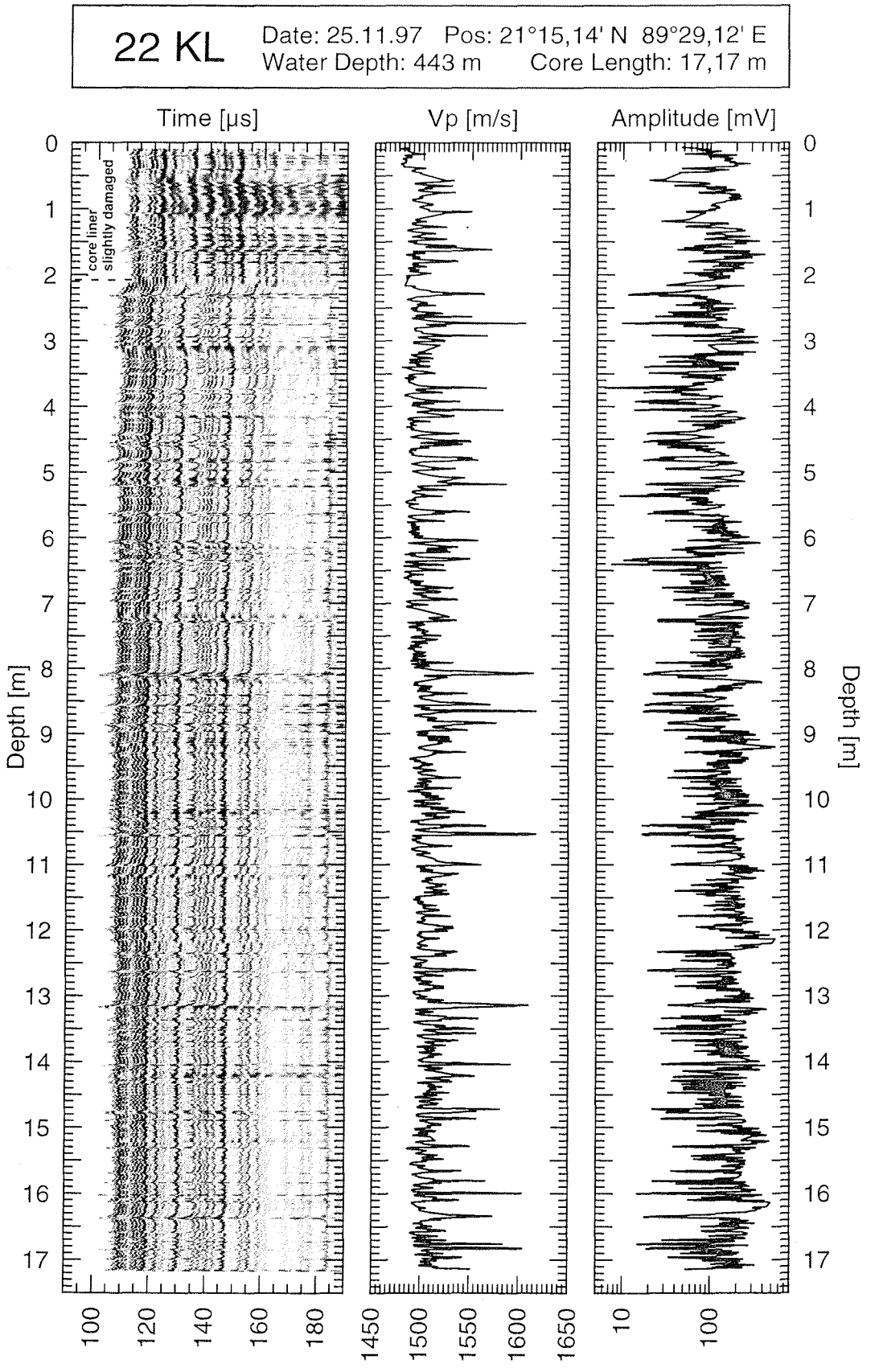

Figure 11.4.9: Grey-shaded full wavefrom transmission seismogram logand P-wave velocity and maximum peak-to-peak amplitude log of piston core 22 KL. P-wave velocities are reduced to 20°C, no corrections are applied to the amplitude data.

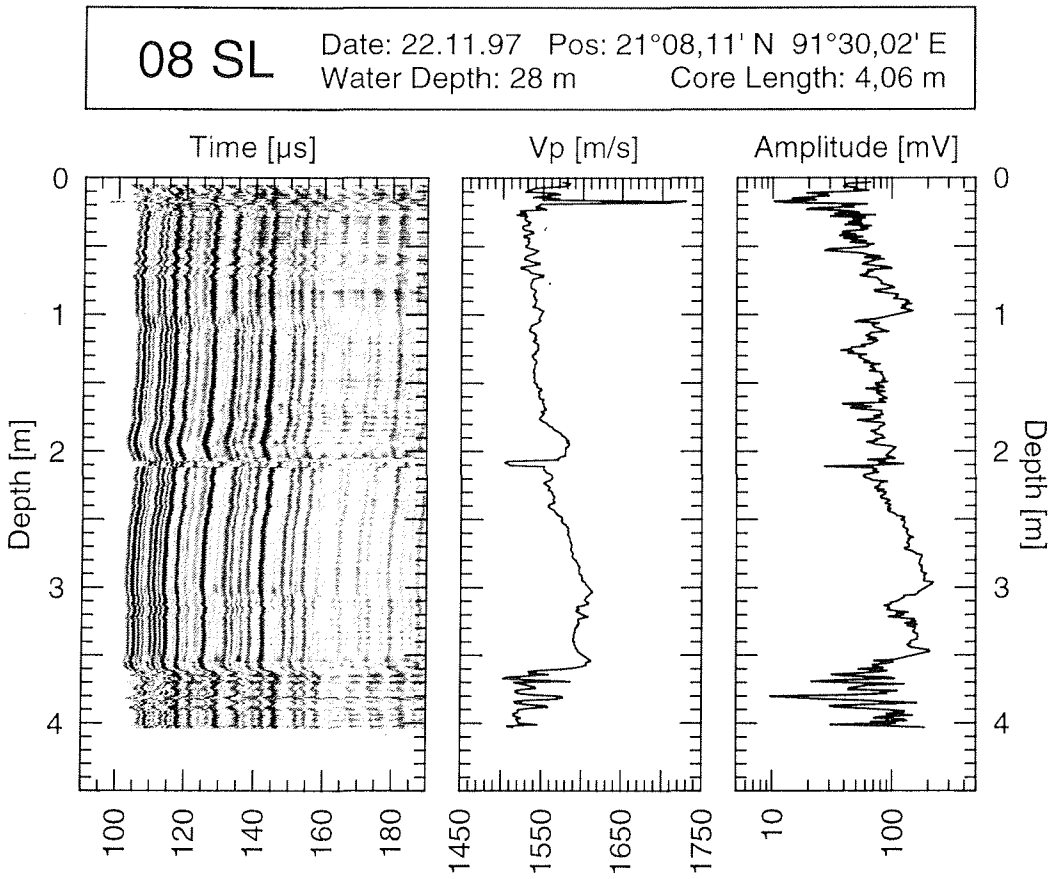

Figure 11.4.8: Grey-shaded full wavefrom transmission seismogram log and P-wave velocity and maximum peak-to-peak amplitude log of gravity core 08 SL. P-wave velocities are reduced to 20°C, no corrections are applied to the amplitude data.

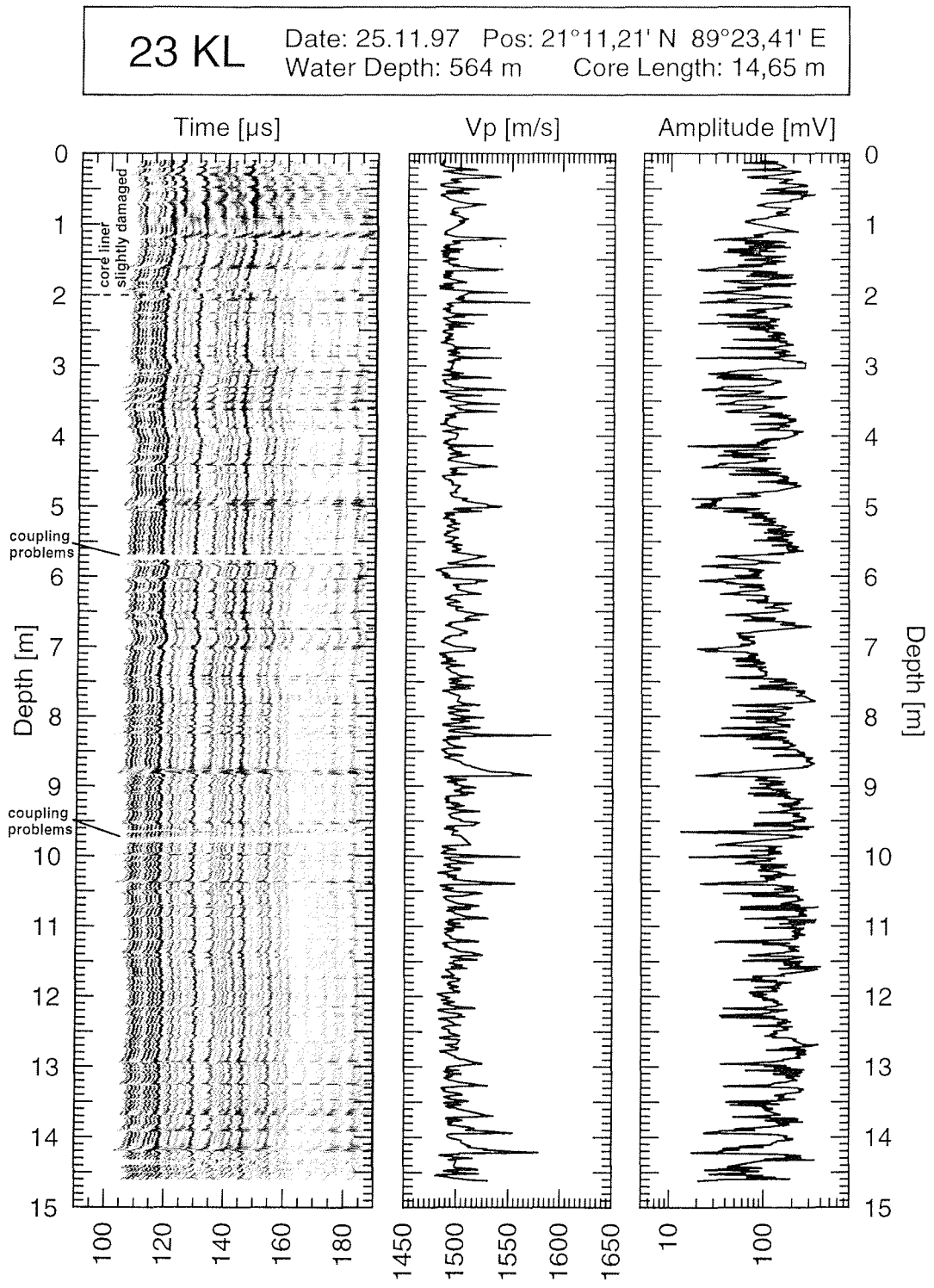

Figure 11.4.10: Grey-shaded full wavefrom transmission seismogram log and P-wave velocity and maximum peak-to-peak amplitude log of piston core 23 KL. P-wave velocities are reduced to 20°C, no corrections are applied to the amplitude data.

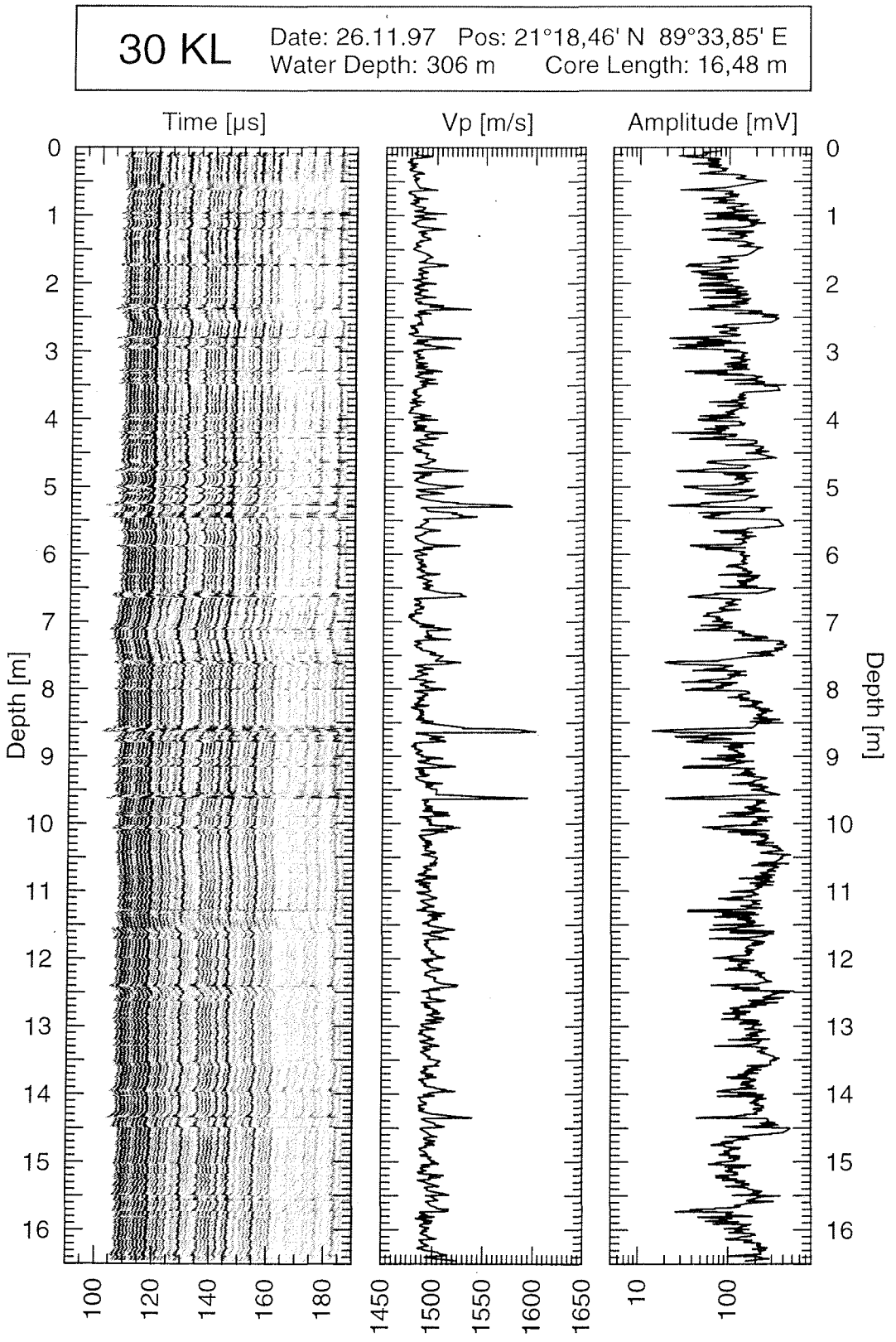

Figure 11.4.11: Grey-shaded full wavefrom transmission seismogram log and P-wave velocity and maximum peak-to-peak amplitude log of piston core 30 KL. P-wave velocities are reduced to 20°C, no corrections are applied to the amplitude data.

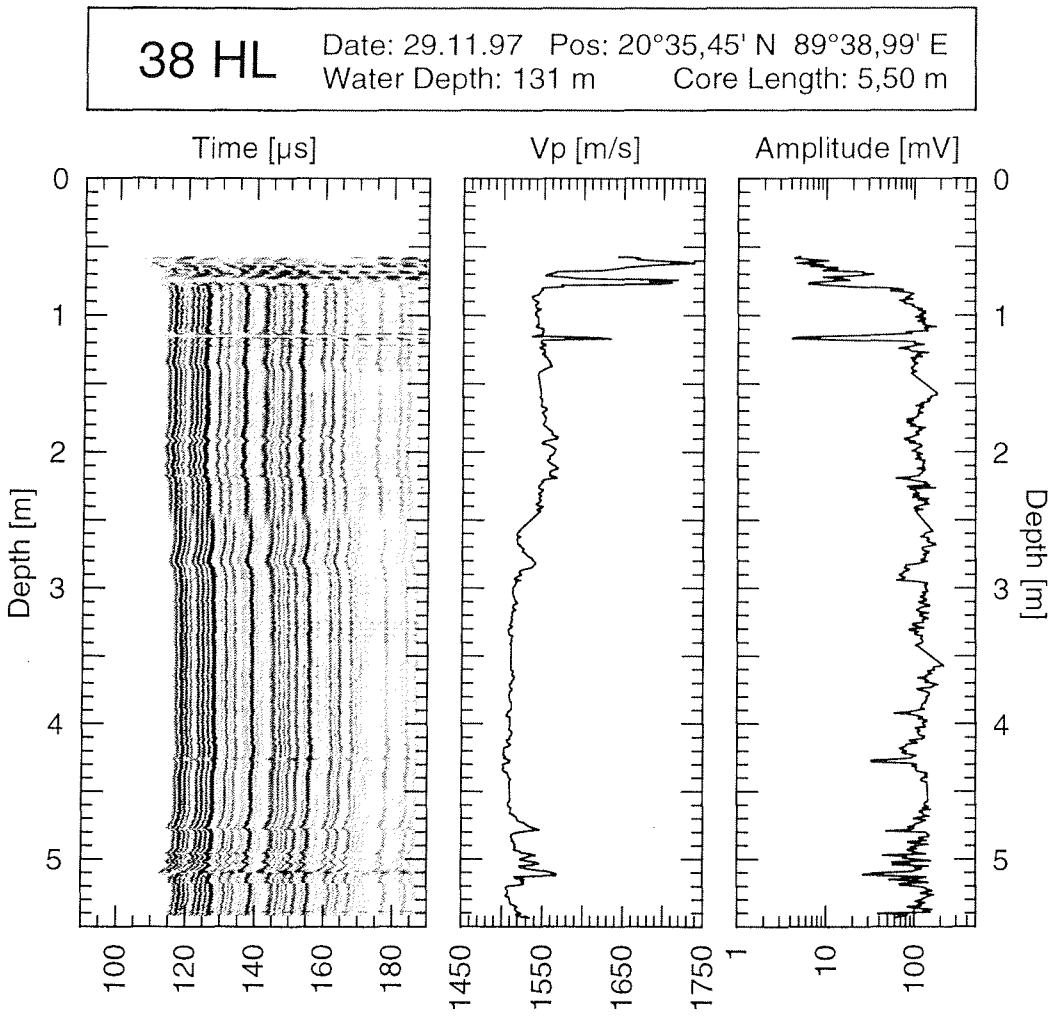

Figure 11.4.12: Grey-shaded full wavefrom transmission seismogram log and P-wave velocity and maximum peak-to-peak amplitude log of hammer core 38 HL. P-wave velocities are reduced to 20°C, no corrections are applied to the amplitude data.

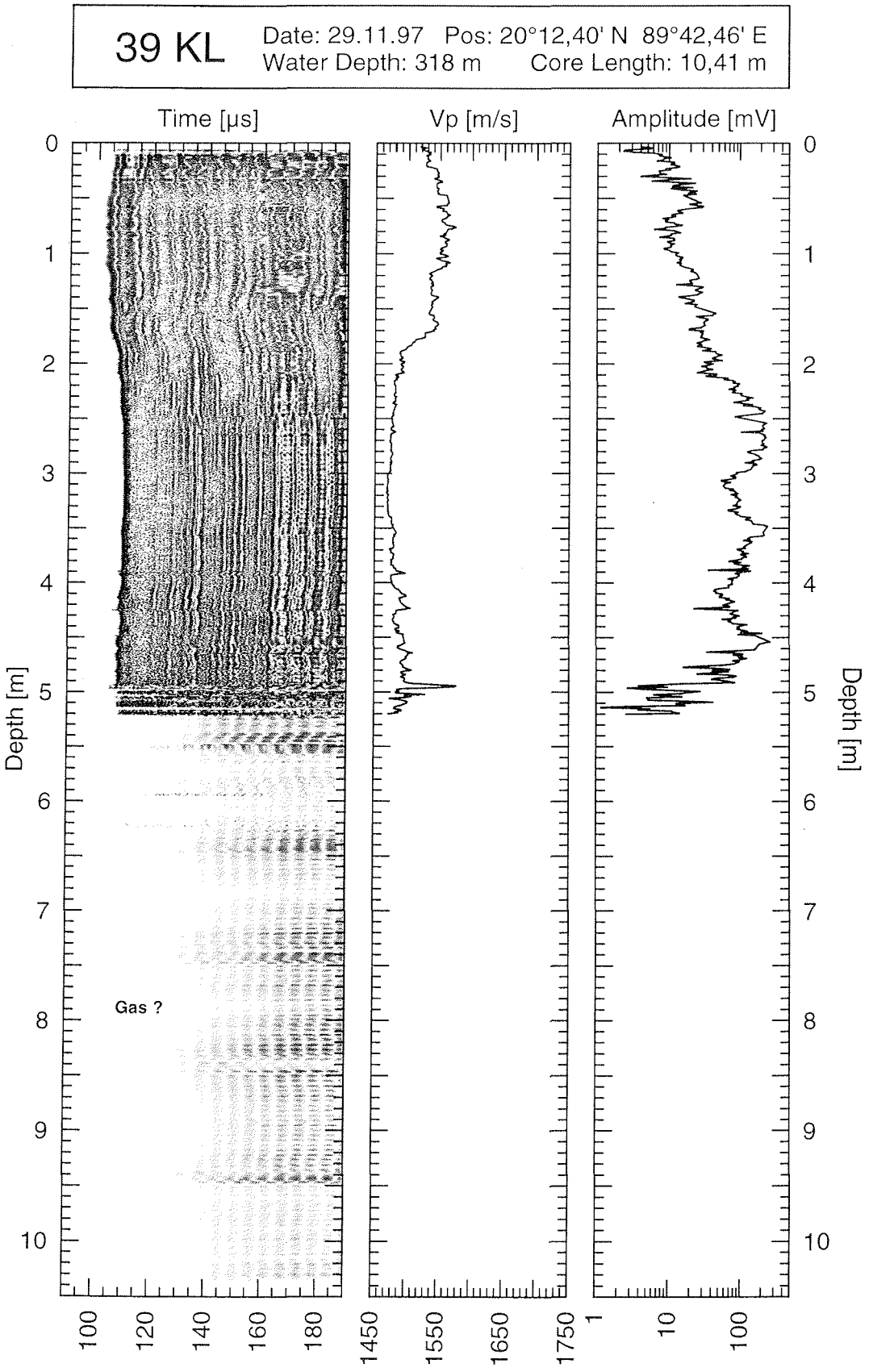

Figure 11.4.13: Grey-shaded full wavefrom transmission seismogram log and P-wave velocity and maximum peak-to-peak amplitude log of piston core 39 KL. P-wave velocities are reduced to 20°C, no corrections are applied to the amplitude data.

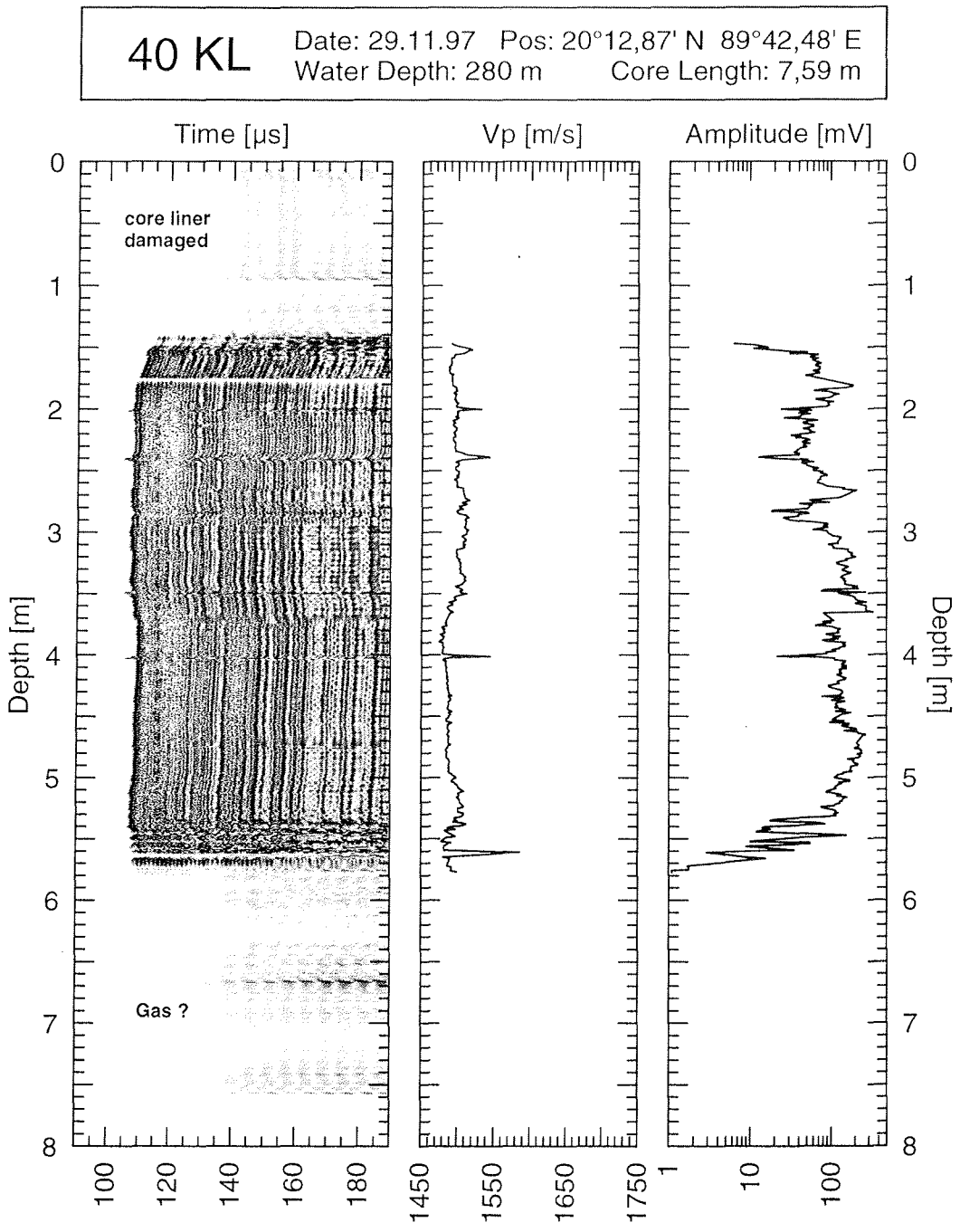

Figure 11.4.14: Grey-shaded full wavefrom transmission seismogram log and P-wave velocity and maximum peak-to-peak amplitude log of piston core 40 KL. P-wave velocities are reduced to 20°C, no corrections are applied to the amplitude data.

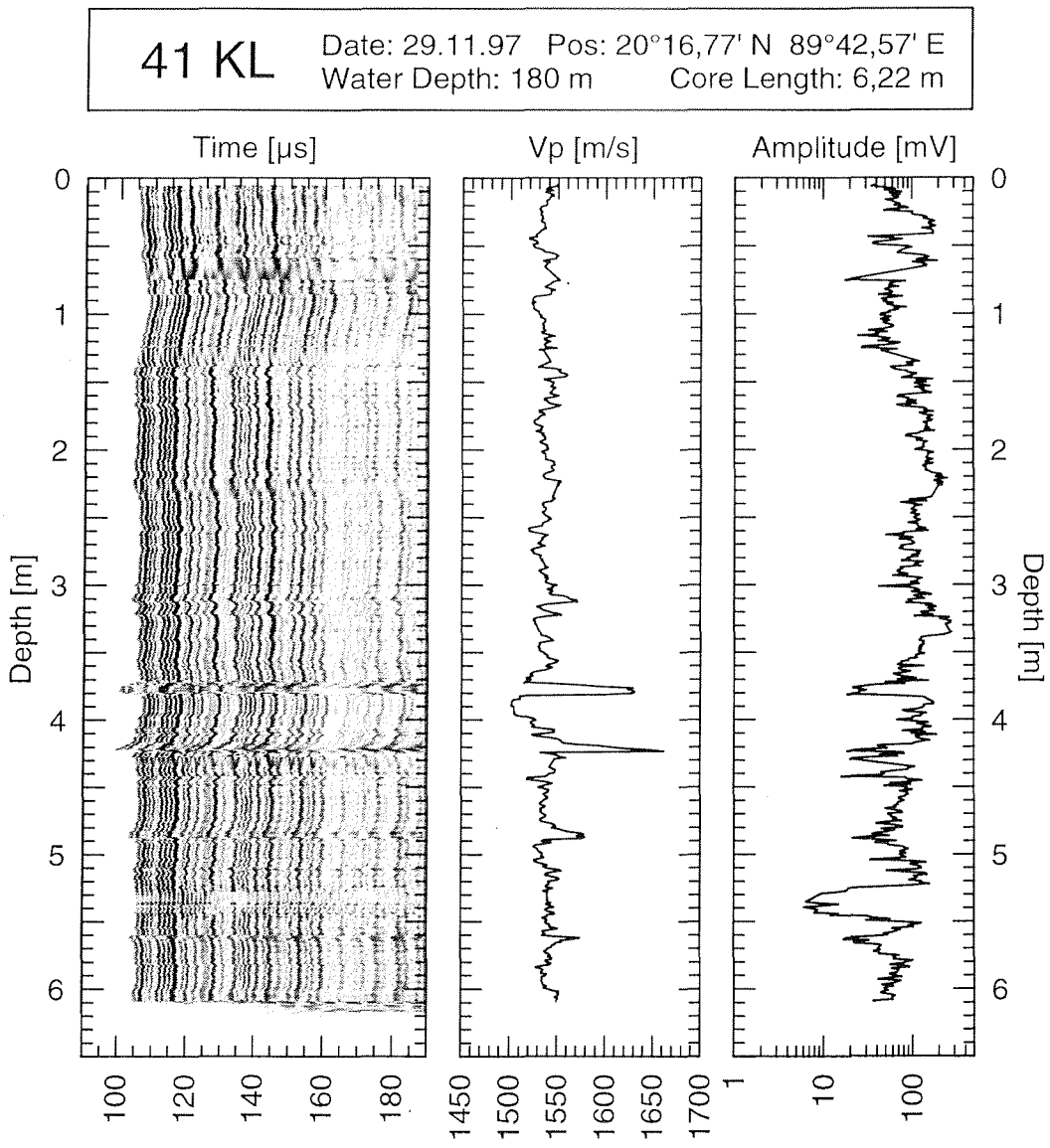

Figure 11.4.15: Grey-shaded full wavefrom transmission seismogram log and P-wave velocity and maximum peak-to-peak amplitude log of piston core 41 KL. P-wave velocities are reduced to 20°C, no corrections are applied to the amplitude data.

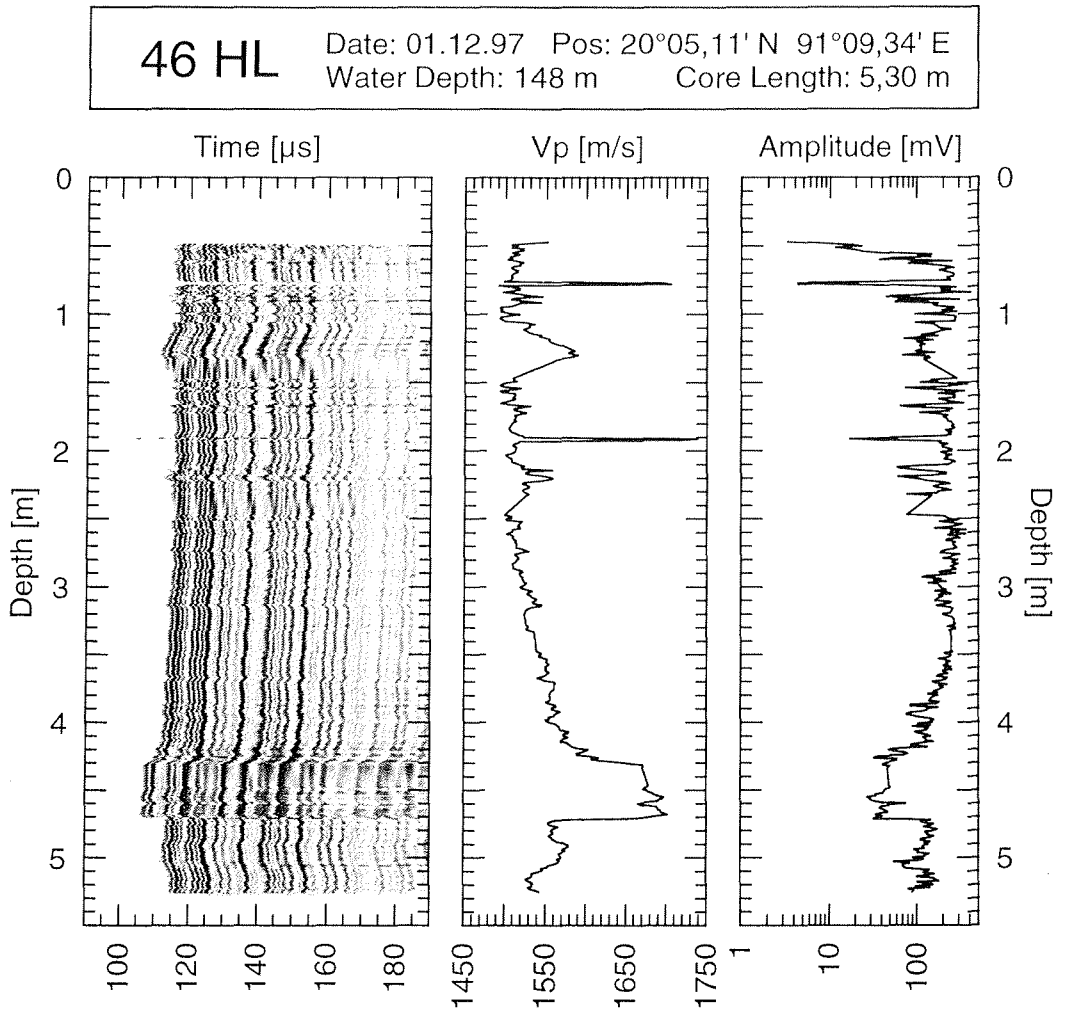

Figure 11.4.16: Grey-shaded full wavefrom transmission seismogram log and P-wave velocity and maximum peak-to-peak amplitude log of hammer core 46 HL. P-wave velocities are reduced to 20°C, no corrections are applied to the amplitude data.

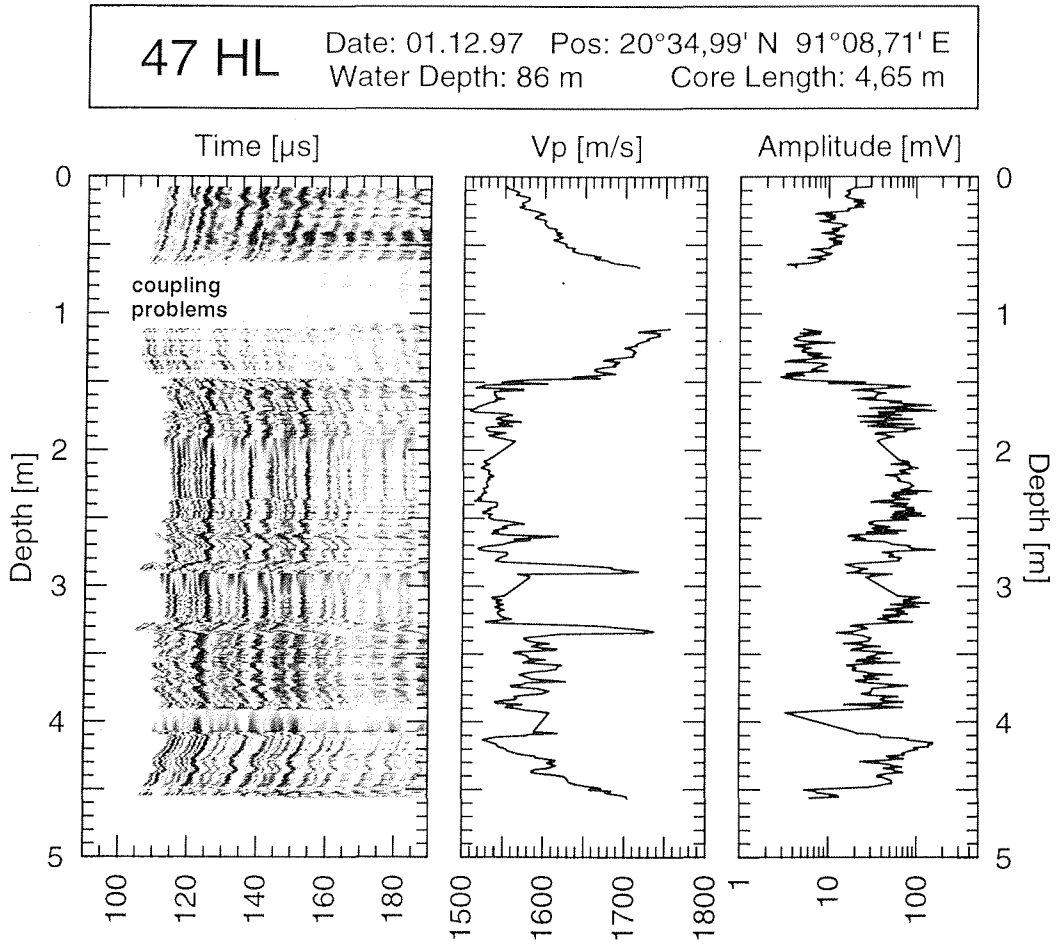

Figure 11.4.17: Grey-shaded full wavefrom transmission seismogram log and P-wave velocity and maximum peak-to-peak amplitude log of hammer core 47 HL. P-wave velocities are reduced to 20°C, no corrections are applied to the amplitude data.

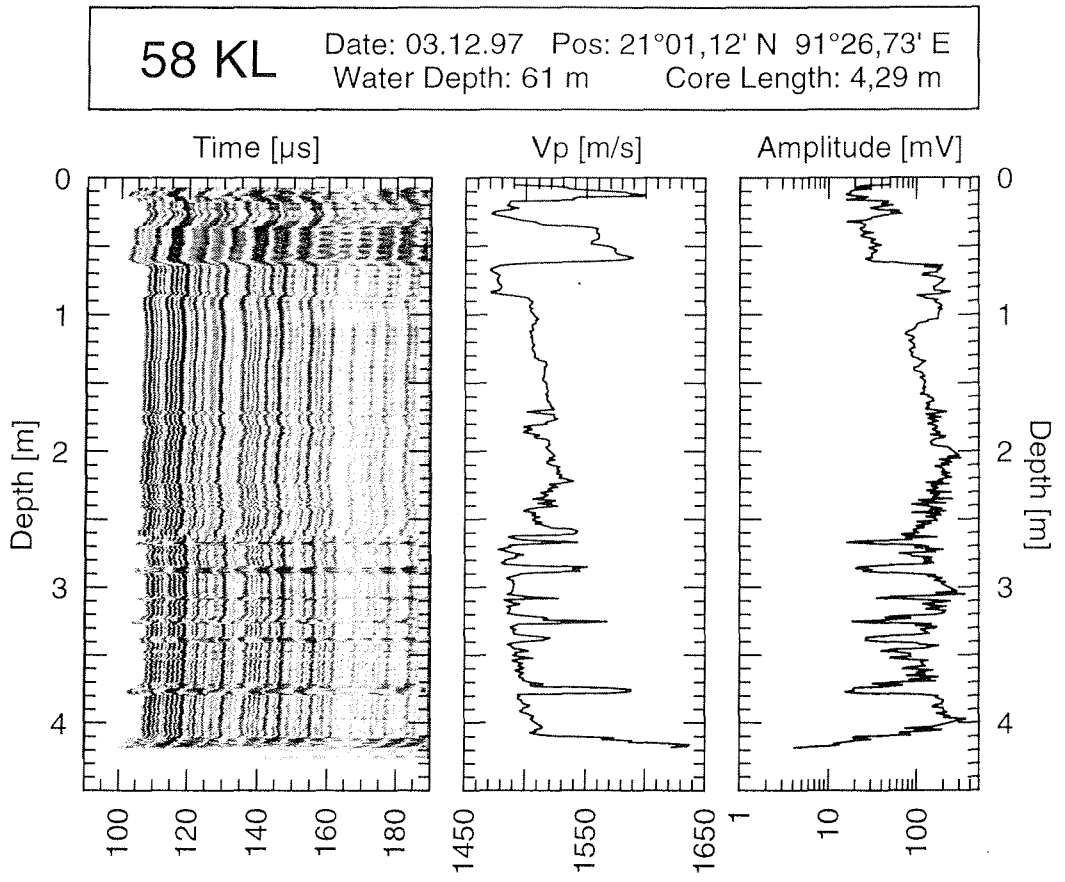

Figure 11.4.18: Grey-shaded full wavefrom transmission seismogram log and P-wave velocity and maximum peak-to-peak amplitude log of piston core 58 KL. P-wave velocities are reduced to 20°C, no corrections are applied to the amplitude data.

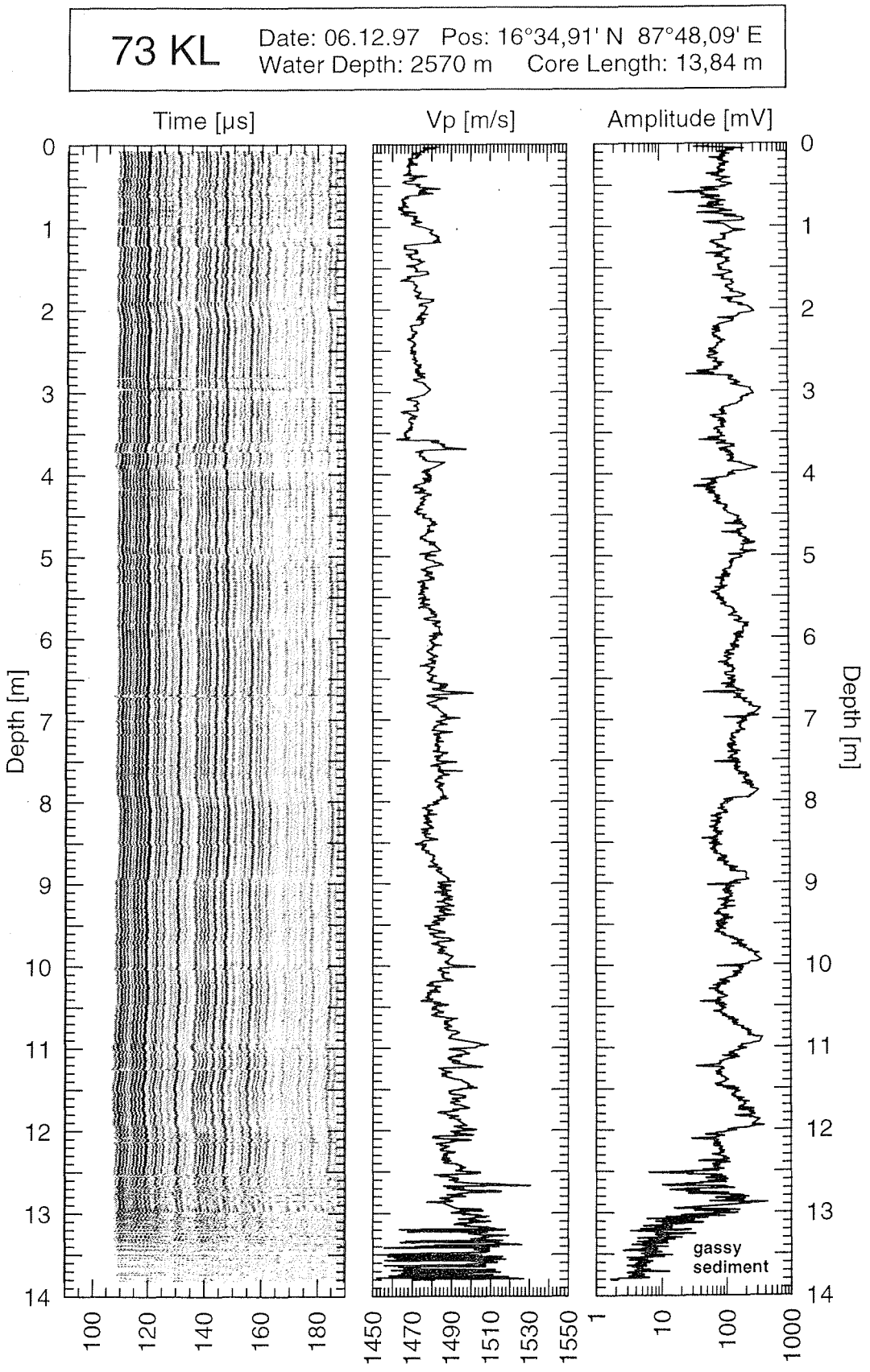

Figure 11.4.19: Grey-shaded full wavefrom transmission seismogram log and P-wave velocity and maximum peak-to-peak amplitude log of piston core 73 KL. P-wave velocities are reduced to 20°C, no corrections are applied to the amplitude data.

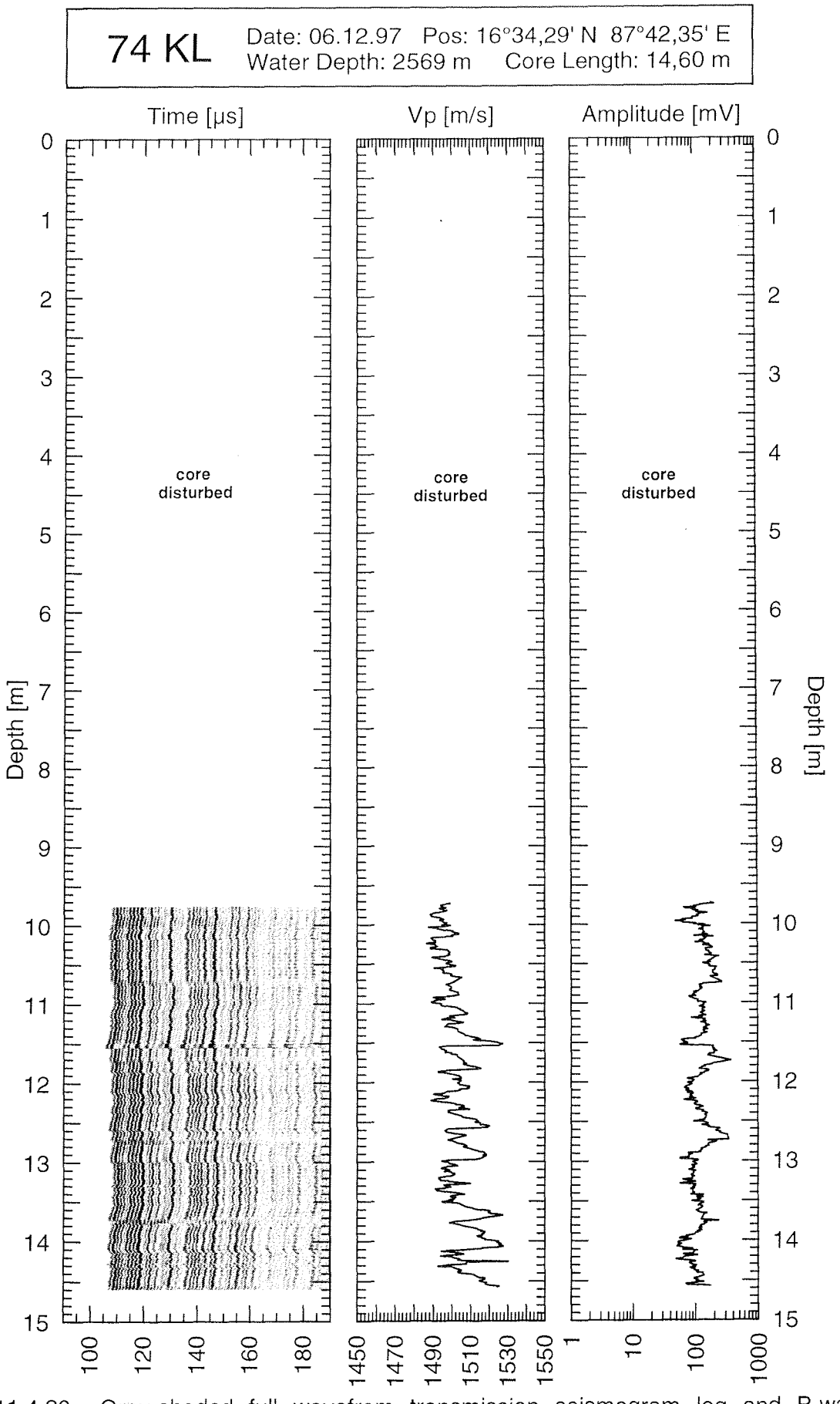

Figure 11.4.20: Grey-shaded full wavefrom transmission seismogram log and P-wave velocity and maximum peak-to-peak amplitude log of piston core 74 KL. P-wave velocities are reduced to 20°C, no corrections are applied to the amplitude data.

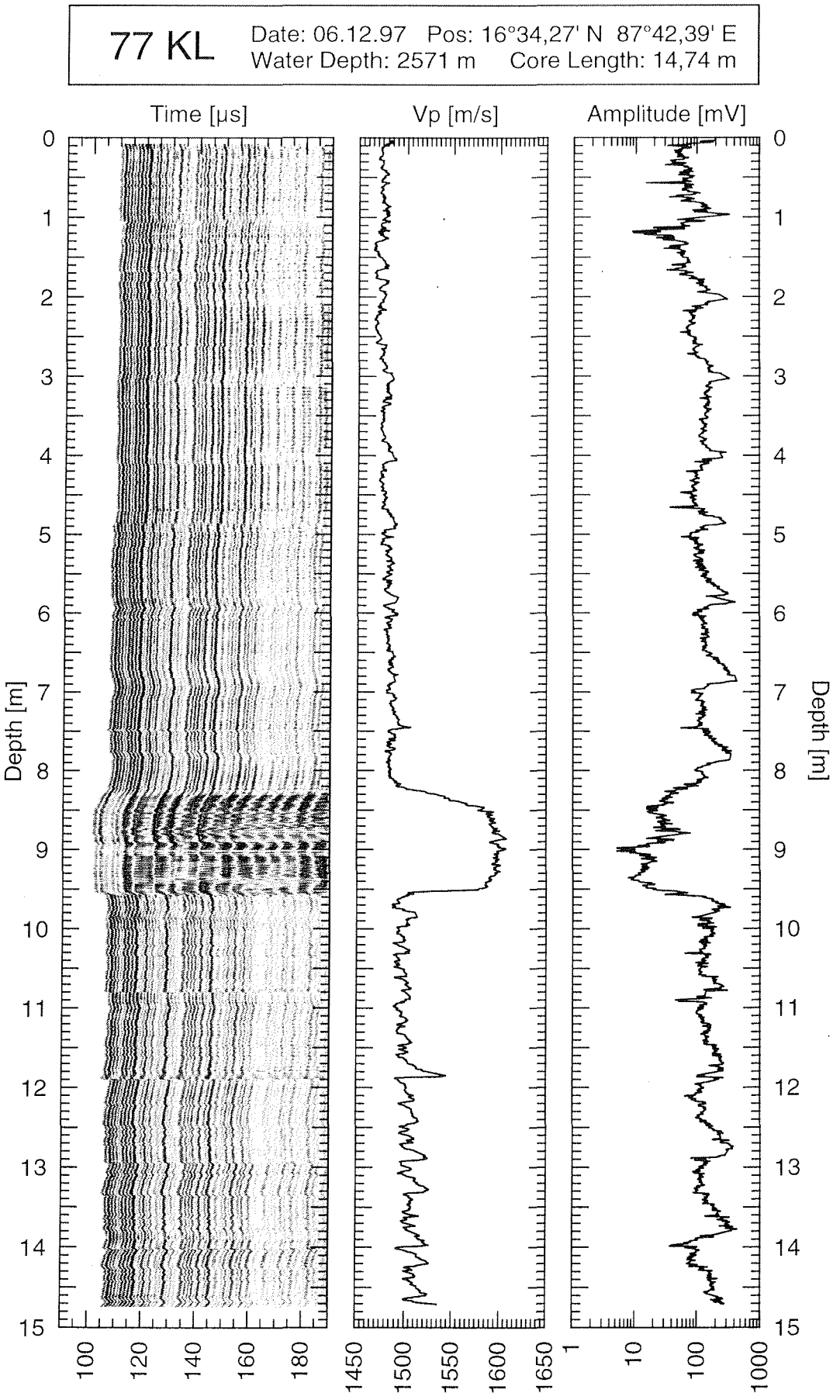

Figure 11.4.21: Grey-shaded full wavefrom transmission seismogram log and P-wave velocity and maximum peak-to-peak amplitude log of piston core 77 KL. P-wave velocities are reduced to 20°C, no corrections are applied to the amplitude data.

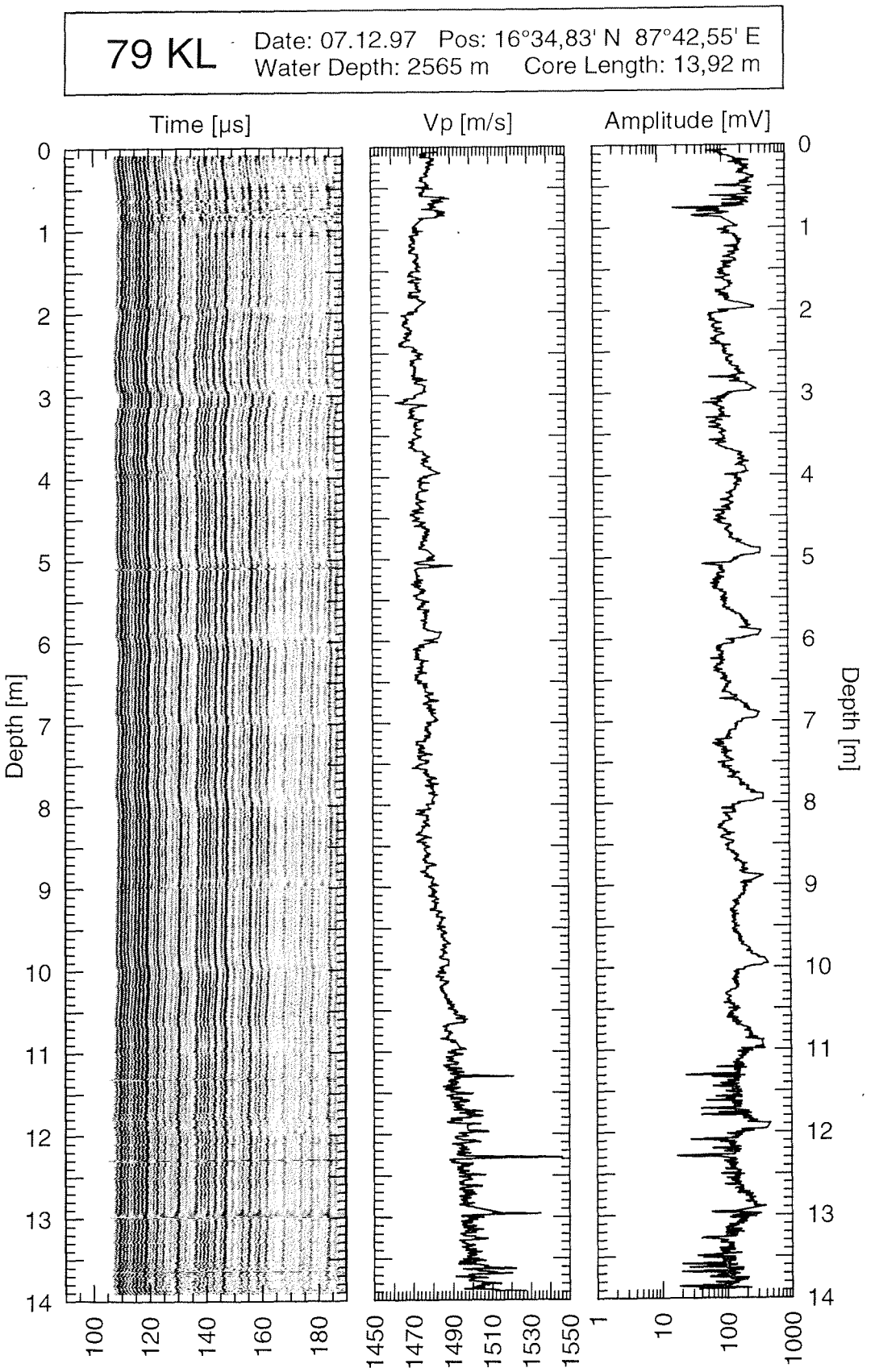

Figure 11.4.22: Grey-shaded full wavefrom transmission seismogram log and P-wave velocity and maximum peak-to-peak amplitude log of piston core 79 KL. P-wave velocities are reduced to 20°C, no corrections are applied to the amplitude data.

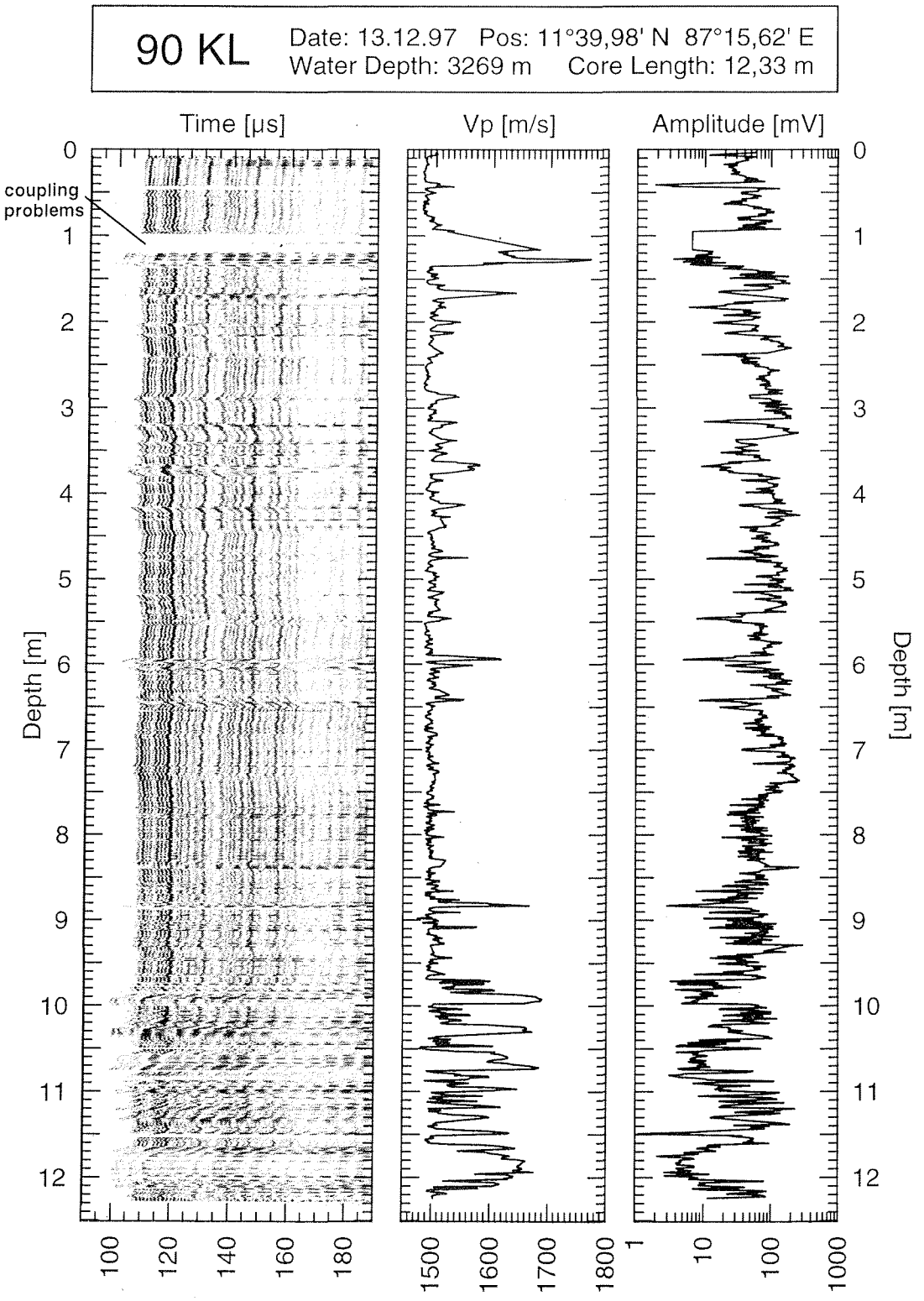

Figure 11.4.23: Grey-shaded full wavefrom transmission seismogram log and P-wave velocity and maximum peak-to-peak amplitude log of piston core 90 KL. P-wave velocities are reduced to 20°C, no corrections are applied to the amplitude data.

Publications of this series:

No. 1 **Wefer, G., E. Suess and cruise participants**
Bericht über die POLARSTERN-Fahrt ANT IV/2, Rio de Janeiro - Punta Arenas, 6.11. - 1.12.1985.
60 pages, Bremen, 1986.

No. 2 **Hoffmann, G.**
Holozänstratigraphie und Küstenlinienverlagerung an der andalusischen Mittelmeerküste.
173 pages, Bremen, 1988. (out of print)

No. 3 **Wefer, G. and cruise participants**
Bericht über die METEOR-Fahrt M 6/6, Libreville - Las Palmas, 18.2. - 23.3.1988.
97 pages, Bremen, 1988.

No. 4 **Wefer, G., G.F. Lutze, T.J. Müller, O. Pfannkuche, W. Schenke, G. Siedler, W. Zenk**
Kurzbericht über die METEOR-Expedition No. 6, Hamburg - Hamburg, 28.10.1987 - 19.5.1988.
29 pages, Bremen, 1988. (out of print)

No. 5 **Fischer, G.**
Stabile Kohlenstoff-Isotope in partikulärer organischer Substanz aus dem Südpolarmeer (Atlantischer Sektor). 161 pages, Bremen, 1989.

No. 6 **Berger, W.H. and G. Wefer**
Partikelfluß und Kohlenstoffkreislauf im Ozean.
Bericht und Kurzfassungen über den Workshop vom 3.-4. Juli 1989 in Bremen.
57 pages, Bremen, 1989.

No. 7 **Wefer, G. and cruise participants**
Bericht über die METEOR - Fahrt M 9/4, Dakar - Santa Cruz, 19.2. - 16.3.1989.
103 pages, Bremen, 1989.

No. 8 **Kölling, M.**
Modellierung geochemischer Prozesse im Sickerwasser und Grundwasser.
135 pages, Bremen, 1990.

No. 9 **Heinze, P.-M.**
Das Auftriebsgeschehen vor Peru im Spätquartär. 204 pages, Bremen, 1990. (out of print)

No. 10 **Willems, H., G. Wefer, M. Rinski, B. Donner, H.-J. Bellmann, L. Eißmann, A. Müller, B.W. Flemming, H.-C. Höfle, J. Merkt, H. Streif, G. Hertweck, H. Kuntze, J. Schwaar, W. Schäfer, M.-G. Schulz, F. Grube, B. Menke**
Beiträge zur Geologie und Paläontologie Norddeutschlands: Exkursionsführer.
202 pages, Bremen, 1990.

No. 11 **Wefer, G. and cruise participants**
Bericht über die METEOR-Fahrt M 12/1, Kapstadt - Funchal, 13.3.1990 - 14.4.1990.
66 pages, Bremen, 1990.

No. 12 **Dahmke, A., H.D. Schulz, A. Kölling, F. Kracht, A. Lücke**
Schwermetallspuren und geochemische Gleichgewichte zwischen Porenlösung und Sediment im Wesermündungsgebiet. BMFT-Projekt MFU 0562, Abschlußbericht. 121 pages, Bremen, 1991.

No. 13 **Rostek, F.**
Physikalische Strukturen von Tiefseesedimenten des Südatlantiks und ihre Erfassung in Echolotregistrierungen. 209 pages, Bremen, 1991.

No. 14 **Baumann, M.**
Die Ablagerung von Tschernobyl-Radiocäsium in der Norwegischen See und in der Nordsee.
133 pages, Bremen, 1991. (out of print)

No. 15 **Kölling, A.**
Frühdiagenetische Prozesse und Stoff-Flüsse in marinen und ästuarinen Sedimenten.
140 pages, Bremen, 1991.

No. 16 **SFB 261 (ed.)**
1. Kolloquium des Sonderforschungsbereichs 261 der Universität Bremen (14.Juni 1991):
Der Südatlantik im Spätquartär: Rekonstruktion von Stoffhaushalt und Stromsystemen.
Kurzfassungen der Vorträge und Poster. 66 pages, Bremen, 1991.

No. 17 **Pätzold, J. and cruise participants**
Bericht und erste Ergebnisse über die METEOR-Fahrt M 15/2, Rio de Janeiro - Vitoria, 18.1. - 7.2.1991. 46 pages, Bremen, 1993.

No. 18 **Wefer, G. and cruise participants**
Bericht und erste Ergebnisse über die METEOR-Fahrt M 16/1, Pointe Noire - Recife, 27.3. - 25.4.1991. 120 pages, Bremen, 1991.

No. 19 **Schulz, H.D. and cruise participants**
Bericht und erste Ergebnisse über die METEOR-Fahrt M 16/2, Recife - Belem, 28.4. - 20.5.1991. 149 pages, Bremen, 1991.

No. 20 **Berner, H.**
Mechanismen der Sedimentbildung in der Fram-Straße, im Arktischen Ozean und in der Norwegischen See. 167 pages, Bremen, 1991.

No. 21 **Schneider, R.**
Spätquartäre Produktivitätsänderungen im östlichen Angola-Becken: Reaktion auf Variationen im Passat-Monsun-Windsystem und in der Advektion des Benguela-Küstenstroms. 198 pages, Bremen, 1991. (out of print)

No. 22 **Hebbeln, D.**
Spätquartäre Stratigraphie und Paläozeanographie in der Fram-Straße. 174 pages, Bremen, 1991.

No. 23 **Lücke, A.**
Umsetzungsprozesse organischer Substanz während der Frühdiagenese in ästuarinen Sedimenten. 137 pages, Bremen, 1991.

No. 24 **Wefer, G. and cruise participants**
Bericht und erste Ergebnisse der METEOR-Fahrt M 20/1, Bremen - Abidjan, 18.11.- 22.12.1991. 74 pages, Bremen, 1992.

No. 25 **Schulz, H.D. and cruise participants**
Bericht und erste Ergebnisse der METEOR-Fahrt M 20/2, Abidjan - Dakar, 27.12.1991 - 3.2.1992. 173 pages, Bremen, 1992.

No. 26 **Gingele, F.**
Zur klimaabhängigen Bildung biogener und terrigener Sedimente und ihrer Veränderung durch die Frühdiagenese im zentralen und östlichen Südatlantik. 202 pages, Bremen, 1992.

No. 27 **Bickert, T.**
Rekonstruktion der spätquartären Bodenwasserzirkulation im östlichen Südatlantik über stabile Isotope benthischer Foraminiferen. 205 pages, Bremen, 1992. (out of print)

No. 28 **Schmidt, H.**
Der Benguela-Strom im Bereich des Walfisch-Rückens im Spätquartär. 172 pages, Bremen, 1992.

No. 29 **Meinecke, G.**
Spätquartäre Oberflächenwassertemperaturen im östlichen äquatorialen Atlantik. 181 pages, Bremen, 1992.

No. 30 **Bathmann, U., U. Bleil, A. Dahmke, P. Müller, A. Nehrkorn, E.-M. Nöthig, M. Olesch, J. Pätzold, H.D. Schulz, V. Smetacek, V. Spieß, G. Wefer, H. Willems**
Bericht des Graduierten Kollegs. Stoff-Flüsse in marinen Geosystemen. Berichtszeitraum Oktober 1990 - Dezember 1992. 396 pages, Bremen, 1992.

No. 31 **Damm, E.**
Frühdiagenetische Verteilung von Schwermetallen in Schlicksedimenten der westlichen Ostsee. 115 pages, Bremen, 1992.

No. 32 **Antia, E.E.**
Sedimentology, Morphodynamics and Facies Association of a mesotidal Barrier Island Shoreface (Spiekeroog, Southern North Sea). 370 pages, Bremen, 1993.

No. 33 **Duinker, J. and G. Wefer (ed.)**
Bericht über den 1. JGOFS-Workshop. 1./2. Dezember 1992 in Bremen. 83 pages, Bremen, 1993.

No. 34 **Kasten, S.**
Die Verteilung von Schwermetallen in den Sedimenten eines stadtbremischen Hafenbeckens. 103 pages, Bremen, 1993.

No. 35 **Spieß, V.**
Digitale Sedimentographie. Neue Wege zu einer hochauflösenden Akustostratigraphie.
199 pages, Bremen, 1993.

No. 36 **Schinzel, U.**
Laborversuche zu frühdiagenetischen Reaktionen von Eisen (III) - Oxidhydraten in marinen Sedimenten.189 pages, Bremen, 1993.

No. 37 **Sieger, R.**
CoTAM - ein Modell zur Modellierung des Schwermetalltransports in Grundwasserleitern.
56 pages, Bremen, 1993. (out of print)

No. 38 **Willems, H. (ed.)**
Geoscientific Investigations in the Tethyan Himalayas. 183 pages, Bremen, 1993.

No. 39 **Hamer, K.**
Entwicklung von Laborversuchen als Grundlage für die Modellierung des Transportverhaltens von Arsenat, Blei, Cadmium und Kupfer in wassergesättigten Säulen. 147 pages, Bremen, 1993.

No. 40 **Sieger, R.**
Modellierung des Stofftransports in porösen Medien unter Ankopplung kinetisch gesteuerter Sorptions- und Redoxprozesse sowie thermischer Gleichgewichte. 158 pages, Bremen, 1993.

No. 41 **Thießen, W.**
Magnetische Eigenschaften von Sedimenten des östlichen Südatlantiks und ihre paläozeanographische Relevanz. 170 pages, Bremen, 1993.

No. 42 **Spieß, V. and cruise participants**
Report and preliminary results of METEOR-Cruise M 23/1, Kapstadt - Rio de Janeiro, 4.-25.2.1993.
139 pages, Bremen, 1994.

No. 43 **Bleil, U. and cruise participants**
Report and preliminary results of METEOR-Cruise M 23/2, Rio de Janeiro - Recife, 27.2.-19.3.1993
133 pages, Bremen, 1994.

No. 44 **Wefer, G. and cruise participants**
Report and preliminary results of METEOR-Cruise M 23/3, Recife - Las Palmas, 21.3. - 12.4.1993
71 pages, Bremen, 1994.

No. 45 **Giese, M. and G. Wefer (ed.)**
Bericht über den 2. JGOFS-Workshop. 18../19. November 1993 in Bremen.
93 pages, Bremen, 1994.

No. 46 **Balzer, W. and cruise participants**
Report and preliminary results of METEOR-Cruise M 22/1, Hamburg - Recife, 22.9. - 21.10.1992.
24 pages, Bremen, 1994.

No. 47 **Stax, R.**
Zyklische Sedimentation von organischem Kohlenstoff in der Japan See: Anzeiger für Änderungen von Paläoozeanographie und Paläoklima im Spätkänozoikum.
150 pages, Bremen, 1994.

No. 48 **Skowronek, F.**
Frühdiagenetische Stoff-Flüsse gelöster Schwermetalle an der Oberfläche von Sedimenten des Weser Ästuares. 107 pages, Bremen, 1994.

No. 49 **Dersch-Hansmann, M.**
Zur Klimaentwicklung in Ostasien während der letzten 5 Millionen Jahre:
Terrigener Sedimenteintrag in die Japan See (ODP Ausfahrt 128). 149 pages, Bremen, 1994.

No. 50 **Zabel, M.**
Frühdiagenetische Stoff-Flüsse in Oberflächen-Sedimenten des äquatorialen und östlichen Südatlantik. 129 pages, Bremen, 1994.

No. 51 **Bleil, U. and cruise participants**
Report and preliminary results of SONNE-Cruise SO 86, Buenos Aires - Capetown, 22.4. - 31.5.93
116 pages, Bremen, 1994.

No. 52 **Symposium: The South Atlantic: Present and Past Circulation.**
Bremen, Germany, 15 - 19 August 1994. Abstracts. 167 pages, Bremen, 1994.

No. 53 **Kretzmann, U.B.**
^{57}Fe-Mössbauer-Spektroskopie an Sedimenten - Möglichkeiten und Grenzen.
183 pages, Bremen, 1994.

No. 54 **Bachmann, M.**
Die Karbonatrampe von Organyà im oberen Oberapt und unteren Unteralb (NE-Spanien, Prov. Lerida): Fazies, Zyklo- und Sequenzstratigraphie. 147 pages, Bremen, 1994. (out of print)

No. 55 **Kemle-von Mücke, S.**
Oberflächenwasserstruktur und -zirkulation des Südostatlantiks im Spätquartär.
151 pages, Bremen, 1994.

No. 56 **Petermann, H.**
Magnetotaktische Bakterien und ihre Magnetosome in Oberflächensedimenten des Südatlantiks.
134 pages, Bremen, 1994.

No. 57 **Mulitza, S.**
Spätquartäre Variationen der oberflächennahen Hydrographie im westlichen äquatorialen Atlantik.
97 pages, Bremen, 1994.

No. 58 **Segl, M. and cruise participants**
Report and preliminary results of METEOR-Cruise M 29/1, Buenos-Aires - Montevideo, 17.6. - 13.7.1994
94 pages, Bremen, 1994.

No. 59 **Bleil, U. and cruise participants**
Report and preliminary results of METEOR-Cruise M 29/2, Montevideo - Rio de Janiero 15.7. - 8.8.1994. 153 pages, Bremen, 1994.

No. 60 **Henrich, R. and cruise participants**
Report and preliminary results of METEOR-Cruise M 29/3, Rio de Janeiro - Las Palmas 11.8. - 5.9.1994. Bremen, 1994 (not published). (out of print)

No. 61 **Sagemann, J.**
Saisonale Variationen von Porenwasserprofilen, Nährstoff-Flüssen und Reaktionen in intertidalen Sedimenten des Weser-Ästuars. 110 pages, Bremen, 1994. (out of print)

No. 62 **Giese, M. and G. Wefer**
Bericht über den 3. JGOFS-Workshop. 5./6. Dezember 1994 in Bremen.
84 pages, Bremen, 1995.

No. 63 **Mann, U.**
Genese kretazischer Schwarzschiefer in Kolumbien: Globale vs. regionale/lokale Prozesse.
153 pages, Bremen, 1995. (out of print)

No. 64 **Willems, H., Wan X., Yin J., Dongdui L., Liu G., S. Dürr, K.-U. Gräfe**
The Mesozoic development of the N-Indian passive margin and of the Xigaze Forearc Basin in southern Tibet, China. – Excursion Guide to IGCP 362 Working-Group Meeting "Integrated Stratigraphy". 113 pages, Bremen, 1995. (out of print)

No. 65 **Hünken, U.**
Liefergebiets - Charakterisierung proterozoischer Goldseifen in Ghana anhand von Fluideinschluß - Untersuchungen. 270 pages, Bremen, 1995.

No. 66 **Nyandwi, N.**
The Nature of the Sediment Distribution Patterns in ther Spiekeroog Backbarrier Area, the East Frisian Islands. 162 pages, Bremen, 1995.

No. 67 **Isenbeck-Schröter, M.**
Transportverhalten von Schwermetallkationen und Oxoanionen in wassergesättigten Sanden. - Laborversuche in Säulen und ihre Modellierung -. 182 pages, Bremen, 1995.

No. 68 **Hebbeln, D. and cruise participants**
Report and preliminary results of SONNE-Cruise SO 102, Valparaiso - Valparaiso, 95
134 pages, Bremen, 1995.

No. 69 **Willems, H. (Sprecher), U.Bathmann, U. Bleil, T. v. Dobeneck, K. Herterich, B.B. Jorgensen, E.-M. Nöthig, M. Olesch, J. Pätzold, H.D. Schulz, V. Smetacek, V. Speiß. G. Wefer**
Bericht des Graduierten-Kollegs Stoff-Flüsse in marine Geosystemen.
Berichtszeitraum Januar 1993 - Dezember 1995., 45 & 468 pages, Bremen, 1995.

No. 70 **Giese, M. and G. Wefer**
Bericht über den 4. JGOFS-Workshop. 20./21. November 1995 in Bremen.
60 pages, Bremen, 1996. (out of print)

No. 71 **Meggers, H.**
Pliozän-quartäre Karbonatsedimentation und Paläozeanographie des Nordatlantiks und des Europäischen Nordmeeres - Hinweise aus planktischen Foraminiferengemeinschaften.
143 pages, Bremen, 1996. (out of print)

No. 72 **Teske, A.**
Phylogenetische und ökologische Untersuchungen an Bakterien des oxidativen und reduktiven marinen Schwefelkreislaufs mittels ribosomaler RNA. 220 pages, Bremen, 1996. (out of print)

No. 73 **Andersen, N.**
Biogeochemische Charakterisierung von Sinkstoffen und Sedimenten aus ostatlantischen Produktions-Systemen mit Hilfe von Biomarkern. 215 pages, Bremen, 1996.

No. 74 **Treppke, U.**
Saisonalität im Diatomeen- und Silikoflagellatenfluß im östlichen tropischen und subtropischen Atlantik. 200 pages, Bremen, 1996.

No. 75 **Schüring, J.**
Die Verwendung von Steinkohlebergematerialien im Deponiebau im Hinblick auf die Pyritverwitterung und die Eignung als geochemische Barriere. 110 pages, Bremen, 1996.

No. 76 **Pätzold, J. and cruise participants**
Report and preliminary results of VICTOR HENSEN cruise JOPS II, Leg 6, Fortaleza - Recife, 10.3. - 26.3. 1995 and Leg 8, Vitoria - Vitoria, 10.4. - 23.4.1995.
87 pages, Bremen, 1996.

No. 77 **Bleil, U. and cruise participants**
Report and preliminary results of METEOR-Cruise M 34/1, Cape Town - Walvis Bay, 3.-26.1.1996.
129 pages, Bremen, 1996.

No. 78 **Schulz, H.D. and cruise participants**
Report and preliminary results of METEOR-Cruise M 34/2, Walvis Bay - Walvis Bay, 29.1.-18.2.96
133 pages, Bremen, 1996.

No. 79 **Wefer, G. and cruise participants**
Report and preliminary results of METEOR-Cruise M 34/3, Walvis Bay - Recife, 21.2.-17.3.1996.
168 pages, Bremen, 1996.

No. 80 **Fischer, G. and cruise participants**
Report and preliminary results of METEOR-Cruise M 34/4, Recife - Bridgetown, 19.3.-15.4.1996.
105 pages, Bremen, 1996.

No. 81 **Kulbrok, F.**
Biostratigraphie, Fazies und Sequenzstratigraphie einer Karbonatrampe in den Schichten der Oberkreide und des Alttertiärs Nordost-Ägyptens (Eastern Desert, N'Golf von Suez, Sinai).
153 pages, Bremen, 1996.

No. 82 **Kasten, S.**
Early Diagenetic Metal Enrichments in Marine Sediments as Documents of Nonsteady-State Depositional Conditions. Bremen, 1996.

No. 83 **Holmes, M.E.**
Reconstruction of Surface Ocean Nitrate Utilization in the Southeast Atlantic Ocean Based on Stable Nitrogen Isotopes. 113 pages, Bremen, 1996.

No. 84 **Rühlemann, C.**
Akkumulation von Carbonat und organischem Kohlenstoff im tropischen Atlantik: Spätquartäre Produktivitäts-Variationen und ihre Steuerungsmechanismen.
139 pages, Bremen, 1996.

No. 85 **Ratmeyer, V.**
Untersuchungen zum Eintrag und Transport lithogener und organischer partikulärer Substanz im östlichen subtropischen Nordatlantik. 154 pages, Bremen, 1996.

No. 86 **Cepek, M.**
Zeitliche und räumliche Variationen von Coccolithophoriden-Gemeinschaften im subtropischen Ost-Atlantik: Untersuchungen an Plankton, Sinkstoffen und Sedimenten.
156 pages, Bremen, 1996.

No. 87 **Otto, S.**
Die Bedeutung von gelöstem organischen Kohlenstoff (DOC) für den Kohlenstoffffluß im Ozean.
150 pages, Bremen, 1996.

No. 88 **Hensen, C.**
Frühdiagenetische Prozesse und Quantifizierung benthischer Stoff-Flüsse in Oberflächen sedimenten des Südatlantiks.
132 pages, Bremen, 1996.

No. 89 **Giese, M. and G. Wefer**
Bericht über den 5. JGOFS-Workshop. 27./28. November 1996 in Bremen.
73 pages, Bremen, 1997.

No. 90 **Wefer, G. and cruise participants**
Report and preliminary results of METEOR-Cruise M 37/1, Lisbon - Las Palmas, 4.-23.12.1996.
79 pages, Bremen, 1997.

No. 91 **Isenbeck-Schröter, M., E. Bedbur, M. Kofod, B. König, T. Schramm & G. Mattheß**
Occurrence of Pesticide Residues in Water - Assessment of the Current Situation in Selected EU Countries. 65 pages, Bremen 1997.

No. 92 **Kühn, M.**
Geochemische Folgereaktionen bei der hydrogeothermalen Energiegewinnung.
129 pages, Bremen 1997.

No. 93 **Determann, S. & K. Herterich**
JGOFS-A6 „Daten und Modelle": Sammlung JGOFS-relevanter Modelle in Deutschland.
26 pages, Bremen, 1997.

No. 94 **Fischer, G. and cruise participants**
Report and preliminary results of METEOR-Cruise M 38/1, Las Palmas - Recife, 25.1.-1.3.1997.
Bremen, 1997.

No. 95 **Bleil, U. and cruise participants**
Report and preliminary results of METEOR-Cruise M 38/2, Recife - Las Palmas, 4.3.-14.4.1997.
126 pages, Bremen, 1997 (in press).

No. 96 **Neuer, S. and cruise participants**
Report and preliminary results of VICTOR HENSEN-Cruise 96/1. Bremen, 1997.

No. 97 **Villinger, H. and cruise participants**
Fahrtbericht SO 111, 20.8. - 16.9.1996. 115 pages, Bremen, 1997.

No. 98 **Lüning, S.**
Late Cretaceous - Early Tertiary sequence stratigraphy, paleoecology and geodynamics of Eastern Sinai, Egypt. 218 pages, Bremen, 1997.

No. 99 **Haese, R.R.**
Beschreibung und Quantifizierung frühdiagenetischer Reaktionen des Eisens in Sedimenten des Südatlantiks. 118 pages, Bremen, 1997.

No. 100 **Lührte, R. von**
Verwertung von Bremer Baggergut als Material zur Oberflächenabdichtung von Deponien - Geochemisches Langzeitverhalten und Schwermetall-Mobilität (Cd, Cu, Ni, Pb, Zn).
Bremen, 1997.

No. 101 **Ebert, M.**
Der Einfluß des Redoxmilieus auf die Mobilität von Chrom im durchströmten Aquifer.
135 pages, Bremen, 1997.

No. 102 **Krögel, F.**
Einfluß von Viskosität und Dichte des Seewassers auf Transport und Ablagerung von Wattsedimenten (Langeooger Rückseitenwatt, südliche Nordsee).
168 pages, Bremen, 1997.

No. 103 **Kerntopf, B.**
Dinoflagellate Distribution Patterns and Preservation in the Equatorial Atlantic and Offshore North-West Africa. 137 pages, Bremen, 1997.

No. 104 **Breitzke, M.**
Elastische Wellenausbreitung in marinen Sedimenten - Neue Entwicklungen der Ultraschall Sedimentphysik und Sedimentechographie. 298 pages, Bremen, 1997.

No. 105 **Marchant, M.**
Rezente und spätquartäre Sedimentation planktischer Foraminiferen im Peru-Chile Strom. 115 pages, Bremen, 1997.

No. 106 **Habicht, K.S.**
Sulfur isotope fractionation in marine sediments and bacterial cultures. 125 pages, Bremen, 1997.

No. 107 **Hamer, K., R.v. Lührte, G. Becker, T. Felis, S. Keffel, B. Strotmann, C. Waschkowitz, M. Kölling, M. Isenbeck-Schröter, H.D. Schulz**
Endbericht zum Forschungsvorhaben 060 des Landes Bremen: Baggergut der Hafengruppe Bremen-Stadt: Modelluntersuchungen zur Schwermetallmobilität und Möglichkeiten der Verwertung von Hafenschlick aus Bremischen Häfen. 98 pages, Bremen, 1997.

No. 108 **Greeff, O.W.**
Entwicklung und Erprobung eines benthischen Landersystemes zur *in situ*-Bestimmung von Sulfatreduktionsraten mariner Sedimente. 121 pages, Bremen, 1997.

No. 109 **Pätzold, M. und G. Wefer**
Bericht über den 6. JGOFS-Workshop am 4./5.12.1997 in Bremen. Im Anhang: Publikationen zum deutschen Beitrag zur Joint Global Ocean Flux Study (JGOFS), Stand 1/1998. 122 pages, Bremen, 1998.

No. 110 **Landenberger, H.**
CoTReM, ein Multi-Komponenten Transport- und Reaktions-Modell. 142 pages, Bremen, 1998.

No. 111 **Villinger, H. und Fahrtteilnehmer**
Fahrtbericht SO 124, 4.10. - 16.10.199. 90 pages, Bremen, 1997.

No. 112 **Gietl, R.**
Biostratigraphie und Sedimentationsmuster einer nordostägyptischen Karbonatrampe unter Berücksichtigung der Alveolinen-Faunen. 142 pages, Bremen, 1998.

No. 113 **Ziebis, W.**
The Impact of the Thalassinidean Shrimp *Callianassa truncata* on the Geochemistry of permeable, coastal Sediments. 158 pages, Bremen 1998.

No. 114 **Schulz, H.D. und Fahrtteilnehmer**
Report and preliminary results of METEOR-Cruise M 41/1, Málaga - Libreville, 13.2.-15.3.1998. Bremen, 1998.

No. 115 **Völker, D.J.**
Untersuchungen an strömungsbeeinflußten Sedimentationsmustern im Südozean. Interpretation sedimentechographischer Daten und numerische Modellierung. Bremen, 1998.

No. 116 **Schlünz, B.**
Riverine Organic Carbon Input into the Ocean in Relation to Late Quaternary Climate Change. 136 pages, Bremen, 1998.

No. 117 **Kuhnert, H.**
Aufzeichnug des Klimas vor Westaustralien in stabilen Isotopen in Korallenskeletten. 109 pages, Bremen, 1998.

No. 118 **Kirst, G.**
Rekonstruktion von Oberflächenwassertemperaturen im östlichen Südatlantik anhand von Alkenonen. 130 pages, Bremen, 1998.

No. 119 **Dürkoop, A.**
Der Brasil-Strom im Spätquartär: Rekonstruktion der oberflächennahen Hydrographie während der letzten 400 000 Jahre. 121 pages, Bremen, 1998.

No. 120 **Lamy, F.**
Spätquartäre Variationen des terrigenen Sedimenteintrags entlang des chilenischen Kontinentalhangs als Abbild von Klimavariabilität im Milanković- und Sub-Milanković-Zeitbereich.
141 pages, Bremen, 1998.